Academic Year 2020-2021

Faculty Pharmaceutical, Biomedical and Veterinary Sciences

Biomedical Sciences

The obstacle course of biomarker discovery research for mood disorders - Protocol optimization and validation for peripheral blood mononuclear cell and neuronal extracellular vesicle isolation and analysis

By:

Selina Cortoos

Master dissertation submitted in completion of the degree of
Master in Biomedical Sciences

Promotor: Prof. Dr. Violette Coppens

Co-promotor: Prof. Dr. Manuel Morrens

Coach: Jobbe Goossens

Scientific Initiative for Neuropsychiatric and Psychopharmacological Studies (SINAPS), Collaborative Antwerp Psychiatric Research Institute (CAPRI), University of Antwerp

Rooienberg 19, 2570 Duffel, Belgium

Table of contents

I. List of abbreviations

2DE	Two-Dimensional Gel Electrophoresis
3-HK	3-hydroxykynurenine
5-HT	Serotonin
5-HTT	Serotonin Transporter (SERT)
5-HTTLPR	Serotonin Transporter-Linked Polymorphic Region
ACTH	Adrenocorticotropic Hormone
APOA1	Apolipoprotein A1
BCA	Bicinchoninic acid
BD	Bipolar Disorder
BD-D	Depression in context of Bipolar Disorder
BD-M	Mania in context of Bipolar Disorder
BDNF	Brain-Derived Neurotrophic Factor
BSA	Bovine Serum Albumin
CAPRI	Collaborative Antwerp Psychiatric Research Institute
CMG	CellMask Green
CRF	Corticotropin Releasing Factor
CV	Coefficient of Variation
DA	Dopamine
DSM-5	Diagnostic and Statistical Manual of Mental Disorders, 5th revision
ECT	Electroconvulsive Therapy
EDTA	Ethylenediaminetetraacetic acid
ELISA	Enzyme-Linked Immuno Sorbent Assay
EV	Extracellular Vesicle
fMRI	Functional Magnetic Resonance Imaging
GO	Gene Ontology
GR-plasma	Gradient-Residue plasma
HC	Healthy Control
HDRS	Hamilton Depression Rating Scale
HLA-DRB1	HLA class II histocompatibility antigen, DRB1-16 beta chain
HPA axis	Hypothalamic-Pituitary-Adrenal axis
HPLC	High Performance Liquid Chromatography
HSD	Honest Significant Differences
HSP70	Heat shock protein 70
ICD-10	International Statistical Classification of Diseases and Related Health Problems, 10th revision
IDO	Indoleamine 2,3-dioxygenase
IL-1Ra	Interleukin-1 Receptor Agonist Protein
iTRAQ	Isobaric Mass-Tag Labelling for Relative and Absolute Quantitation
KAT/CCBL1	Kynurenine aminotransferase I / Cysteine Conjugate-Beta Lyase 1
KMO	Kynurenine 3-monooxygenase
KYN	Kynurenine
KYNA	Kynurenic acid
L1CAM	L1 Cell Adhesion Molecule
LC-MS	Liquid Chromatography-Mass Spectrometry
LFQ	Label Free Quantification
MAO-I	Monoamine Oxidase Inhibitor
MDD	Major Depressive Disorder
MIF	Macrophage Migration Inhibition Factor
MINI	Mini International Neuropsychiatric Interview
M-PER	Mammalian Protein Extraction Reagent
MS	Mass Spectrometry
MTBE	Methyl Tert-Butyl Ether
NA/NE	Noradrenaline/Norepinephrine
nEV	Neuronal extracellular vesicle
NTA	Nanoparticle Tracking Analysis

OD	Optical Density
PBMC	Peripheral Blood Mononuclear Cell
PBS	Phosphate Buffered Saline
PET	Positron Emission Tomography
PMSF	Phenylmethylsulfonyl Fluoride
QUIN	Quinolinic acid
R^2	Coefficient of Determination
RAB7A	Rab-Related Protein 7a
RBC	Red Blood Cells
RIPA buffer	Radio-Immunoprecipitation Assay buffer
ROCK2	Rho-Associated Coiled-Coil Containing Protein Kinase 2
rpm	Revolutions per minute
rTMS	Repetitive Transcranial Magnetic Stimulation
SD	Standard Deviation
SDS	Sodium Dodecyl Sulphate
SEC	Size Exclusion Chromatography
SINAPS	Scientific Initiative for Neuropsychiatric And Psychopharmacological Studies
SNRI	Serotonin-Noradrenaline Reuptake Inhibitor
SRM/MRM	Selected/Multiple Reaction Monitoring
SSRI	Selective Serotonin Reuptake Inhibitor
SST	Serum Separator Tube
SZ	Schizophrenia
TCA	Tricyclic Antidepressants
TCEP	Tris(2-carboxyethyl)phosphine
TEAB	Triethylammonium bicarbonate
TimsTOF	Trapped Ion Mobility Spectrometry Time of Flight
TPH	Tryptophan Hydroxylase
TRP	Tryptophan
TRYCAT	Tryptophan Catabolite
WHO	World Health Organization
XA	Xanthurenic Acid
XPO7	Exportin-7

II. Abstract

Introduction: Psychiatric mood disorders are debilitating mental illnesses, with recent studies of the World Health Organization predicting that major depressive disorder will become the leading cause of disability worldwide within the coming 10 years. However, a part of those diagnosed with major depressive disorder actually suffer from bipolar disorder, a related, but differently treated disease. Due to the extensive similarity in symptoms between major depressive disorder (MDD) and depression in a context of bipolar disorder (BD-D), and the fact that differential diagnosis merely relies on the subjective evaluation of symptoms, this often leads to misdiagnosis and consequently incorrect treatment. The use of a biomarker panel as a diagnostic method could potentially overcome these problems and ensure a more accurate diagnosis. Previous research focused on biomarker identification in whole blood, plasma, and serum, although without any clinical success. This project hence aimed at scrutinizing peripheral blood mononuclear cells for differentially expressed proteins as biomarker candidates to discriminate MDD from BD-D (*project 1*). Moreover, we technically validated enzyme-linked immunosorbent assays (ELISAs) for immunogenic tryptophan and kynurenine metabolites on blood samples (*project 2*), and initiated protocol optimization for the isolation of neuronal extracellular vesicles from plasma (*project 3*).

Methodology: *Project 1*: Patients with major depressive disorder (n=46), patients with bipolar disorder in a depressive state (n=21), and healthy controls (n=48) were recruited and peripheral blood mononuclear cell samples were collected. For protocol validation of the first liquid chromatography – mass spectrometry run, non-patient test samples were used. *Project 2*: Test blood samples were acquired from healthy volunteers, from which serum, plasma, gradient-residue (GR) plasma, and peripheral blood mononuclear cells were isolated. ELISAs for tryptophan, kynurenine, kynurenic acid, and quinolinic acid were performed according to the manufacturer's protocol. *Project 3*: Size exclusion chromatography and an immunoprecipitation with anti-L1CAM antibody were performed to isolate neuronal extracellular vesicles from plasma. Samples were further processed for analysis with ZetaView, liquid chromatography – mass spectrometry, silver staining, and Western blots with anti-CD81, anti-APOA1, anti-albumin, and anti-HSP70 antibodies.

Results: *Project 1*: A test run indicated heavy haemoglobin contamination of our peripheral blood mononuclear cell samples. Protocol optimization regarding purification of the samples is currently ongoing. *Project 2*: Tryptophan, kynurenine, kynurenic acid, and quinolinic acid ELISAs were precise with accurate control concentrations. Concentrations in plasma and GR-plasma were within the expected ranges and were not significantly different for any of the catabolites. GR-plasma had the lowest coefficient of variation, thus possibly being the best source for liquid blood fraction ELISAs. For kynurenic acid, serum concentrations were significantly higher than in plasma, while for quinolinic acid, the opposite was observed. Concentrations in peripheral blood mononuclear cells were mostly under the detection limit. *Project 3*: ZetaView analysis showed the presence of particles in the samples, and a low amount of extracellular vesicles. The silver staining showed no specific bands for our samples, while on the Western blots, only albumin was detected. The mass spectrometry results showed no extracellular vesicle-specific proteins were present in our test samples.

Conclusion: *Project 1*: Haemoglobin contamination of the preliminary test samples interfered with the mass spectrometry analysis. In future experiments, optimization of peripheral blood mononuclear cell collection is required to prevent erythrocyte lysis during the final steps of isolation. The already acquired samples will be used for the second project. *Project 2*: The repeatability and precision of the kits was successfully validated for use on patient samples. GR-plasma can be used in surplus of normal plasma with an eye to waste-reduction purposes and increased sample availability for additional analyses. The number of peripheral blood mononuclear cells should be higher in future assays to get results within the ELISA detection limits. *Project 3*: Extensive protocol optimizations will be needed to successfully isolate extracellular vesicles from plasma, as to use them for potential biomarker discovery purposes in psychiatry.

III. Dutch summary – Nederlandse samenvatting

Introductie: Psychiatrische stemmingsstoornissen behoren tot de meest slopende mentale ziekten. Zo hebben studies van de Wereldgezondheidsorganisatie geschat dat majeure depressie de grootste oorzaak van invaliditeit zal worden in de komende 10 jaar. Een groot deel van de patiënten gediagnosticeerd met majeure depressie leidt echter aan een bipolaire stoornis, een gerelateerde, maar anders behandelde ziekte. Door de grote gelijkenis in symptomen tussen majeure depressie (MDD) en depressie in de context van een bipolaire stoornis (BD-D), en het feit dat differentiële diagnose enkel gebaseerd is op een subjectieve symptoomevaluatie, leidt dit vaak tot misdiagnoses en foutieve behandelingen. Het gebruik van een biomerker panel als diagnostische techniek zou deze problemen potentieel kunnen voorkomen en een meer accurate diagnose kunnen garanderen. Eerdere studies waren gefocust op biomerker identificatie in volledig bloed, plasma en serum, echter zonder klinisch succes. Deze thesis was dan ook gericht op het gebruik van perifere mononucleaire cellen voor het vinden van differentieel geëxpresseerde eiwitten als biomerker-kandidaten voor de differentiatie tussen MDD en BD-D (*project 1*). Verder werden technische validaties van *enzyme-linked immunosorbent assays* (ELISAs) van het kynurenine metabolisme uitgevoerd (*project 2*), en werd het isolatieprotocol voor neuronale extracellulaire vesikels uit plasma geoptimaliseerd (*project 3*).

Methodologie: *Project 1:* Patiënten met majeure depressie (n=46), depressieve patiënten met een bipolaire stoornis (n=21), en gezonde controles (n=48) werden gerekruteerd en perifere mononucleaire cellen werden verzameld. Voor protocoloptimalisatie van de eerste chromatografie – massaspectrometrie analyse werden teststalen gebruikt. *Project 2:* Teststalen werden verzameld van gezonde vrijwilligers waaruit serum, plasma, gradiënt-residu (GR) plasma, en mononucleaire cellen werden opgezuiverd. Tryptofaan, kynurenine, kynureenzuur, en chinolinezuur ELISAs werden uitgevoerd volgens de instructies van de fabrikant. *Project 3:* Gelchromatografie en een immunoprecipitatie met een anti-L1CAM antilichaam werden uitgevoerd om neuronale extracellulaire vesikels te isoleren uit plasma. Stalen werden gebruikt voor verdere analyse met ZetaView, chromatografie – massaspectrometrie, zilverkleuring, en Western blots met anti-CD81, anti-APOA1, anti-albumine, en anti-HSP70 antilichamen.

Resultaten: *Project 1:* De analyse van de teststalen onthulde een sterke hemoglobine-contaminatie van onze mononucleaire cellen. Protocoloptimalisatie voor de zuivering van de stalen is momenteel lopende. *Project 2:* Tryptofaan, kynurenine, kynureenzuur, en chinolinezuur ELISAs waren nauwkeurig met accurate controle concentraties. Concentraties in plasma en GR-plasma waren binnen de verwachte marges en voor geen enkele metaboliet significant verschillend. GR-plasma had bovendien de laagste variatiecoëfficiënt, waardoor dit mogelijks de beste bron is voor ELISAs op bloedstalen. Kynureenzuur concentraties waren significant hoger in serum dan in plasma, terwijl voor chinolinezuur het omgekeerde werd opgemerkt. Concentraties in de perifere mononucleaire cellen bevonden zich voornamelijk onder de detectielimiet. *Project 3:* ZetaView analyse toonde de aanwezigheid van verscheidene partikels aan, waaronder lage concentraties extracellulaire vesikels. De zilverkleuring toonde geen specifieke bandenpatronen, terwijl op de Western blots enkel albumine werd gedetecteerd. The massaspectrometrie resultaten toonden dat er geen eiwitten specifiek voor extracellulaire vesikels in onze stalen aanwezig waren.

Conclusie: *Project 1:* De hemoglobine contaminatie van onze stalen verhinderde de verdere analyse met de massaspectrometer. Het isolatieprotocol voor perifere mononucleaire cellen moet geoptimaliseerd worden om de lysis van rode bloedcellen in de laatste stappen van de isolatie te voorkomen. De reeds verzamelde stalen zullen gebruikt worden voor het tweede project. *Project 2:* De reproduceerbaarheid en precisie van de kits werden succesvol gevalideerd voor gebruik op patiëntstalen. GR-plasma kan bovendien worden gebruikt als aanvulling op normaal plasma met het oog op afvalbeperking en staalbeschikbaarheid. Het aantal perifere mononucleaire cellen zal moeten worden verhoogd om resultaten binnen de ELISA detectielimieten te verkrijgen. *Project 3:* Uitvoerige protocoloptimalisaties zullen nodig zijn om succesvol extracellulaire vesikels van plasma te isoleren.

1. Introduction

1.1. Major depressive disorder and bipolar disorder

Psychiatric mood or affective disorders, like major depressive disorder (MDD) and bipolar disorder (BD), are debilitating mental illnesses associated with high mortality and life-long suffering for those who are affected. MDD is predominantly characterized by symptoms as anhedonia, low energy, feelings of low self-esteem, and periods of extreme depression (Chiriţă et al., 2015). Globally, MDD affects an estimated 264 million people, making it the most common psychiatric disorder worldwide. Moreover, the World Health Organization (WHO) has estimated that MDD will become the leading cause of disability worldwide within the coming 10 years, overtaking cardiovascular disease (Funk et al., 2010). BD on the other hand is hallmarked by recurring episodes of mania, hypomania, depression or mixed states, with euthymic periods in-between (Musetti et al., 2013), and affects an estimated 45 million people worldwide (James et al., 2018; Hirschfeld, 2014).

Both MDD and BD have poor clinical outcomes, such as low rates of response and remission and high incidences of symptom recurrence – over 50% of patients relapses within six months of apparent clinical remission – but also cognitive and functional impairment, often with lingering residual symptoms (Sim et al., 2015). Because of their very complex and multifactorial aetiopathogenesis, the biology of MDD and BD remains poorly understood (Chen et al., 2015). As a result, discriminatory diagnosis solely relies on the subjective evaluation of clinical signs. The disorders' complexity and overlapping symptoms cause alarmingly high rates of misdiagnosis (Singh and Rajput, 2006) and consequential incorrect psycho-pharmacotherapeutic treatment (Preece et al., 2018). It has been estimated that approximately 40% of patients with BD were initially misdiagnosed with MDD, misguiding their medication (Forte et al., 2015). Moreover, failure to treat psychiatric patients adequately, regularly leads to feelings of despair and helplessness, further aggravating their condition (Nasrallah, 2015). Likewise, inappropriate treatment with antidepressant monotherapy can trigger manic episodes or rapid cycling in previously undetected bipolar depression (Singh and Rajput, 2006; Ghaemi et al., 2000). It remains thus of the utmost importance to diagnose psychiatric patients more effectively and objectively, so as to treat each specific mood disorder more efficiently with proper pharmacotherapies. As of today, no such diagnostic method exists. The discovery of discriminatory biomarkers thus remains essential in the diagnosis and treatment of psychiatric mood disorders like MDD and BD (Ren et al., 2017).

1.2. Underlying disease mechanisms and previous findings

MDD and BD are inhomogeneous and complex disorders that act at different levels; psychologically, biologically, genetically, and socially. Unfortunately, the exact mechanisms underlying the emergence of depressive episodes are still poorly understood due to their complex nature. Likewise, because of the considerable variation between patients, different aspects like subtypes, prognosis, response to treatment, comorbidity with other disorders and neurobiological and psychosocial factors must be taken into account (Chiriţă et al., 2015). The most important neurobiological factors in MDD, as well as depression in context of bipolar disorder (BD-D), will be discussed below.

1.2.1. *(Epi)genetic and environmental factors*

First, several environmental and (epi)genetic factors may trigger and aggravate MDD and BD-D. Individuals with a family history of psychiatric mood disorders often show a more deleterious reaction to stressful life events, which may ultimately lead to the development of a depressive episode. However, twin studies have estimated that only about 37% of the total trait variance in MDD is due to genetic variation (Sullivan et al., 2000), in comparison to a heritability of 70-80% in BD (Craddock and Sklar, 2013). Mood disorders can thus not be considered purely genetic disorders. Nevertheless, the gene coding for the serotonin transporter has been shown to be involved in the occurrence of major depressive episodes. According to a prospective-longitudinal birth cohort study by *Caspi et al.*, a functional polymorphism in the promotor region of the serotonin transporter 5-HTT may moderate the effect of stress on depression. Patients hetero- or homozygous for the short 5-HTT gene-linked

polymorphic region (5-HTTLPR) allele were deemed more vulnerable to the development of a depressive episode, depending on the number of stressful events in the recent past. Moreover, a significant interaction was found between the occurrence of stressful life events and the capability to predict suicide ideation or attempts among individuals carrying at least one short allele (Caspi et al., 2003). These findings support the gene-by-environment interaction model for MDD and BD-D within the field of epigenetics (Chiriţă et al., 2015).

These underlying epigenetic modifications can alter the function of specific genes, dependent on the environmental experiences, without changing the DNA sequence (Penner-Goeke and Binder, 2019). This could possibly explain several aspects of depression like high discordance rates between monozygotic twins, the role of mistreatment during childhood, and the significantly higher prevalence in women, possibly caused by skewed X-chromosome inactivation (Mill and Petronis, 2007). Overall, there are at least two important epigenetic modifications that are thought to be involved in MDD and BD-D: DNA methylation (in the influence of maternal behaviour on the adult emotional processing) and histone acetylation (in the antidepressant mechanism of action). More epigenetic mechanisms are supposedly involved as well, but are not fully elucidated as of yet (Drevets, 1998; Chiriţă et al., 2015).

1.2.2. *Neural circuitry and neurotransmitters*

Several prefrontal and limbic brain regions can regulate emotion, learning, memory, executive function, and reward systems. Those regions include the ventromedial prefrontal cortex, the dorsolateral prefrontal cortex, the lateral orbital prefrontal cortex, the anterior cingulate cortex, the hippocampus, the amygdala and the ventral striatum (Berton and Nestler, 2006). In post-mortem and neuroimaging studies of patients with MDD, a reduced grey-matter volume has been reported. Likewise, in BD patients, the amygdala, hippocampus, and white and grey matter in the frontal brain areas have significantly reduced volumes (de Sá et al., 2016). Research has also pointed to a reduced number of glial cells in the subgenual prefrontal cortex and the hippocampus (Dager et al., 2004). Those regions are thought to mediate feelings like guilt and worthlessness and correlate with dysthymic mood and impaired memory, all frequent cognitive aspects of depression (Krishnan and Nestler, 2008). Also cerebral metabolism alterations and reduced blood flow, both in unipolar and bipolar depression, have been detected (Dager et al., 2004). However, abovementioned findings are often complicated by medication history and comorbid diagnoses, causing limited success in demonstrating a clear cause-effect relation of these pathological changes (Krishnan and Nestler, 2008).

Experiments assessing brain function – like positron-emission tomography (PET) and functional magnetic resonance imaging (fMRI) – show that activity in the amygdala and subgenual cingulate cortex are strongly correlated with negative emotions. Neuronal activity within these regions is chronically increased in MDD patients, and transiently increased in healthy volunteers when they experience feelings of sadness (Drevets, 2001). In MDD patients, hyperactivity in the ventromedial prefrontal cortex and lateral orbital prefrontal cortex, and a hypoactivity in the dorsolateral prefrontal cortex are described (Hirschfeld and Weissman, 2002). Furthermore, a decrease in communication between the anterior cingulate cortex and the amygdala has been suggested, which could possibly be an indication for a decreased capacity of the cortex to mediate dysphoric emotions in the subcortical areas (Anand et al., 2005). BD-D patients on the other hand show an increased activity in the left ventral portion of the prefrontal cortex, while the amygdala exhibits a bilateral decrease in activation (Blumberg et al., 2003). These networks in the forebrain are considerably modulated by neuronal projections of monoamines from the midbrain and brainstem nuclei. Those monoamines are serotonin (5-HT) from the dorsal raphe in the periaqueductal grey area, dopamine (DA) from the ventral tegmental area, and noradrenaline (NA, also referred to as norepinephrine (NE)) from the locus coeruleus (Krishnan and Nestler, 2008). The ‘monoamine hypothesis’ of depression states that the cause of depression lies in the decreased monoamine function in the brain. A decrease in serotonin may therefore be associated with increased anxiety, obsessions, and compulsions, whereas a reduction in noradrenaline may be linked with loss of alertness, energy, attention, and interest in life. A decrease in dopamine, on the other hand, may contribute to loss of motivation, reward, and

pleasure. In patients with MDD and BD-D, increased levels of dopamine transporters and consequently decreased dopamine levels were detected, while in bipolar individuals in a manic state, an increase in dopamine levels has been found (Berk et al., 2007; Gorwood, 2008). Besides this 'monoamine hypothesis', there is also the 'BDNF hypothesis', which states that the level of brain-derived neurotrophic factor (BDNF) is reduced in patients with MDD and BD, independent of the latter's mood state (Sen et al., 2008; de Sá et al., 2016). BDNF is a neurotrophin responsible for the neurogenesis in the brain, and a reduction may lead to depression-related symptoms (Chiriţă et al., 2015). However, more recent findings have shown that a revision of this hypothesis may be needed, since the opposite has also been observed (Krishnan and Nestler, 2008).

1.2.3. *Neuroendocrine dysregulation and neuroimmune interactions*

Depression and stress often go hand in hand; a stressful life event can precipitate a depressive episode in a person vulnerable to those events. As mentioned before, childhood stress and maltreatment in early life may increase the risk of depression in the adult life (Kim et al., 2020). This relationship between depression and stress could be due to a possible dysfunction of the hypothalamic-pituitary-adrenal axis (HPA axis) (Dean and Keshavan, 2017; Varghese and Brown, 2001). Those dysfunctions may vary between a hypersecretion of corticotropin releasing factor (CRF), impaired glucocorticoid-receptor-mediated negative feedback of the HPA axis, hyperresponsiveness to adrenocorticotropic hormone (ACTH), hypercortisolaemia, reduced suppression of cortisol in dexamethasone treatment, or enlarged adrenal glands (Pruessner et al., 2003). Physical or psychological stress may thus increase glucocorticoid levels, causing several depression-like symptoms and volume reductions of the hippocampus (Krishnan and Nestler, 2008).

Additionally, there have been indications for a link between immune mechanisms and the development of MDD or BD. Elevated levels of circulating cytokines, which are the humoral mediators of the innate and adaptive immune system, have been found in patients with MDD (Felger and Lotrich, 2013) and BD-D (Muneer, 2016). Those pro-inflammatory cytokines such as IFN-α, TNF-α, IL-6 and IL-1β, cause 'sickness behaviours' which encompass symptoms like fatigue and anhedonia, not unlike the illness experience when our body is fighting off an infection (Dean and Keshavan, 2017; Chiriţă et al., 2015). The inconsistency in clinical studies examining depression-associated increases in circulating cytokines suggests that only a subset of MDD and BD cases are caused by immune activation, including those associated with certain autoimmune conditions. Future studies of this 'neuroinflammatory hypothesis' should focus on elucidating the behavioural effects of cytokines and the involved neural circuitry, while defining the intercellular interactions between neurons, glia and macrophages (microglia) (Krishnan and Nestler, 2008).

More recently, a relation between the change in metabolism of essential amino acid tryptophan (TRP) and the occurrence of MDD has been found. Two main pathways are responsible for the metabolization of TRP; the serotonin (5-HT) pathway, initiated by the tryptophan 5-monooxygenase (tryptophan hydroxylase (TPH)) enzyme, and the kynurenine (KYN) pathway, initiated by the indoleamine 2,3-dioxygenase (IDO) enzyme (Miura et al., 2008; Doolin et al., 2018). Tryptophan may thus well be the intersection mediator linking the 'monoamine hypothesis' to the 'neuroinflammatory hypothesis'. IDO activity is induced by immunological changes such as increases of the aforementioned proinflammatory cytokines, indicating a possible association between IDO activation and the aetiology of MDD and BD-D. Since activated IDO metabolizes TRP to KYN, TPH is deprived from its substrate, eventually leading to a decrease in serotonin and an increase in tryptophan catabolites (TRYCAT) such as kynurenine, kynurenic acid (KYNA), and quinolinic acid (QUIN) (*Figure 1*) (Maes et al., 2007; Miura et al., 2008; Arnone et al., 2018). These TRYCAT may either have neurotoxic (KYN and QUIN) or neuroprotective (KYNA) effects. Imbalance of the neurodegenerative and neuroprotective activities of these catabolites could subsequently contribute to atrophy of the hippocampus in chronic depression (Doolin et al., 2018; Arnone et al., 2018). Illustratively, decreased KYNA concentrations (Allen et al., 2018) and an increase in the tryptophan breakdown index (KYN:TRP ratio) (Schwieler et al., 2016; Doolin et al., 2018) have been reported in depressed patients compared to healthy controls.

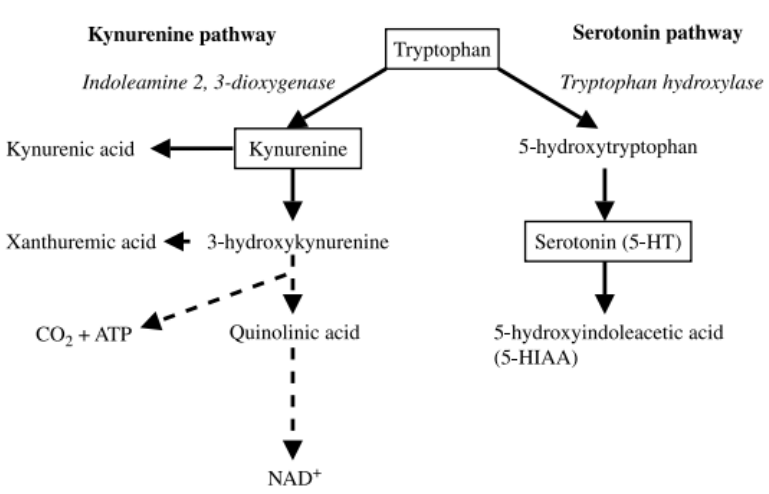

Figure 1 | **Kynurenine pathway (left) and serotonin pathway (right) of the tryptophan metabolism.** Left: Tryptophan (TRP) is metabolized by indoleamine 2,3-dioxygenase (IDO) to kynurenine (KYN). KYN can be further metabolized to kynurenic acid (KYNA), xanthurenic acid (XA), and quinolinic acid (QUIN). Right: Tryptophan is metabolized by tryptophan hydroxylase (TPH) to 5-hydroxytryptophan (5-HTP) and serotonin (5-HT) (Miura et al., 2008).

1.3. Current diagnosis and treatments

1.3.1. *Diagnostic methods*

As mentioned earlier, treatment choice is currently solely based on subjective evaluation of the patient anamnesis by the consulting psychiatrist or treating physician and often suffers from misdiagnosis. Currently, predetermined criteria for different mood disorders are described in the International Statistical Classification of Diseases and Related Health Problems, 10th revision (ICD-10) and the Diagnostic and Statistical Manual of Mental Disorders, 5th revision (DSM-5) (*Table 1)* (Preece et al., 2018).

Table 1 | **Diagnostic criteria for major depressive disorder and bipolar disorder.**

	Major depressive episode	Manic episode	Hypomanic episode
Symptoms	(1) Depressed mood (2) Diminished interest or pleasure (3) Decrease or increase in weight or appetite (4) Insomnia or hypersomnia (5) Psychomotor agitation or retardation (6) Fatigue or loss of energy (7) Feelings of worthlessness or guilt (8) Concentration or decision-making difficulties (9) Recurrent thoughts of death or suicide	(1) Inflated self-esteem or grandiosity (2) Decreased need for sleep (3) More talkative than usual or pressure to keep talking (4) Flight of ideas or racing thoughts (5) Distractibility (6) Increase in goal-directed activity or psychomotor agitation (7) Excessive involvement in activities with potentially painful consequences	
Number and duration of symptoms required	– Five (or more) symptoms; at least one symptom is either depressed mood or diminished interest or pleasure – Most of the day, nearly every day, for at least two weeks	– Three (or more) symptoms; four if the mood is only irritable – Most of the day, nearly every day, for at least one week	
Diagnosis of MDD	Required	Exclusion criterion	Exclusion criterion
Diagnosis of BD I	Not required	Required	Not required
Diagnosis of BD II	Required	Exclusion criterion	Required

A table of the characteristics of a major depressive episode, a manic episode, and a hypomanic episode and how they are applied in the diagnosis of major depressive disorder and bipolar disorder type I and type II, as defined in the DSM-5. MDD: major depressive disorder, BD I: bipolar disorder type I, BD II: bipolar disorder type II (Preece et al., 2018).

Since an objective biological diagnostic method is not yet available for physicians to use, they rely on the diagnostic manuals provided by the WHO. However, these manuals often categorize patients in strictly designated groups, while symptoms often overlap between different psychiatric disorders. This further complicates the potential treatment because of frequent misdiagnosis of MDD and BD-D (Kim and Ahn, 2002; McIntyre et al., 2019). The high rate of misdiagnosis of MDD vs. BD stems from the observation that most BD patients only seek treatment when feeling depressed, and not while being manic. Symptoms such as grandiosity, energy and increased motivation are often not considered negative events by those who experience them, therefore not requiring a doctor's visit (Bowden, 2005). However, more often than not, the first mood disturbance episode in BD is depression, rather than mania (Perugi et al., 2000). This phenomenon often leads to the impression that the patient is

solely depressed and is therefore easily misdiagnosed as having MDD, rather than BD-D. Consequences of misdiagnosis range from increased chronicity of episodes, to inappropriate treatment with antidepressant monotherapy, often resulting in a manic episode or triggering rapid cycling BD (Ghaemi et al., 2000). The subsequent delay in appropriate treatment increases the risk of recurrences, but may also cause a substantial rise in suicide attempts and hospitalization: the lifetime risk of suicide attempts in BD patients ranges between 25% and 50%, in comparison to 15% in MDD (Singh and Rajput, 2006; Walker et al., 2015). These alarmingly high numbers underscore the dire need for objective, biological diagnostic methods in order to provide an adequate, individually personalized treatment for each patient.

1.3.2. *Treatments*

Current treatment guidelines for MDD recommend pharmacotherapies such as selective serotonin reuptake inhibitors (SSRIs) and serotonin-noradrenaline reuptake inhibitors (SNRIs) as first-line treatments (Koenig and Thase, 2009; Gautam et al., 2017). Monoamine oxidase inhibitors (MAO-I) and tricyclic antidepressants (TCAs) are often only used as a second-line treatment due to safety and tolerability issues (Carvalho et al., 2016). Antidepressants such as TCAs, SSRIs, and SNRIs have shown to increase levels of serotonin in the brain, building further on the 'monoamine hypothesis'. Moreover, chronic treatment with SSRIs has revealed a downregulation of presynaptic 5-HT1A auto-receptors, increasing the serotonin concentration in the long-term (Dean and Keshavan, 2017). Still, the response rates to antidepressants are estimated to be as low as 30% in MDD, with an even lower effectiveness in BD-D (Preece et al., 2018). Furthermore, in some cases, the addition of an anti-inflammatory agent to antidepressant treatment has been successful in the reduction of depressive symptoms in MDD (Tyring et al., 2006). For BD patients, treatment guidelines suggest antipsychotics, valproate, and lithium as first-line mania treatment, yet pharmacotherapy options are limited and often ineffective in the depressive state of BD (Fountoulakis et al., 2005; Shah et al., 2017). Since most BD patients show a poor response to most antidepressants, the addition of an antipsychotic such as quetiapine, or a change of medication to a mood stabilizer to decrease the risk of switching to a manic episode, is often required (Shim et al., 2017).

Additionally, electroconvulsive therapy (ECT) and repetitive transcranial magnetic stimulation (rTMS) have known an uprise in the use for predominantly treatment-resistant MDD, but in some cases also for BD (Chen et al., 2017). However, both ECT and rTMS have been shown to possibly induce (hypo)manic episodes in both unipolar and bipolar depression, making the supplementation of a mood stabilizer often required (Rachid, 2017; Saatcioglu and Guduk, 2009).

1.4. Biomarker discovery: state-of-the-art

In the past, several studies have looked at potential biomarkers for MDD and BD. Most of those studies used targeted methods, while the use of non-targeted approaches is only scarcely investigated in psychiatric biomarker discovery. Hypothesis-driven or targeted approaches are based on the detection of known proteins and the measurement of their abundance in the sample, while hypothesis-free or non-targeted techniques allow for the identification of molecules that do not necessarily have a mechanistic relation to psychiatric pathologies. Both targeted and non-targeted approaches will be analysed further below, as well as the most frequently used sample sources for use in proteomic analysis. Additionally, state-of-the-art literature on possible discriminatory diagnostic biomarkers will be discussed.

1.4.1. *Targeted approaches*

Techniques based on the immunoassay technology, such as ELISAs and Western blot, are the gold standard for the validation and application of protein biomarkers. They use antibodies as a measurement of protein concentrations and are relatively easy to implement in a clinical setting. However, due to possible cross-reactivity, limited antibody availability, and large sample volume requirements, the technical and biological reproducibility are often limited (Hoofnagle and Wener, 2009). For this reason, targeted mass-spectrometry (MS)-based technologies such as selected/multiple

reaction monitoring (SRM/MRM) have known an uprise in biomarker discovery research. These techniques allow for a sensitive and robust protein quantitation with a high reproducibility. In the past, several potential diagnostic biomarkers for MDD and BD identified with targeted methods have been reported, including BDNF, ceruloplasmin, apolipoprotein C-III, and angiotensin-converting enzyme (Preece et al., 2018). However, none of these studies have been able to identify a biomarker that is applicable in a clinical setting, while also being highly predictive and specific (Taurines et al., 2011). Therefore, it might be beneficial to focus more on hypothesis-free approaches that do not assume a certain theory but start out from a global analysis of the sample. This is not possible with targeted methods, since those are only able to profile a limited number of proteins (*for additional review, see (Goossens et al., 2021)*).

1.4.2. *Non-targeted approaches*

As targeted biomarker discovery ventures have not yielded any satisfactory candidates as of yet, research focus has shifted towards non-targeted '-omics' approaches in the recent years. Hypothesis-free approaches like proteomics and genomics may thus be the key methodologies in discovering the aetiology and pathophysiology of MDD and BD. Given the possible inconsistency in translational regulation and post-translational events, proteomics might prove advantageous over genomics (Xu et al., 2012). Additionally, since proteins are the functional molecules of the cell, they reflect the current biological status of a patient more accurately. As such, a proteomic approach could allow for the detection of functional disease-related and state-dependent changes in an individual (Martins-de-Souza et al., 2010). The preferred method today is the use of MS coupled with other separation techniques, allowing for high-throughput analysis with an increased specificity and sensitivity (Preece et al., 2018). Liquid chromatography-MS (LC-MS) has become the most effective method in providing a thorough analysis and profiling disease-related alterations. Since LC-MS has the capability to detect changes in function, structure, abundance, and expression of proteins, it is the method of choice in early biomarker discovery (Patel, 2014).

1.4.3. *Sample sources*

Due to recent advancements in proteomic technologies, it is possible to collect protein information such as protein structure, protein-protein interactions, protein degradation and posttranslational modifications from tissues and bodily fluids such as serum, plasma, saliva, and urine (Preece et al., 2018). Evidently, as both MDD and BD are neuropsychiatric disorders, sampling of cerebrospinal fluid or brain tissue would be the most obvious choice for proteome analysis in order to identify potential biomarkers. However, lumbar punctures and brain biopsies are very invasive techniques that are not routinely performed in a psychiatric clinic or research setting (Xu et al., 2012). Peripheral blood samples, on the other hand, are very easy to obtain and also suitable for use in psychiatry since the peripheral blood absorbs approximately 500mL cerebrospinal fluid per day (Hye et al., 2006). Moreover, since the blood-brain barrier permeability seems to be disturbed in MDD and BD patients, a protein exchange may occur between the brain and the peripheral blood circulation (Hampel et al., 1997). In comparison to free-circulating serum or plasma, peripheral blood mononuclear cells (PBMC) have more steady protein levels and are furthermore abundantly present in a simple blood sample, making them an excellent candidate for proteome analysis (Grievink et al., 2016). Moreover, PBMC display similar protein expression profiles as the post-mortem brain, with the presence of BDNF receptors, serotonin, and dopamine (Rollins et al., 2010). The peripheral bloodstream, and more specifically PBMC, may thus be an important and promising sample source for proteome analysis in MDD and BD patients.

Additionally, extracellular vesicles or EVs – sometimes also referred to as exosomes – are present in saliva, urine and plasma and play a role in many physiological processes. EVs are a group of cell-derived vesicles that are released to the extracellular environment and carry molecular signals involved in the cellular communication (Lee et al., 2012; Samanta et al., 2018). There has been emerging evidence for the involvement of modified EV surfaces and cargo signatures (proteins and

microRNAs) in people with MDD (Nasca et al., 2020; Soares et al., 2021) and BD-D (Fries et al., 2019; Mansur et al., 2020), which could possibly envision a new potential biomarker source for the diagnosis and treatment of depression and other psychiatric disorders (Kano et al., 2019). The implication of EVs – more specifically those derived from the brain (neuronal extracellular vesicles or nEVs) – in psychiatric disorders is nevertheless still poorly understood. Nonetheless, they are a very accessible sample source when isolated from plasma for the possible discovery of discriminatory diagnostic biomarkers in the future (Saeedi et al., 2019).

1.4.4. *Discriminatory diagnostic biomarkers in MDD vs. BD-D: state-of-the-art*

Because of the complexity and heterogenicity of psychiatric diseases, it seems unlikely that a single biomarker will have an accurate and reliable discriminatory diagnostic potential. Therefore, most probably a biomarker panel will be required, as to more reliably differentiate between diseased and healthy people, but also among patients with MDD vs. BD-D. Preece et al. provided a comprehensive overview of the current knowledge on potential differential biomarkers in whole blood, plasma, and serum of MDD and BD patients, as identified with MS and validated with immunoassays.

Across 17 studies, 155 proteins were found that were differentially expressed between healthy controls and MDD or BD patients (MDD vs. control, BD vs. control) (*Figure 2*). Some of those proteins were reported in multiple studies; ceruloplasmin was found in 5 out of 10 studies comparing MDD with controls; alpha-2-macroglobuline, Apolipoprotein B-100, Apolipoprotein D, BDNF, interleukin-1 receptor antagonist protein (IL-1Ra), macrophage migration inhibitor factor (MIF) and protein S100-A12 were all reported in 3 out of 10 studies that compared MDD with healthy controls. Additionally, Apolipoprotein A-I was reported in 5 out of 7 BD vs. control studies, while serotransferrin was found in four (the remaining 101 BD proteins were only reported in less than 3 studies). These identified proteins all have functional roles in inflammation, immune response, metabolism or cell signalling. Furthermore, 29 proteins were identified that were reported in both MDD and BD vs. control studies, implying their possible involvement in pathological mechanisms and disease-related alterations, present in both MDD and BD. Those proteins that have been found repeatedly within the same group, could possibly lead to the discovery of diagnostic biomarkers and should be further investigated via targeted approaches (Preece et al., 2018).

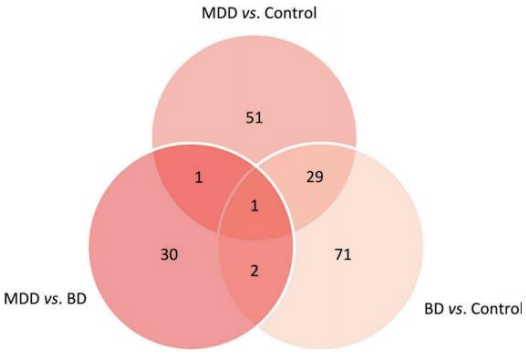

Figure *2* | **Venn diagram of the identified proteins from group-wise comparisons of MDD vs. BD, MDD vs. control, and BD vs. control.** 185 proteins were reported in total as potential diagnostic biomarkers across all 19 reviewed studies. 34 proteins were identified in the 2 studies comparing MDD vs. BD, 82 proteins were identified in the 10 studies comparing MDD vs. control, and 103 proteins were identified in the 7 studies that compared BD vs. control. MDD: major depressive disorder, BD: bipolar disorder (Preece et al., 2018).

Concerning differential discriminatory biomarkers, the 2 studies that directly compared MDD vs. BD, found a total of 34 differentially expressed proteins (*Figure 2*). Those included B2RAN2 and ENG (Ren et al., 2017), and C3, ROCK2 and C4BPα (Chen et al., 2015). They were found to have important key roles in the pathophysiology of depression and could serve as new candidate biomarkers for differentiation between MDD vs. BD-D in the clinic. Increased plasma concentrations of C3, for example, could be an indication for an MDD diagnosis or a depressive episode in BD (Chen et al., 2015).

Additionally, a more recently published research article by Rhee et al. found 14 differentially expressed proteins between MDD and BD patients, using LC-MS/MS analysis. The proteins that were significantly overexpressed in patients with MDD were Rab-related protein 7a (RAB7A) and Rho-associated coiled-coil containing protein kinase 2 (ROCK2), whereas Exportin-7 (XPO7) was significantly overexpressed in BD patients (Rhee et al., 2020). Only ROCK2 had previously been identified as a

potential differential diagnostic biomarker by the aforementioned study by Chen et al (Chen et al., 2015). This may indicate a possible relation between MDD and the presence of ROCK2 in the peripheral blood. The limited overlap between these two studies might possibly be explained by heterogeneous study designs, as the used proteomic technique and statistical methods varied between studies. (Preece et al., 2018).

1.4.5. *Gaps in state-of-the-art knowledge*

An important and persistent limitation in the state-of-the-art knowledge is the heterogeneity in studies, evidently impacting the validity of discovered biomarker data. Additionally, the frequent small sample sizes in studies cause an insufficiently high statistical power, ultimately preventing potential biomarkers from being used in a clinical setting (Young et al., 2016). Most identified biomarkers are non-specific and are thus fallible as a clinically applicable biological method of diagnosis. Additionally, current research largely focuses on biomarkers that differentiate between healthy controls and patients with either MDD or BD (Preece et al., 2018). However, in clinical practice it is more relevant to differentiate different illnesses from each other. The studies that did compare MDD with BD, all used non-targeted techniques like MS, validated by ELISA (Chen et al., 2015), iTRAQ LC-MS/MS (Ren et al., 2017), or label-free LC-MS/MS (Rhee et al., 2020), all on plasma or serum samples. As mentioned earlier, PBMC may show greater promise as biomarker vehicle than plasma or serum since their protein levels are less volatile and their proteomic profile reveals higher similarities to the post-mortem brain of psychiatric patients (Končarević et al., 2014; Grievink et al., 2016; Rollins et al., 2010).

1.5. Goal of the project

1.5.1. *Expertise of the host laboratory CAPRI – SINAPS*

The Collaborative Antwerp Psychiatric Research Institute (CAPRI) is a research centre specialized in mental health and neuropsychiatry at the University of Antwerp. CAPRI has delivered significant research efforts in the field of psychiatry and psychology and aims to improve diagnostics and treatments of various psychiatric diseases. As of today, numerous studies have been performed concerning cognitive neuroscience, psychopathology, psychopharmacology, psychotherapy, and biomarker discovery. The Scientific Initiative for Neuropsychiatric and Psychopharmacological Studies (SINAPS) is the research organization founded by CAPRI and the University Psychiatric Centre Duffel and specializes in scientific studies in the field of neuropsychiatry. SINAPS has immediate access to a large psychiatric patient population and a fully functional biomedical lab. CAPRI – SINAPS therefore has ample expertise and is adequately equipped to perform discriminatory biomarker discovery studies for MDD vs BD-D.

CAPRI and SINAPS have already carried out numerous studies concerning biomarker discovery and the identification of the underlying pathophysiological processes in MDD, BD and schizophrenia (SZ). Illustratively, van den Ameele et al. described the involvement of neurotrophic and inflammatory markers as kynurenine metabolites to be involved in the aetiopathogenesis of BD (van den Ameele et al., 2020; van den Ameele et al., 2017). Moreover, blood-based kynurenine pathway alterations in SZ spectrum disorders were identified by Morrens et al. (Morrens et al., 2020), but also the effects of ECT on the concentration of peripheral inflammatory markers and their influence on the hippocampal volume were studied (Belge et al., 2020).

Additionally, a preliminary and explorative proof-of-concept study by Coppens and colleagues from SINAPS, previously aimed to establish a record of possible discriminatory biomarkers in PBMC for MDD vs. BD-D on the one hand, but also BD-M (mania in context of bipolar depression) vs. SZ on the other hand, of which the latter two are beyond the scope of this Master's thesis. Because of the explorative nature of the study, only very small sample sizes were used (MDD, n=5; BD-D, n=3) which makes the comparison with the elaborate review of Preece et al. somewhat tricky. However, one protein was found to be contraregulated significantly in MDD vs. BD-D, namely HLA-DRB1 (HLA class II histocompatibility antigen, DRB1-16 beta chain), which has already been implicated in various psychiatric disorders. This antigen was significantly downregulated in MDD patients, while being

upregulated in BD-D patients (Coppens et al., 2020). A list of all 66 possible discriminatory biomarkers for MDD and BD-D as identified by Coppens et al. can be found in *appendix Table 10.* Nevertheless, this preliminary study had some important limitations: because only a handful of patients were studied in each experimental group – most of which had recently been started on medication – replication in drug-free patients in substantially larger cohorts is envisaged. Additionally, since the approaches that could allow for clinical biomarking require a thorough follow-up to confirm their biomarker potential, some additional experiments have to be performed on considerably larger cohorts.

1.5.2. *Aims of the thesis*

The goal of this Master's thesis was to follow-up on the aforementioned explorative proof-of-concept study by Coppens and colleagues from SINAPS with the required experiments, eventually aiming to validate potential readily accessible diagnostic biomarkers. For this purpose, PBMC were collected from MDD and BD-D patients to be used for non-targeted LC-MS analysis. Our aim was to find proteins that are differentially expressed between MDD vs. BD-D on the one hand, and MDD and BD vs. controls on the other hand. The identified proteins could then potentially be further investigated in future experiments as to eventually develop a biomarker panel with high discriminatory capacity for distinguishing between MDD and BD-D patients.

1.5.3. *Alternative projects – contingency plans*

Preliminary results indicated our PBMC samples were of insufficient quality to perform reliable LC-MS-based proteomics (*see results section 3.1 and discussion section 4.1*). Therefore, the focus of the internship and thesis shifted to two parallel projects. SINAPS also investigates blood-based kynurenine pathway aberrations in psychiatric patients (van den Ameele et al., 2020; Morrens et al., 2020; De Picker et al., 2019; Hebbrecht et al., 2021). Recently, ELISAs have been developed to measure several kynurenine pathway metabolites. As the currently utilized methodologies for tryptophan metabolite quantification remain cumbersome, I performed exploratory experiments to investigate the validity of TRYCAT quantification by ELISA. Additionally, I got the opportunity to do a part of my internship at the Centre for Proteomics at the University of Antwerp Groenenborger Campus, where I joined in on an exploratory project focused on the isolation of neuronal extracellular vesicles (nEV) from plasma and their potential role in psychiatric disorders (Ilgın and Topuzoğlu, 2018; Vakili et al., 2020; Soares et al., 2021).

2. Methodologies

2.1. Discriminatory diagnostic biomarkers for MDD vs. BD-D using LC-MS

To achieve the abovementioned goals, a patient selection was already performed based on pre-specified inclusion and exclusion criteria. PBMC were collected in all patients over the past two years and during the internship. These PBMC samples were to be used for analysis by label-free LC-MS whereafter the results would have been analysed with various data analysis methods. Subsequently, the biomarker candidates would have been validated by immunoassays like ELISAs and Western blots, after which the fold change expressions and protein abundance would have been calculated (*Figure 3*). Unfortunately, due to problems with the PBMC samples, the last three steps in the experiment could not be completed and the project was temporarily discontinued.

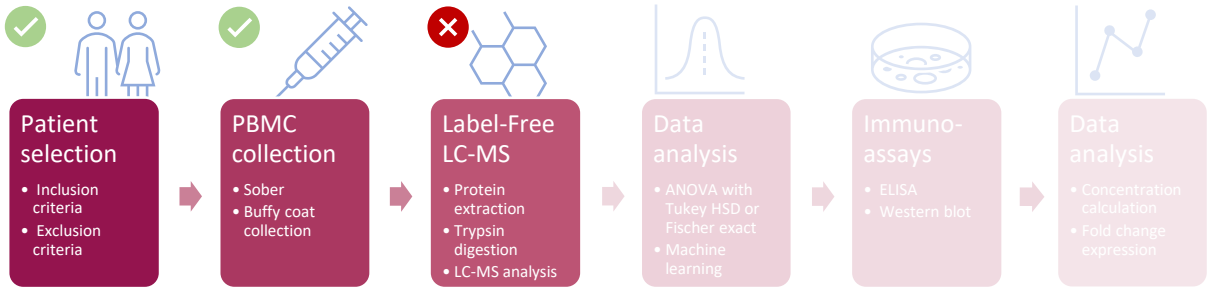

Figure 3 | **Schematic representation of the initial experimental setup.** Patient selection and PBMC collection were completed successfully, however the label-free LC-MS step could not be completed and the project was put on hold. PBMC: peripheral blood mononuclear cells; LC-MS: liquid chromatography-mass spectrometry; ELISA: enzyme-linked immune sorbent assay; HSD: honest significant differences.

2.1.1. *Study participant recruitment*

MDD patients (n=46), and BD patients in a depressive state (n=21) were recruited from the University Psychiatric Centre Duffel, as well 48 healthy controls (HCs) via advertising. Diagnoses were made according to the guidelines in the DSM-5 and confirmed by the Mini International Neuropsychiatric Interview (MINI). Inclusion criteria were: men and women between the ages of 18 and 55; and for MDD patients or BD patients in a depressed state, a Hamilton Depression Rating Scale (HDRS) score of ≥17. Exclusion criteria were: autoimmune diseases, a history or recent occurrence of chronic inflammatory disease, substance dependence in the last 6 months, and acute physical diseases. Additionally, exclusion criteria for HC were: a history of psychopathologies or having a first-degree relative with a history of psychiatric illness. Clinical scale assessments were performed by psychiatrists and trained personnel. All participants gave their written consent to partake in the study, which is approved by the local ethical committee.

2.1.2. *Collection of PBMC*

Venous blood was collected between 7h30 and 10h AM in patients that fasted overnight for at least 8 hours. 10mL whole blood was collected in 10mL K2-EDTA-coated collection tubes of which 5mL was used for PBMC isolation. 3,5mL of Histopaque-1077 (Sigma-Aldrich, REF 10771, UK) or Ficoll-Paque PLUS (Cytiva, REF 17-1440-03, Sweden) was carefully pipetted through the central hole of a 15mL SepMate tube (Stemcell Technologies, REF 85415, France). Keeping the SepMate tube vertical, 5mL whole blood was pipetted down the side of the tube, only mixing with the density gradient above the insert. The SepMate tube was centrifuged at 1200 x g for 10 minutes at room temperature, with the brake on. After centrifugation, some of the supernatant above the buffy coat was removed, leaving at least 0,5cm supernatant above the buffy coat. The remaining supernatant and buffy coat above the insert of the SepMate tube was poured into a new standard 15mL tube. The enriched PBMC were then washed with 6mL PBS pH 7,4 (Gibco, REF 10010-031, USA), mixed gently, and centrifuged at 300 x g for 8 minutes at room temperature, with the brake on. After centrifugation, the supernatant was removed by pouring and the pellet was resuspended in 1mL PBS. Another 5mL PBS was added, mixed

gently, and centrifuged again at 300 x g for 8 minutes at room temperature, with the brake on. After the second wash, the supernatant was discarded by pouring and the pellet was resuspended in 1mL PBS. The remaining solution (approximately 1,2mL) was split in three Eppendorf tubes, each containing approximately 400µL. The tubes were subsequently centrifuged at 400 x g for 5 minutes at room temperature, with the brake on. After centrifugation, the supernatant was removed carefully with a micropipette without touching the pellet, making the latter completely dry. Finally, the pellets in the Eppendorf tubes were stored at -80°C until further use.

2.1.3. *Quantitative proteomic analysis*

Before running the valuable patient and healthy control samples onto the LC-MS, the protocol was performed using preliminary test samples acquired using the same aforementioned protocol[1].

2.1.3.1. *Protein extraction*

The test PBMC samples were solubilized in 200µL Radio-Immunoprecipitation Assay (RIPA) buffer (Thermo Scientific, REF 89900, Rockford, Illinois, USA) in a LoBind Eppendorf tube, whereafter Halt Protease Inhibitor Single-Use Cocktail EDTA-free (Thermo Scientific, REF 78425, Rockford, Illinois, USA) and Halt Phosphatase Inhibitor Single-Use Cocktail (Thermo Scientific, REF 78428, Rockford, Illinois, USA) were added in a 1:100 volume ratio. All samples were then sonicated twice for 30 seconds and shaken on ice for at least 15 minutes. The lysates were subsequently centrifuged at 16 000 x g for 10 minutes at 4°C. Hereafter, the supernatant was transferred to a new LoBind Eppendorf tube, and again centrifuged at 16 000 x g for 10 minutes at 4°C. The supernatant was again collected in a new tube and used for concentration measurement.

2.1.3.2. *Concentration measurement*

A bicinchoninic acid (BCA) assay (Thermo Scientific, REF 23225, Rockford, Illinois, USA) was used to determine the total protein concentration in each sample. 5µL of all standards, buffer (reference), working reagent (blank), and each PBMC sample were pipetted onto a 96-well plate, whereafter 40µL working reagent was added to each well. The plate was shaken for 30 seconds, covered in tin foil, and put in the oven at 37°C for 30 minutes. After incubation, the plate was cooled to room temperature and the concentrations were measured with a NanoDrop 2000 spectrophotometer (Thermo Scientific, REF ND-2000, Rockford, Illinois, USA).

2.1.3.3. *In-solution digest*

After protein concentrations were determined, 10µg was taken from each sample, lengthened to a final concentration of 0,1% with 1% RapiGest SF (Waters, REF 186001861, Milford, Massachusetts, USA) and incubated for 5 minutes at 100°C. After incubation, the samples were cooled down and vortexed. Hereafter, a reduction was performed by adding 10mM (final concentration) tris(2-carboxyethyl)phosphine (TCEP [Sigma-Aldrich, REF C4706, USA]) and incubating for 1 hour at 55°C. After incubation, an alkylation was done by adding 19mM (final concentration) iodoacetamide (iodoacetamide [Sigma-Aldrich, REF I1149, USA] in 1.0M, pH 8,5 triethylammonium bicarbonate buffer [TEAB, Sigma-Aldrich, REF T7408, USA]) to each sample and incubating for 30 minutes in the dark at room temperature. Hereafter, 1mL pre-chilled (-20°C) acetone (Acros Organics by Thermo Fisher Scientific, REF 268310010, Geel, Antwerp, Belgium) was added to each sample and frozen overnight at -20°C. After overnight incubation, the samples were centrifuged at 10 000 x g for 15 minutes at 4°C, and carefully inverted to decant the acetone without disturbing the white pellet. Remaining acetone was carefully removed with a pipette without touching the pellet. The pellet was then resolved in 10µL 200mM TEAB, before adding 1/40 trypsin (Trypsin Gold MS Grade [Promega, REF V5280, USA] in mass grade water [BioSolve, REF 232141, France]) and incubating at 37°C overnight.

[1] The proteomic sample preparation and LC-MS run of the preliminary test samples was performed by the Centre for Proteomics before the start of the internship.

2.1.3.4. *Sample clean-up and LC-MS analysis*

The next day, samples were cleaned on Pierce C18 spin columns (Thermo Scientific, REF 89873, Rockford, Illinois, USA). First, the C18 cartridges were washed twice with 200µL activation buffer (50% acetonitrile [BioSolve, REF 012041, France] and 0,1% formic acid [BioSolve, REF 069141, France]), with centrifuging at 1 500 x g for 1 minute after each wash. After both washes with activation buffer, the cartridges were washed twice with 200µL equilibration buffer (5% acetonitrile and 0,1% formic acid), with centrifuging at 1 500 x g for 1 minute after each wash. Then, all samples were diluted in 400µL loading buffer (5% acetonitrile and 0,1% formic acid) and loaded onto the C18 columns. The cartridges were centrifuged at 1 500 x g for 1 minute, after which the remaining sample was loaded onto the cartridges and centrifuged again at the same conditions. Hereafter, the cartridges were washed twice with 200µL washing buffer (5% acetonitrile and 0,1% formic acid), with centrifuging at 1 500 x g for 1 minute after both washes. Finally, the proteins were eluted from the C18 spin column with 2 x 20µL elution buffer (70% acetonitrile and 0,1% formic acid), whereafter all LoBind Eppendorf tubes with the eluted peptides were placed in a Thermo Fisher Scientific Savant SpeedVac Vacuum Concentrator to dry down all peptides. This procedure was followed by loading 0,5µg of the samples onto the LC fractionation system, consisting of a µPAC C18 trapping column (PharmaFluidics, REF COL-trpnano 16G1B2, Zwijnaarde, Ghent, Belgium) and subsequently a 200cm µPAC C18 column (PharmaFluidics, REF COL-nano200G1B, Zwijnaarde, Ghent, Belgium). The latter was coupled online to a QExactive-Plus Orbitrap MS. The resulting test data was analysed by the MaxQuant Software (open source) and searched against the human UniProt/SwissProt database by using the Andromeda search engine.

2.2. Enzyme-linked immunosorbent assays for tryptophan and its metabolites

Unfortunately, the results of the test PBMC samples were unsatisfactory (*see section 3.1*), causing the initial experimental set-up to not be completed. Due to the severe haemoglobin contamination, an alternative was required to make use of these samples. Since targeted techniques like ELISAs are not influenced as much by the presence of high-abundant proteins, the already collected MDD and BD-D patient samples could possibly be used to determine concentrations of the TRYCAT metabolites and enzymes of the kynurenine pathway of the tryptophan metabolism. Given that there has been emerging evidence of altered tryptophan catabolite concentrations in plasma in patients with MDD (Liu et al., 2018), we wanted to test this hypothesis in PBMC. The catabolites of interest were tryptophan (TRP), kynurenine (KYN), kynurenic acid (KYNA), and quinolinic acid (QUIN), of which the concentrations were determined and analysed in test samples as a technical validation of the technique. In literature, ratios of the catabolites are used as proxy surrogate indicators of enzyme activity: [KYN]/[TRP] is often used as an indication of Indoleamine 2,3-dioxygenase (IDO) concentration (Suzuki et al., 2010; de Jong et al., 2011), [3-hydroxykynurenine (3-HK)]/[KYN] as an indication of Kynurenine 3-monooxygenase (KMO) concentration (Birner et al., 2017), and [KYNA]/[KYN] for the concentration of Kynurenine aminotransferase I (KAT/CCBL1) (Han et al., 2010; Quan et al., 2020). However, to our knowledge, there has been no clear confirmation on whether these catabolite ratios are reliable surrogate indicators of enzyme concentrations. Furthermore, nearly all studies concerning the kynurenine pathway have been performed on plasma, serum or whole blood. However, due to the rising evidence for the implication of PBMC in the pathophysiology of neuropsychiatric disorders, our focus was on the alterations of the aforementioned catabolites in PBMC. Eventually, if differential expression of certain catabolites or enzymes are found in MDD vs BD-D patients, a potential biomarker panel could possibly be established in the future. During the limited time span of the internship, only the catabolite ELISAs were performed, the enzyme ELISAs will be carried out at a later time.

2.2.1. *Sample collection*

In order to technically validate the acquired ELISA kits on PBMC, test blood samples from healthy volunteers were obtained. Even though the research is focused on the presence of tryptophan pathway catabolites and enzymes in PBMC, also plasma and serum samples were collected for an additional validation and comparison of the results.

2.2.1.1. *Plasma and serum*

For plasma collection, healthy volunteers were recruited in the morning and 10mL whole blood was collected in 10mL K2-EDTA-coated collection tubes (BD Vacutainer, REF 367525, UK). 5mL whole blood was used for PBMC isolation, the remaining 5mL in the EDTA-coated tube was centrifuged at 2000 x g for 10 minutes at 4°C, with the brake on. After centrifugation, the plasma was collected and stored in Eppendorf tubes at -80°C until further use. For serum collection, healthy volunteers were recruited in the morning and 2,5mL whole blood was collected in 2,5mL serum separator tubes (SSTs) II advance (BD Vacutainer, REF 366882, UK). The SST II advance tube was centrifuged at 2500 x g for 10 minutes at room temperature, with the brake on. After centrifugation, the serum was collected and stored in Eppendorf tubes at -80°C until further use.

2.2.1.2. *PBMC*

Healthy volunteers were recruited in the morning and 10mL whole blood was collected in 10mL K2-EDTA-coated collection tubes. 5mL whole blood was used for PBMC isolation, the remaining 5mL was used for plasma collection. 3,5mL of Histopaque-1077 (Sigma-Aldrich, REF 10771, UK) or Ficoll-Paque PLUS (Cytiva, REF 17-1440-03, Sweden) was carefully pipetted through the central hole of a 15mL SepMate tube (Stemcell Technologies, REF 85415, France). Keeping the SepMate tube vertical, 5mL whole blood was pipetted down the side of the tube, only mixing with the density gradient above the insert. The SepMate tube was centrifuged at 1200 x g for 10 minutes at room temperature, with the brake on. After centrifugation, some of the supernatant (will be referred to as gradient-residue plasma) above the buffy coat was removed, collected in Eppendorf tubes, and stored at -80°C until further use. The remaining supernatant and buffy coat above the insert of the SepMate tube was poured into a new standard 15mL tube. The enriched PBMC were then washed with 6mL PBS pH 7,4 (Gibco, REF 10010-031, USA), and centrifuged at 300 x g for 8 minutes at room temperature, with the brake on. After centrifugation, the supernatant was removed by pouring and the pellet was resuspended in 1mL PBS. Another 5mL PBS was added, mixed gently, and centrifuged again at 300 x g for 8 minutes at room temperature, with the brake on. After the second wash, the supernatant was discarded by pouring and the pellet was resuspended in 1mL PBS. The remaining solution (approximately 1,2mL) was split in three Eppendorf tubes, each containing approximately 400µL. The tubes were subsequently centrifuged at 400 x g for 5 minutes at room temperature, with the brake on. After centrifugation, the supernatant was removed carefully with a micropipette without touching the pellet, making the latter completely dry. Finally, the pellets in the Eppendorf tubes were stored at -80°C until further use.

2.2.2. *Sample preparation*

Before starting the ELISAs, sample preparation of the frozen PBMC samples was required. At least one day before performing the ELISA protocol, the frozen PBMC were brought to room temperature to thaw completely, and then stored at -80°C again to complete a freeze-thaw cycle to ensure full cell lysis. An hour before starting the ELISA protocols, the PBMC were again brought to room temperature and the dry pellet was resuspended in PBS pH 7,4. An alternative cell lysis protocol was used for the first two KYNA ELISAs[2]. The cells were acquired according to the aforementioned method, but the cell pellet was lysed in cell extraction buffer (Invitrogen by Thermo Fisher Scientific, REF FNN0011, Rockford, Illinois, USA), supplemented with 1mM phenylmethylsulfonyl fluoride (PMSF [Thermo Scientific, REF 36978, Rockford, Illinois, USA]) and protease inhibitor cocktail (Sigma-Aldrich, REF P2714, UK) for 30 minutes, on ice, with vortexing at 10 minute intervals. The cell extract was subsequently centrifuged at 13 000 rpm for 10 minutes at 4°C. The clear lysate was aliquoted to clean Eppendorf tubes and stored at -80°C until further use. Additionally, plasma, gradient-residue plasma (GR-plasma), and serum samples were thawed and brought to room temperature an hour before starting the ELISA protocols.

[2] This protocol was used only for the KYNA ELISAs performed on 21st of December 2020 and 21st of January 2021.

2.2.3. *Tryptophan and kynurenine pathway catabolites (TRYCAT) ELISAs*

In general, all ELISA kit reagents and samples were brought to room temperature and mixed gently by inversion before use. Repeated freezing and thawing of reagents and samples was avoided. All dilutions or reconstitutions were performed with ultra-pure water. Once an ELISA had been started, all steps were completed without interruption.

2.2.3.1. *Tryptophan (TRP)*

To detect the amount of tryptophan in our samples, the BA-E-2700 ELISA kit from ImmuSmol was used. This kit has been optimized for detection of tryptophan in urine, serum and plasma samples, and is not guaranteed to work on PBMC. Therefore, a technical validation of the kit on test samples of PBMC was required. For plasma and serum, haemolytic and especially lipemic samples should not be used. 20µL of all standards, controls and samples were pipetted into standard polypropylene tubes, whereafter 200µL of PBS (ImmuSmol, REF BA-E-2788, Bordeaux, France) was added to each tube. Subsequently, 25µL precipitating reagent (ImmuSmol, REF BA-E-2721, Bordeaux, France) was added and all tubes were vortexed thoroughly and centrifuged for 15 minutes at 3000 x g. 25µL of the resulting clear supernatant was used for the derivatization and thus pipetted into the appropriate wells of the kit's reaction plate (ImmuSmol, REF BA-D-0024, Bordeaux, France). Then, 50µL of equalizing reagent (prepared by adding 12,5mL of assay buffer [ImmuSmol, REF BA-E-2413, Bordeaux, France] to the lyophilized equalizing reagent [ImmuSmol, REF BA-E-2428, Bordeaux, France] and storing the reconstituted equalizing reagent in aliquots for max. 1 month at -20°C) was pipetted into all wells, whereafter 10µL of D-reagent (ImmuSmol, REF BA-E-2446, Bordeaux, France) was added. The plate was then covered with adhesive foil and incubated for 2 hours at room temperature on a shaker at approximately 600rpm. After the incubation, 100µL of Q-buffer (ImmuSmol, REF BA-E-2458, Bordeaux, France) was pipetted into all wells, followed by a 10 minute incubation at the same conditions as the previous incubation step. After 10 minutes, 25µL of all well volumes was pipetted into their respective wells on the tryptophan microtiter strips (ImmuSmol, REF BA-E-2731, Bordeaux, France). Next, 50µL of the tryptophan antiserum (ImmuSmol, REF BA-E-2710, Bordeaux, France) was added to all wells and mixed. The plate was then covered with clean adhesive foil and incubated for 15-20 hours (overnight) at 2-8°C. After the overnight incubation, the foil was removed and the content of the wells was discarded. The plate was washed three times by adding 300µL of prepared ELISA wash buffer (2mL wash buffer concentrate (50X) [ImmuSmol, REF BA-E-0030, Bordeaux, France] diluted to a final volume of 100mL with ultra-pure water), the content was discarded and blotted dry after each wash by tapping the inverted plate on absorbent material. Subsequently, 100µL of the enzyme conjugate (ImmuSmol, REF BA-E-0040, Bordeaux, France) was pipetted into all wells and the plate was incubated for 30 minutes on a shaker at approximately 600rpm. After incubation, the contents of the wells were discarded and the plate was washed again three times by adding 300µL of the previously prepared ELISA wash buffer, while discarding the contents and blotting dry after each washing step by tapping the inverted plate on absorbent material. Then, 100µL of substrate (ImmuSmol, REF BA-E-0055, Bordeaux, France) was added to all wells and the plate was incubated for 25 minutes at room temperature on a shaker at approximately 600rpm. Direct exposure to sunlight was avoided. Immediately after incubation, 100µL of stop solution (ImmuSmol, REF BA-E-0080, Bordeaux, France) was pipetted into each well and the plate was shaken briefly to ensure a homogeneous distribution of the solution. The absorbance of the solution in the wells was read within 10 minutes of adding the stop solution, using a microplate reader set to 450nm.

2.2.3.2. *Kynurenine (KYN)*

For the kynurenine ELISA, the BA-E-2200 ELISA kit from ImmuSmol was used. This kit has been optimized for detection of L-kynurenine in serum and plasma samples, and is not guaranteed to work on PBMC. Therefore, a technical validation of the kit on test samples of PBMC was required. Before starting the protocol, the incubator was preheated to 37°C. 10µL of all standards, controls and samples were pipetted into the appropriate wells of the microtiter plate (ImmuSmol, REF BA-D-0032, Bordeaux,

France). Subsequently, 250µL of acylation buffer (ImmuSmol, REF BA-E-2211, Bordeaux, France) was added to all wells, whereafter 25µL of acylation reagent (ImmuSmol, REF BA-E-2212, Bordeaux, France) was added and the plate was mixed shortly. The microtiter plate was covered with adhesive foil and incubated for 90 minutes at 37°C. After this incubation period, 20µL of all well volumes was pipetted into their respective wells on the kynurenine microtiter strips (ImmuSmol, REF BA-E-2231, Bordeaux, France) and placed on a new plate. Next, 50µL of the kynurenine antiserum (ImmuSmol, REF BA-E-2210, Bordeaux, France) was added to all wells and mixed. The plate was then covered with clean adhesive foil and incubated for 15-20 hours (overnight) at 2-8°C. After the overnight incubation, the foil was removed and the content of the wells was discarded. The plate was washed four times by adding 300µL of prepared ELISA wash buffer (2mL wash buffer concentrate (50X) [ImmuSmol, REF BA-E-0030, Bordeaux, France] diluted to a final volume of 100mL with ultra-pure water), the content was discarded and blotted dry after each wash by tapping the inverted plate on absorbent material. Subsequently, 100µL of the enzyme conjugate (ImmuSmol, REF BA-E-0040, Bordeaux, France) was pipetted into all wells and the plate was incubated for 30 minutes on a shaker at approximately 600rpm. After incubation, the contents of the wells were discarded and the plate was washed again four times by adding 300µL of the previously prepared ELISA wash buffer, while discarding the contents and blotting dry after each washing step by tapping the inverted plate on absorbent material. Then, 100µL substrate (ImmuSmol, REF BA-E-0055, Bordeaux, France) was added to all wells and the plate was incubated for 25 minutes at room temperature on a shaker at approximately 600rpm. Direct exposure to sunlight was avoided. Immediately after incubation, 100µL stop solution (ImmuSmol, REF BA-E-0080, Bordeaux, France) was pipetted into each well and the plate was shaken briefly to ensure a homogeneous distribution of the solution. The absorbance of the solution in the wells was read within 10 minutes of adding the stop solution, using a microplate reader set to 450nm.

2.2.3.3. *Kynurenic acid (KYNA)*

For the detection and measurement of kynurenic acid in our samples, the IS-I-0200 ELISA kit from ImmuSmol was used. This kit has been optimized for detection of kynurenic acid in serum samples, and is not guaranteed to work in plasma or PBMC samples. Therefore, a technical validation of the kit on test samples of plasma and PBMC was required. 50µL of all standards, controls and samples were pipetted into the appropriate wells of the kit's extraction plate (ImmuSmol, REF BA-R-8318, Bordeaux, France). Subsequently, 25µL of the extraction reagent (ImmuSmol, REF IS-I-0212, Bordeaux, France) was pipetted into all wells, whereafter the plate was covered with adhesive foil and incubated for 1 hour at room temperature on a shaker at approximately 500rpm. During the incubation period, the incubator was preheated to 37°C. After 1 hour of incubation, the foil was removed and the contents of the wells were discarded. The extraction plate was washed once by adding 300µL of extraction wash buffer (ImmuSmol, REF IS-I-0213, Bordeaux, France) to each well, discarding the content of the wells and blotting dry by tapping the inverted plate on absorbent material. After washing, 140µL of the acylation reagent (prepared by reconstituting 1 vial of lyophilized acylation reagent [ImmuSmol, REF IS-I-0215, Bordeaux, France] – just before use – with 15mL of acylation buffer [ImmuSmol, REF BA-E-2211, Bordeaux, France]) was pipetted into all wells and mixed shortly. Hereafter, the plate was covered with adhesive foil and incubated for 90 minutes at 37°C. After this incubation period, the wells were stirred on a shaker for 2 minutes at 500rpm to homogenize the medium before pipetting the contents. Then, 50µL of all well volumes was pipetted into their respective wells on the kynurenic acid microtiter strips (ImmuSmol, REF IS-I-0231, Bordeaux, France) and placed on a new plate. Next, 100µL of the kynurenic acid antiserum (prepared by mixing equal volumes (1:1) of kynurenic acid antiserum concentrate (2X) [ImmuSmol, REF IS-I-0210, Bordeaux, France] with kynurenic acid antiserum diluent [ImmuSmol, REF IS-I-0211, Bordeaux, France] in a standard polypropylene tube) was added to all wells and mixed shortly. The plate was then covered with clean adhesive foil and incubated for 15-20 hours (overnight) at 2-8°C. After the overnight incubation, the foil was removed and the content of the wells was discarded. The plate was washed four times by adding 300µL of prepared ELISA wash buffer (2mL wash buffer concentrate (50X) [ImmuSmol, REF BA-E-0030, Bordeaux, France] diluted to a final volume

of 100mL with ultra-pure water), the content was discarded and blotted dry after each wash by tapping the inverted plate on absorbent material. Subsequently, 100µL of the enzyme conjugate (ImmuSmol, REF BA-E-0040, Bordeaux, France) was pipetted into all wells and the plate was incubated for 30 minutes on a shaker at approximately 500rpm. After incubation, the contents of the wells were discarded and the plate was washed again four times by adding 300µL of the previously prepared ELISA wash buffer, while discarding the contents and blotting dry after each washing step by tapping the inverted plate on absorbent material. Then, 100µL substrate (ImmuSmol, REF BA-E-0055, Bordeaux, France) was added to all wells and the plate was incubated for 25 minutes at room temperature on a shaker at approximately 500rpm. Direct exposure to sunlight was avoided. Immediately after incubation, 100µL stop solution (ImmuSmol, REF BA-E-0080, Bordeaux, France) was pipetted into each well and the plate was shaken briefly to ensure a homogeneous distribution of the solution. The absorbance of the solution in the wells was read within 10 minutes of adding the stop solution, using a microplate reader set to 450nm.

2.2.3.4. *Quinolinic acid (QUIN)*

Finally, for the measurement of quinolinic acid concentration in our samples, the IS-I-0100 ELISA kit from ImmuSmol was used. This kit has been optimized for detection of quinolinic acid in serum samples, and is not guaranteed to work in plasma or PBMC samples. Therefore, a technical validation of the kit on test samples of plasma and PBMC was required. Before starting the protocol, the incubator was preheated to 37°C. 25µL of all standards, controls and samples were pipetted into the appropriate wells of the kit's reaction plate (ImmuSmol, REF IS-I-0324, Bordeaux, France), whereafter 25µL of reaction diluent (ImmuSmol, REF IS-I-0128, Bordeaux, France) was added into all wells and mixed shortly. Subsequently, 100µL of the acylation reagent (prepared by reconstituting 1 vial of lyophilized acylation reagent [ImmuSmol, REF IS-I-0115, Bordeaux, France] – just before use – with 12mL of acylation buffer [ImmuSmol, REF BA-E-2211, Bordeaux, France]) was pipetted into all wells and again mixed shortly. Then, the plate was covered with adhesive foil and incubated for 2 hours at 37°C. After this incubation period, the wells were stirred on a shaker for 2 minutes at 500rpm to homogenize the medium before pipetting the contents. Then, 40µL of all well volumes was pipetted into their respective wells on the quinolinic acid microtiter strips (ImmuSmol, REF IS-I-0131, Bordeaux, France) and placed on a new plate. Next, 50µL of the quinolinic acid antiserum (prepared by mixing equal volumes (1:1) of quinolinic acid antiserum concentrate (2X) [ImmuSmol, REF IS-I-0110, Bordeaux, France] with quinolinic acid antiserum diluent [ImmuSmol, REF IS-I-0111, Bordeaux, France] in a standard polypropylene tube) was added to all wells and mixed shortly. The plate was then covered with clean adhesive foil and incubated for 15-20 hours (overnight) at 2-8°C. After the overnight incubation, the foil was removed and the content of the wells was discarded. The plate was washed four times by adding 300µL of prepared ELISA wash buffer (2mL wash buffer concentrate (50X) [ImmuSmol, REF BA-E-0030, Bordeaux, France] diluted to a final volume of 100mL with ultra-pure water), the content was discarded and blotted dry after each wash by tapping the inverted plate on absorbent material. Subsequently, 100µL of the enzyme conjugate (ImmuSmol, REF BA-E-0040, Bordeaux, France) was pipetted into all wells and the plate was incubated for 30 minutes on a shaker at approximately 500rpm. After incubation, the contents of the wells were discarded and the plate was washed again four times by adding 300µL of the previously prepared ELISA wash buffer, while discarding the contents and blotting dry after each washing step by tapping the inverted plate on absorbent material. Then, 100µL substrate (ImmuSmol, REF BA-E-0055, Bordeaux, France) was added to all wells and the plate was incubated for 25 minutes at room temperature on a shaker at approximately 500rpm. Direct exposure to sunlight was avoided. Immediately after incubation, 100µL stop solution (ImmuSmol, REF BA-E-0080, Bordeaux, France) was pipetted into each well and the plate was shaken briefly to ensure a homogeneous distribution of the solution. The absorbance of the solution in the wells was read within 10 minutes of adding the stop solution, using a microplate reader set to 450nm.

2.2.4. *Data processing and analysis*

2.2.4.1. *Calculation of metabolite concentrations*

The ELISA results were calculated according to the manufacturer's instructions, being the same for tryptophan and kynurenine, and for kynurenic and quinolinic acid, respectively. For tryptophan and kynurenine, a calibration curve was obtained by calculating the mean absorbances (optical densities or ODs) of all standards and plotting them on the y-axis against the corresponding logarithmic standard concentrations on the x-axis. For kynurenic acid and quinolinic acid, a calibration curve was obtained by calculating the mean absorbances of all standards and then determining the B/B_0 values for each standard. These B/B_0 values were then plotted on the y-axis against the corresponding logarithmic standard concentrations on the x-as. For all four ELISAs, linear regression was used for the curve fitting and the subsequent calculation of the sample concentrations.

2.2.4.2. *Statistical analysis*

Because the ELISAs were performed primarily for technical validation of the kits on a qualitative level, coefficients of determination (R^2s) and coefficients of variation (CVs) were calculated to analyse the precision and repeatability of the assays. Additionally, F-tests and unpaired student's t-tests were performed to assess the significance of the variance in the data and whether or not differences between normal plasma and GR-plasma on the one hand, and plasma and serum on the other hand, were significant or not. Furthermore, with an eye to waste-reduction purposes in future assays, the correlation between normal plasma and GR-plasma was determined by calculating the coefficient of determination and the Pearson's coefficient of correlation.

2.3. Proteomic analysis of extracellular vesicles isolated from plasma

Since the results of the proteomic analysis of our test PBMC samples were unsatisfactory and intercepted the continuation of the PBMC project, the Centre for Proteomics offered the possibility to join in on an ongoing PhD project by Yael Hirschberg as to still gain experience in proteomic sample preparation and LC-MS analysis. In this project, neuron-derived EVs were isolated from plasma using size exclusion chromatography and a mouse anti-human CD171 biotinylated antibody (L1CAM, L1 Cell Adhesion Molecule). Then, a sample preparation for proteomic analysis was performed, whereafter proteomic techniques like silver staining, Western blot, and LC-MS were carried out, as well as a Nanoparticle Tracking Analysis (NTA). If the isolation of nEVs from plasma samples is successful, the same protocols could be used at SINAPS to isolate nEVs from patient and healthy control plasma samples, to eventually start a new project focused on the discovery of differential biomarkers within these nEVs.

2.3.1. *Neuronal extracellular vesicle isolation from plasma*

2.3.1.1. *Plasma collection and processing*

Five healthy volunteers were recruited in the morning and 20mL whole blood was collected per person in two 10mL K2-EDTA-coated collection tubes (BD Vacutainer, REF 367525, UK) for a total of 100mL whole blood. The EDTA-coated tubes were centrifuged at 2000 x g for 10 minutes at 4°C, with the brake on. After centrifugation, approximately 45mL plasma was collected and stored in 90 aliquots of 500µL in 1,5mL LoBind Eppendorf tubes (Eppendorf, REF 0030108442, Germany) at -80°C until further use.

For each isolation experiment, four aliquots of previously collected plasma were thawed and brought to room temperature. Next, one tablet of cOmplete Protease Inhibitor Cocktail (Roche Applied Sciences, REF 11697498001, Indianapolis, Indiana, USA) was solubilized in 500µL ultra-pure water, of which 5µL was added to each plasma aliquot (one tablet can be used for 50mL solution, so a 1/100 dilution was required for 500µL plasma sample). Subsequently, one tablet of Pierce Phosphatase Inhibitor Mini Tablets (Thermo Scientific, REF A32957, Rockford, Illinois, USA) was solubilized in 500µL ultra-pure water, of which 25µL was added to each plasma aliquot (one tablet can be used for 10mL solution, so a 1/20 dilution was required for 500µL plasma sample). The aliquots were vortexed thoroughly and centrifuged at 1500 x g for 20 minutes at room temperature. Only the supernatant was used in the following steps.

2.3.1.2. *Size exclusion chromatography (SEC)*

For the size exclusion chromatography or SEC, Izon's qEVoriginal 35nm SEC columns (Izon Science Ltd., New Zealand) were used. Particles loaded on the SEC column are separated based on their size by the porous, polysaccharide resin. Smaller particles become trapped in the pores, which delays their exit from the column. First, the column was rinsed with 15mL PBS (Gibco, REF 21600-010, USA), whereafter 500µL of the first plasma aliquot was loaded on the column. Since the column should never be dry, PBS filtered with Millex Syringe Filter Unit, 0,22µm (Millipore, REF SLGP033RS, Darmstadt, Hessen, Germany) was loaded onto the column repeatedly during the whole process. Subsequently, fractions of 500µL were collected, of which the first 3mL (fractions 1-6) were void and fractions 7-9 were EVs. Fraction 8 contains the highest concentration of EVs (approximately 1.7 EVs/mL x 10^{10}, according to the manufacturer) and was used in the following steps. This process was repeated for a second plasma aliquot, the other two were not loaded on the SEC column and were thus not purified before further use.

2.3.1.3. *Bead preparation*

For the immunoprecipitation of our nEVs, magnetic streptavidin beads were used, which were later linked to biotinylated L1CAM antibody, or biotin only for the negative control samples. The beads used for the isolation were Dynabeads M-270 Streptavidin 10mg/mL (Invitrogen by Thermo Fisher Scientific, REF 65306, Norway), which were resuspended and vortexed before use. Next, 6 x 150µL beads (9mg/900µL beads, 4 x 1,5mg beads per sample + 2 x 1,5mg beads for the pre-clearance step[3]) were transferred to four new 1,5mL LoBind Eppendorf tubes and placed on a magnet. The beads were allowed to collect at the tube wall for 1 minute, whereafter the supernatant was removed. Then, the beads were washed three times with 1mL of PBS and mixed by vortexing. Between each wash, the tubes were placed on a magnet, and the beads were allowed to collect at the tube wall for 1 minute, whereafter the supernatant was removed.

2.3.1.4. *Binding biotinylated antibody to beads*

For the antibody binding, biotinylated mouse anti-human CD171/L1CAM antibody 0,5mg/mL (clone eBio5G3, eBioscience, San Diego, California, USA) was used. 2 x 15µg (= 2 x 30µL) anti-L1CAM antibody (1mg Dynabeads binds 10µg biotinylated antibody, 15µg antibody for 1,5mg beads per sample) in 270µL PBS was added to two of the tubes with beads and incubated for 1 hour on a shaker. The other four tubes with beads were incubated with biotin only, and were used as negative controls (C, D) and pre-clearance beads (pc-EV, pc-plasma) (*Table 2*). After the incubation period, the beads were washed three times with 1mL PBS – 0,1% BSA (Sigma-Aldrich, REF A9418, USA) and mixed by inversion. The tubes were placed on a magnet, and the beads were allowed to collect at the tube wall for 1 minute, whereafter the supernatant was removed. Then, the beads were washed once more with 1mL PBS, after which the tubes were placed on a magnet and the beads were again allowed to collect at the tube wall for 1 minute, whereafter the supernatant was removed. The six tubes with beads (two bound to biotinylated antibody, four bound to biotin only) were stored in 100µL PBS until further use.

2.3.1.5. *Affinity purification*

Before starting the purification of the EVs, a pre-clearance step of the plasma samples was performed to prevent non-specific binding to the antibody-conjugated beads[3]. Both plasma EV fraction aliquots were added to the pc-EV biotinylated beads, while both non-purified plasma aliquots were added to the pc-plasma biotinylated beads and incubated for 30 minutes. Then, 500µL pre-cleared (EV) plasma was added to each tube containing 1,5mg beads (A, B, C and D) according to the scheme as seen in *Table 2*. Each tube was subsequently incubated for 30 minutes at 4°C on a shaker. After incubation, all four tubes were placed on a magnet, and the beads were allowed to collect at the tube wall for 1 minute, whereafter the supernatant was removed. Next, all tubes were washed twice with 400µL wash buffer 1 (PBS – 0,1% IGEPAL CA-630 [Sigma-Aldrich, REF I8896, USA]) and brought to a new 1,5 LoBind

[3] The pre-clearance step was added only after the first run showed unsatisfactory results (*see results section 3.3*).

Eppendorf tube after the first wash. All tubes were then placed on a magnet, and the beads were allowed to collect at the tube wall for 1 minute, whereafter the supernatant was removed. Hereafter, all tubes were washed once with 400µL wash buffer 2 (PBS + 220mM NaCl [PanReac AppliChem ITW Reagents, REF A70006, Germany]), placed on a magnet, and the supernatant was again removed after allowing the beads to collect at the tube wall for 1 minute. Then, all tubes were washed one more time with 400µL wash buffer 3 (50mM Tris pH 7,5 [PanReac AppliChem ITW Reagents, REF A4263, Germany]) and brought to a clean 1,5mL LoBind Eppendorf tube after thorough resuspension. The tubes were again placed on a magnet, and the beads were allowed to collect at the tube wall for 1 minute, whereafter the supernatant was removed. Finally, a first elution was collected after adding 50µL 0,2M glycine pH 2 (Alfa Aesar, REF J61855, UK), incubating for 5 minutes and bringing the supernatant to a new 1,5mL LoBind Eppendorf tube. A second elution was also collected to make sure all beads were clean, again adding 50µL 0,2M glycine pH 2 and bringing the supernatant to a new 1,5mL LoBind Eppendorf tube. Of each of the eight 50µL elutions, 20µL was brought to new LoBind Eppendorf tubes to be used for the sample preparation for proteomic analysis. To the remaining 30µL, 270µL Tris pH 7,5 buffer[4] was added to keep the EVs in ideal conditions (pH between 6 and 9) for NTA with ZetaView. All tubes were subsequently stored at -20°C until further use.

Table 2 | **Scheme of the plasma/beads combinations per sample.**

SAMPLE	CONTENTS
A (+/+)	EV fraction (SEC) + L1CAM-biotin complex
B (-/+)	Non-purified plasma + L1CAM-biotin complex
C (+/-)	EV fraction (SEC) + biotin only
D (-/-)	Non-purified plasma + biotin only
pc-EV	Pre-clearance beads (biotin only) for EV fraction (Samples A+C)
pc-plasma	Pre-clearance beads (biotin only) for non-purified plasma (Samples B+D)

2.3.2. *Sample preparation for proteomic analysis*

Now the EVs were isolated, the 20µL elution samples were prepared for proteomic analysis on the mass spectrometer, but also for a silver staining and Western blot. For this purpose, the S-trap micro spin column digestion protocol (Protifi LLC, Farmingdale, New York, USA) was used.

2.3.2.1. *Solubilization, reduction & alkylation*

First, all eight 20µL elution samples were thawed and brought to room temperature. During the first sample preparation, 5µL 10% SDS (Sigma-Aldrich, REF L3771, USA) was added to each 20µL elution to solubilize the samples. All samples were then placed in a bath sonicator for at least 15 minutes, before being placed individually under an ultrasonic probe sonicator for 50 seconds in 10 second intervals and cooled on ice in-between sessions. During sonication, elution A_1 was lost due to burning through the bottom of the tube. From elutions A_2, B_1, C_1, and D_1, 5µL was taken for silver staining, whereafter elutions B_1 and B_2, C_1 and C_2, and D_1 and D_2 were pooled. Then, a reduction was performed by adding 0,87µL tris(2-carboxyethyl)phosphine (TCEP [Sigma-Aldrich, REF C4706, USA]) to elution's A_2 LoBind Eppendorf tube (1/23 of initial sample volume of 20µL) and 1,96µL TCEP to samples B_{1+2}, C_{1+2}, and D_{1+2} (1/23 of initial sample volume of 45µL). All tubes were then incubated for 15 minutes at 55°C. This incubation was followed by an alkylation by adding 0,87µL iodoacetamide (0,018g iodoacetamide [Sigma-Aldrich, REF I1149, USA] in 100µL 100mM ammonium bicarbonate [Sigma-Aldrich, REF 09830, USA]) to sample A_2 (1/23 of initial sample volume of 20µL) and 1,96µL iodoacetamide to pooled samples B, C, and D (1/23 of initial sample volume of 45µL). All samples were then incubated for 30 minutes in the dark at room temperature. After incubation, 2,2µL 12% phosphoric acid (BioSolve, REF 161605, France) was added to sample A_2 (1/10 of initial sample volume + added TCEP and iodoacetamide volumes of 21,74µL) and 4,9µL 12% phosphoric acid to samples B, C, and D (1/10 of

[4] During the first isolation, a PBS – 2% BSA – 0,1% Tween-20 (Sigma-Aldrich, REF P1379, USA) buffer was used, but this showed unsatisfactory ZetaView results (*see results section 3.3.1*).

initial sample volume + added TCEP and iodoacetamide volumes of 48,92µL) to ensure complete denaturation of proteins and achieve a pH of ≤1.

During the second sample preparation[5], first 5µL was taken from each 20µL elution for silver staining and prepared according to the same protocol. Of the remaining 15µL samples, elution 1 and 2 were constituted in one LoBind Eppendorf tube, leading to four samples of 30µL. Of each sample, 10µL was brought to a new LoBind Eppendorf tube, whereafter 3µL 10% SDS was added to solubilize the samples. All samples were then placed in a bath sonicator for at least 15 minutes, before being placed individually under an ultrasonic probe sonicator for 50 seconds in 10 second intervals and cooled on ice in-between sessions. After thorough sonication, a reduction was performed by adding 0,57µL TCEP to each LoBind Eppendorf tube (1/23 of initial sample volume of 13µL) and incubated for 15 minutes at 55°C. Then, an alkylation was done by adding 0,57µL iodoacetamide (0,018g iodoacetamide in 100µL 100mM ammonium bicarbonate) to each sample (1/23 of initial sample volume of 13µL) and incubated for 30 minutes in the dark at room temperature. After incubation, 1,4µL 12% phosphoric acid (1/10 of initial sample volume + added TCEP and iodoacetamide volumes of 14,14µL) was added to each tube to ensure complete denaturation of proteins and achieve a pH of ≤1.

2.3.2.2. *Trap proteins*

To sample A_2 of the first sample preparation, 144µL (6 times the total volume of the sample of 24µL) of binding/wash buffer (100mM triethylammonium bicarbonate (TEAB [Sigma-Aldrich, REF T7408, USA]) in 90% methanol [BioSolve, REF 136841, France]) was added, to pooled samples B, C, and D, 324µL binding buffer was added (6 times the total volume of the sample of 54µL). To each sample of the second sample preparation, 93µL of binding/wash buffer was added (6 times the total volume of the sample of 15,5µL). All samples were vortexed thoroughly. The S-traps micro columns (Protifi LLC, REF C02-micro, Farmingdale, New York, USA) were then placed into four new 2ml Eppendorf tubes for waste flow through, whereafter all samples were loaded onto their respective S-trap columns. All four S-trap columns were subsequently centrifuged at 4000 x g for 30 seconds to trap the proteins.

2.3.2.3. *Clean proteins*

After the initial centrifugation step, 150µL binding/wash buffer was added to each S-trap micro column and centrifuged at 4000 x g for 30 seconds. This washing step was performed five times in total, while discarding the waste contents of the 2mL Eppendorf tube in-between washing steps. Additionally, between each centrifugation, the S-trap micro units were rotated 180 degrees to ensure the spin columns did experience a homogenous flow when using a fixed-angle rotor. After five washes, the S-trap columns were centrifuged once more at 4000 x g for 1 minute to fully remove all binding/wash buffer. Then, each S-trap micro column was transferred to a clean 2mL LoBind Eppendorf tube for the protein digestion.

2.3.2.4. *Incubate and digest proteins*

Protein digestion was performed by adding 20µL digestion buffer (1µL 1µg/µL trypsin [100µL Trypsin Gold MS Grade (Promega, REF V5280, USA) in 100µL mass grade water (BioSolve, REF 232141, France)] in 19µL 50mM TEAB per sample, 1µg trypsin per sample) to each S-trap micro column. It was visually confirmed no air bubbles were present at the top of the S-trap to ensure the digestion buffer could enter the trap. All S-traps were capped loosely (not airtight) to limit loss by evaporation and ensure the solution was not forced out of the S-trap during incubation. All samples were then incubated overnight at 37°C on a wet paper towel in a plastic bag to saturate the air with water vapor and thus limit evaporation.

[5] In the LC-MS results of the first run, concentrations turned out to be too high (*see results section 3.3.4*), which lead us to perform a second sample preparation using a smaller amount of material.

2.3.2.5. *Elute peptides for analysis*

After overnight incubation, 40µL of elution buffer 1 (50mM TEAB in water) was added to all S-traps containing the digestion buffer and centrifuged at 4000 x g for 1 minute. Hereafter, 40µL of elution buffer 2 (0,2% formic acid [BioSolve, REF 069141, France] in mass grade water) was added to all S-trap columns and again centrifuged at 4000 x g for 1 minute. Then, 40µL of elution buffer 3 (50% acetonitrile [BioSolve, REF 012041, France] in mass grade water) was added onto the S-trap micro columns and again centrifuged at 4000 x g for 1 minute. All LoBind Eppendorf tubes with the eluted peptides were then placed in a Thermo Fisher Scientific Savant SpeedVac Vacuum Concentrator to dry down all eluted peptides.

2.3.3. *Nanoparticle Tracking Analysis*

The ZetaView (Particle Metrix, Germany) is an instrument used for Nanoparticle Tracking Analysis (NTA) and measures hydrodynamic particle size, zeta potential and concentration based on the Brownian motion of these particles. Based on the diffusion movements of the particles in the sample, the hydrodynamic diameter of the particles can be determined. All these parameters can then be used to distinguish sub-populations of particles such as EVs. The particles are visualized by the scattering of light from a laser beam, which is recorded by a camera.

2.3.3.1. *Scatter mode*

In ZetaView's scatter mode, all particles in the sample are measured. This gives a general idea of the amount of particles present in the sample, without specifying what kind of particles. In scatter mode, 160µL of the initial 600µL of each EV sample (elution 1 and 2) was diluted with 640µL filtered PBS for a 1/5 dilution of the sample. Then, all samples were injected with a syringe into the ZetaView for analysis in scatter mode.

2.3.3.2. *Fluorescence mode*

In fluorescence mode, a labelled antibody is added to each sample, which makes it possible to look at specific predefined particles in the sample. The antibody that was added to specifically look at EVs is CellMask Green Plasma Membrane Stain (CMG [Invitrogen by Thermo Fisher Scientific, REF C37608, Rockford, Illinois, USA]), which colours lipid membranes. However, not only EVs were characterized this way, but also *e.g.* lipoproteins (HDL, LDL) which are a frequent contamination of EV samples. Even though fluorescence mode gives thus a more specific view of the sample, contaminations may still cause it to be a more general view. For fluorescence mode, a 1/2 dilution was made for samples A and B by adding 1µL CMG (already a 1/100 dilution) to 400µL sample, incubating for 1 hour in the dark at room temperature, and adding 400µL filtered PBS, resulting in an optimal dilution to avoid getting noise signal from the antibody. Additionally, a 1/3 dilution was made for samples C and D by adding 1µL CMG (already a 1/100 dilution) to 300µL sample, incubating for 1 hour in the dark at room temperature, and adding 600µL filtered PBS. Then, all samples were injected with a syringe into the ZetaView for analysis in fluorescence mode.

2.3.4. *SDS-PAGE*

SDS-PAGE polyacrylamide gels were prepared for respective analysis by silver staining and Western blot. First, the loading buffer was prepared by adding 100µL β-mercaptoethanol (Bio-Rad, REF 1610710, Hercules, California, USA) to 900µL 4x Laemmli sample buffer (Bio-Rad, REF 1610747, Hercules, California, USA) under a laminar airflow cabinet and vortexing thoroughly. Then, the samples were prepared by taking 5µL of each sample and adding 32,5µL PBS and 12,5µL loading buffer (4x dilution), whereafter each sample was vortexed thoroughly and heated for 5 minutes at 95°C. In the meantime, the Mini-PROTEAN TGX Stain-Free 4-20% Precast gel (Bio-Rad, REF 4568094, Hercules, California, USA) was prepared and the Mini-PROTEAN Tetra Vertical Electrophoresis Cell (Bio-Rad, REF 1658004, Hercules, California, USA) was assembled according to the manufacturer's instructions. The holder and cell were filled with previously prepared SDS-PAGE running buffer (100mL 10x Tris/Glycine/SDS [Bio-Rad, REF 1610732, Hercules, California, USA] in 900mL ultra-pure water). After

the samples were heated, they were loaded into their respective slots in the gel, as well as 3µL of a Precision Plus Western C Protein Standard ladder (Bio-Rad, REF 1610376, Hercules, California, USA) for reference. For the Western blot, EVs extracted from a human lung epithelial control cell line NCI-H1975 (American Type Culture Collection, REF CRL-5908, Manassas, Virginia, USA) were loaded onto the gel as well. The gel was ran for 32 minutes at 200V and 35mA until visual confirmation that the blue dye had reached the bottom of the gel. The gel was then carefully removed from the holder and used for silver staining or Western blot.

2.3.4.1. *Silver staining*

For the silver staining, the Pierce Silver Stain Kit for Mass Spectrometry (Thermo Scientific, REF 24600, Rockford, Illinois, USA) was used. First, the polyacrylamide gel was placed in a clean plastic staining tray, which was gently being shaken during the whole procedure. The gel was first washed twice in ultra-pure water for 5 minutes, replacing the water in-between the two washes. Then, the gel was fixed in fixing solution consisting of 30% ethanol and 10% acetic acid in water (7,5mL ethanol [BioSolve, REF 052541, France], 2,5mL acetic acid [BioSolve, REF 010741, France], 15mL ultra-pure water) for 15 minutes at room temperature. Hereafter, the solution was removed and the gel was fixed for another 15 minutes in new fixing solution. Then, the gel was washed twice in 10% ethanol solution (5mL ethanol, 45mL ultra-pure water) for 5 minutes, replacing the ethanol in-between the two washes. After both 10% ethanol washes, the gel was washed twice with ultra-pure water, replacing the water in-between the two washes. Subsequently, the gel was incubated in freshly prepared sensitizer working solution (50µL sensitizer [Thermo Scientific, REF 1859065] in 25mL ultra-pure water) for exactly 1 minute, whereafter the gel was washed twice with two changes of ultra-pure water for 1 minute each. Next, the gel was incubated in freshly prepared stain working solution (250µL enhancer [Thermo Scientific, REF 1856220] in 25mL silver stain [Thermo Scientific, REF 1856218]) for 5 minutes, whereafter the gel was quickly washed twice with two changes of ultra-pure water for 20 seconds each. Immediately after both washes, freshly prepared developer working solution (250µL enhancer in 25mL developer [Thermo Scientific, REF 1856219]) was added and incubated for at least 10 minutes until the bands were clearly visible. After developing, the developer working solution was replaced with prepared 5% acetic acid stop solution (1,5mL acetic acid, 23,75mL ultra-pure water) and incubated for 10 minutes. Finally, the gel was removed from the staining tray for analysis.

2.3.4.2. *Western blot*

Before starting the Western blot, the polyacrylamide gel was placed in 20% ethanol (10mL ethanol in 40mL ultra-pure water) for 5 minutes to remove the SDS. Then, the gel was placed in ultra-pure water for 5 minutes, whereafter the gel was placed in transfer buffer (200mL Trans-Blot Turbo 5x Transfer Buffer [Bio-Rad, REF 10026938, Hercules, California, USA], 600mL ultra-pure water, 200mL 85% ethanol) for another 5 minutes. For the blotting, the Trans-Blot Turbo RTA Transfer System Transfer Pack (Bio-Rad, REF 1704270, Hercules, California, USA) was used with Pierce nitrocellulose membranes (Thermo Scientific, REF 77012, Rockford, Illinois, USA). The nitrocellulose membrane and two transfer stacks of filter pads were soaked in transfer buffer for 2-3 minutes. One of the wetted ion reservoir transfer stacks was subsequently placed on the bottom of the transfer cassette with the wetted nitrocellulose membrane placed on top. Then, the gel was placed on top of the membrane, whereafter a second ion reservoir transfer stack was added on top. A blot roller was used to remove any trapped air bubbles. The cassette was closed and placed in a Trans-Blot Turbo Transfer System (Bio-Rad, REF 1704150, Hercules, California, USA) for 30 minutes at 25V and 1A. During blotting, blocking buffer was prepared by mixing 2,5g of skim milk with 50mL of 1x PBST wash buffer (2,5mL Pierce 20x PBS Tween-20 Buffer [Thermo Scientific, REF 28352, Rockford, Illinois, USA] in 47,5mL ultra-pure water) and mixing thoroughly. The blocking buffer was subsequently centrifuged at 500 x g for 10 minutes. After blotting was completed, the nitrocellulose membrane was removed and blocked with blocking buffer for 90 minutes at room temperature on a shaker at 60rpm. After blocking, the membrane was washed shortly in 1x PBST wash buffer to remove excess skim milk.

For primary antibody incubation, four different antibodies were used: Mouse Monoclonal IgG2b Anti-CD81 (Santa Cruz Biotechnology, REF sc-166029, USA), Rabbit Polyclonal Anti-albumin (Cell Signaling Technology, REF 4929, USA), Mouse Monoclonal IgG2b Anti-APOA1 (Santa Cruz Biotechnology, REF sc-376818, USA), and Mouse Monoclonal IgG2a Anti-HSP70 (Santa Cruz Biotechnology, REF sc-24, USA). The antibodies were diluted in 5mL of signal enhancer solution 1 of the Millipore SignalBoost Immunoreaction Enhancer Kit (Merck Millipore, REF 407207-1KIT, Darmstadt, Hessen, Germany) to concentrations of 1/100, 1/1000, 1/200 and 1/500, respectively. The membranes were incubated for 75 to 90 minutes in the prepared primary antibody solutions on a shaker at 60rpm. After primary antibody incubation, the membranes were washed four times for 5 minutes with 1x PBST wash buffer at 60rpm. For secondary antibody incubation, two different antibodies were used: Peroxidase AffiniPure Donkey Anti-Mouse IgG (H+L) (Jackson Immuno Research Europe Ltd., REF 715-035-150, UK) for CD81, APOA1 and HSP70, and HRP-linked Goat Anti-Rabbit IgG (Cell Signaling Technology, REF 7074, USA) for albumin. The secondary antibodies were diluted in 5mL of signal enhancer solution 2 of the Millipore SignalBoost Immunoreaction Enhancer Kit to concentrations of 1/5000 and 1/1000, respectively. Subsequently, the membranes were incubated for 75 to 90 minutes in the prepared secondary antibody solutions on a shaker at 60rpm. After secondary antibody incubation, the membranes were washed four times for 5 minutes with 1x PBST wash buffer at 60rpm. Then, equal parts of detection reagent 1 and detection reagent 2 of the GE Healthcare Amersham ECL Prime Western Blotting System (Cytiva Life Sciences, REF GERPN2232, Amersham, UK) were mixed together in a tray. The blots were subsequently placed in the substrate for 5 minutes, with the protein side facing downwards. Afterwards, the blots were placed in the ChemiDoc XRS+ Imaging System (Bio-Rad, REF 1708265, Hercules, California, USA) for blot imaging and analysis.

2.3.5. *Mass spectrometry*

Before loading the samples on the UHPLC-TimsTOF Pro (Trapped Ion Mobility Spectrometry Time of Flight) LC-MS system (Bruker Daltonics, Billerica, Massachusetts, USA), peptide concentrations of each sample were determined with a NanoDrop 2000 spectrophotometer (Thermo Scientific, REF ND-2000, Rockford, Illinois, USA). The required amount of sample for 1µg of peptide was calculated for each sample. Each volume was subsequently lengthened to 10µL with mobile phase A (0,1% formic acid in mass grade water) and loaded onto the LC fractionation system, consisting of a reversed phase nanoEase M/Z Symmetry C18 (100Å, 5µm, 180µm x 20 mm) trap column (Waters, REF 186008821, Milford, Massachusetts, USA) and a reversed phase nanoEase M/Z HSS T3 C18 (100Å, 1,8µm, 75µm x 250µm) analytical column (Waters, REF 186008818, Milford, Massachusetts, USA). The latter was coupled online to a UHPLC-TimsTOF Pro for mass spectrometry analysis. The resulting data was analysed by the MaxQuant Software (open source) and searched against the human UniProt/SwissProt database by using the Andromeda search engine.

3. Results

3.1. Discriminatory diagnostic biomarkers for MDD vs. BD-D using LC-MS

Before loading precious patient and control samples onto the LC-MS system, training blood samples were acquired and processed for experimental reliability analysis. Three individual aliquots of the same sample were ran on the LC-MS system, each aliquot in triplicate to investigate into run reliability. The histogram below represents the amount of high-abundant proteins in the sample (*Figure 4*). As illustrated below, a small number of proteins (n = 70 out of a total of 1771 proteins = 3%) is most often detected (counted > 20 times), while the largest amount of proteins (916 of a total of 1771 = 51,7%) is not or only once quantified. As such, a small collection of high-abundant proteins masks detection of a large collection of low-abundant proteins.

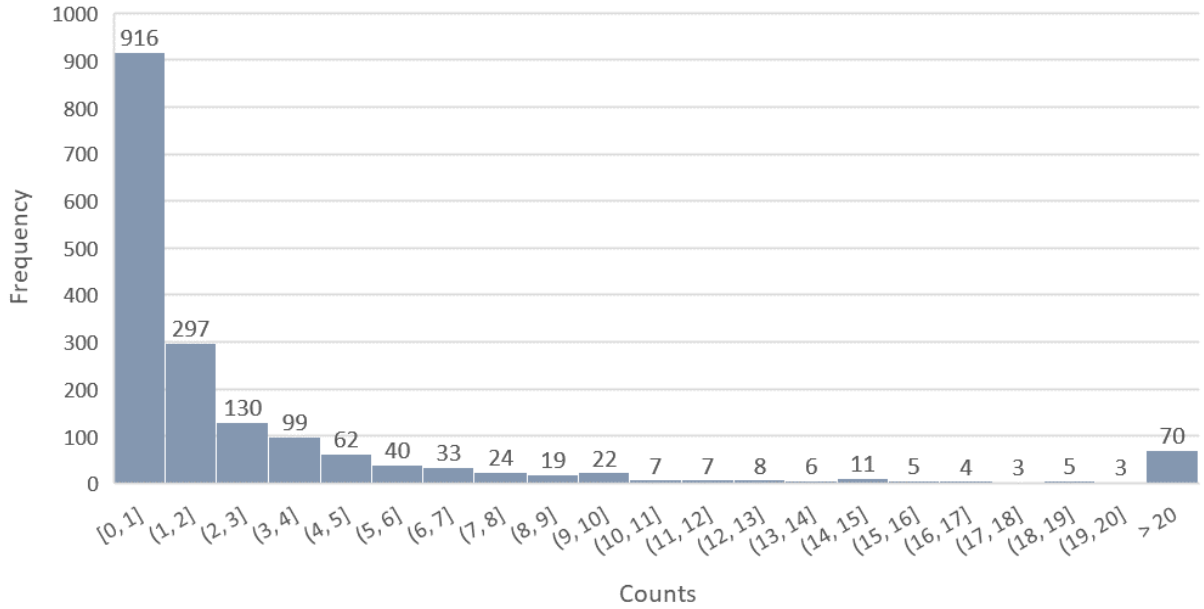

Figure 4 | **Histogram showing the frequency of protein counts.** The amount of counts per protein are shown on the x-axis, the frequency by which each count occurs in the dataset, is shown on the y-axis.

To get more accurate detection of the low-abundant proteins, the samples have to be depleted of the high-abundant ones. For this, a bar chart was created to easily detect the most prominent outliers in the samples, as can be seen in *Figure 5*.

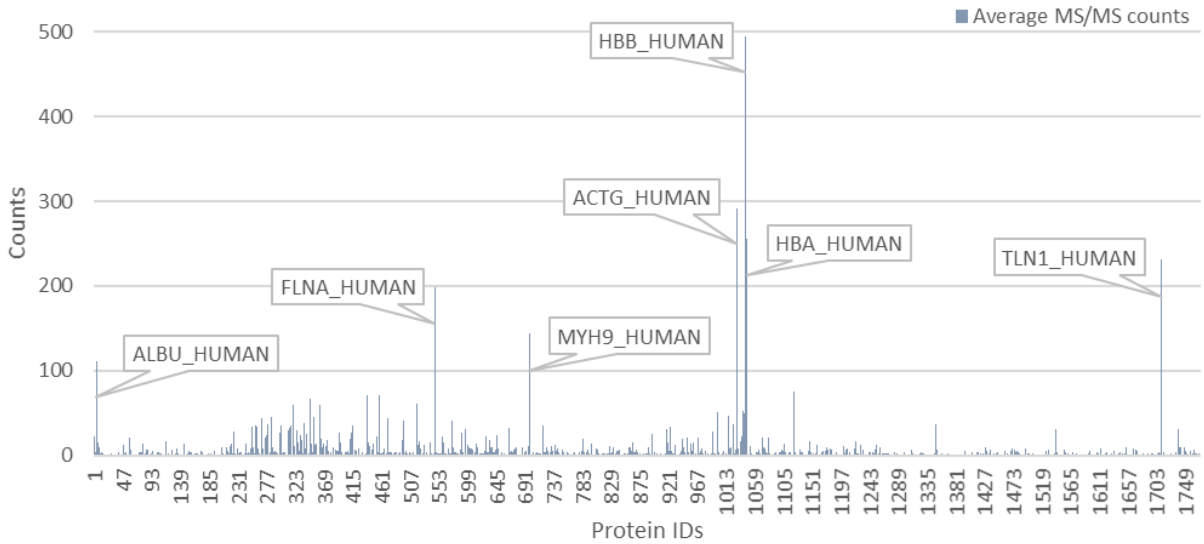

Figure 5 | **Bar chart showing the counts of all identifications.** The protein IDs of the dataset (as generated by MaxQuant) are shown on the x-axis, the counts per protein are shown on the y-axis.

As depicted in *Figure 5*, the HBB_HUMAN (haemoglobin subunit beta) peak reaches near 500 average counts per sample, making it the most contaminating protein in the sample. Also possibly masking proteins (over 100 average counts per sample) are ACTG_HUMAN (gamma-actin), HBA_HUMAN (Haemoglobin subunit alpha), TLN1_HUMAN (talin-1), FLNA_HUMAN (filamin-A), MYH9_HUMAN (myosin-9), and ALBU_HUMAN (albumin). Since these high-abundant proteins mask the low-abundant proteins in the sample, it is impossible to look for very low-abundant proteins in the MDD and BD-D patient samples and compare this to control samples. To illustrate the difference of identifications between our three different samples, two scatterplots were made for all nine sample runs by plotting the total amount of different identifications against the amount of total MS^2 events (*Figure 6*), and plotting the amount of identified haemoglobin-related peptides against the total amount of identifications (*Figure 7*). The data used for this visualisation can be found in *Table 3*.

Table 3 | **LC-MS data for the amount of haemoglobin subunit alpha, beta, delta, gamma-1 and epsilon peptides, the amount of total protein identifications, and the amount of total MS^2 events per sample, per run.**

	SAMPLE 1			SAMPLE 2			SAMPLE 3		
	Run 1	**Run 2**	**Run 3**	**Run 1**	**Run 2**	**Run 3**	**Run 1**	**Run 2**	**Run 3**
Haemoglobin peptides	47	58	41	46	41	42	41	47	45
Total protein identifications	545	485	764	1439	1432	1426	1047	975	1095
Total MS^2 events	3165	2958	5136	10817	11390	10335	7960	7796	8733

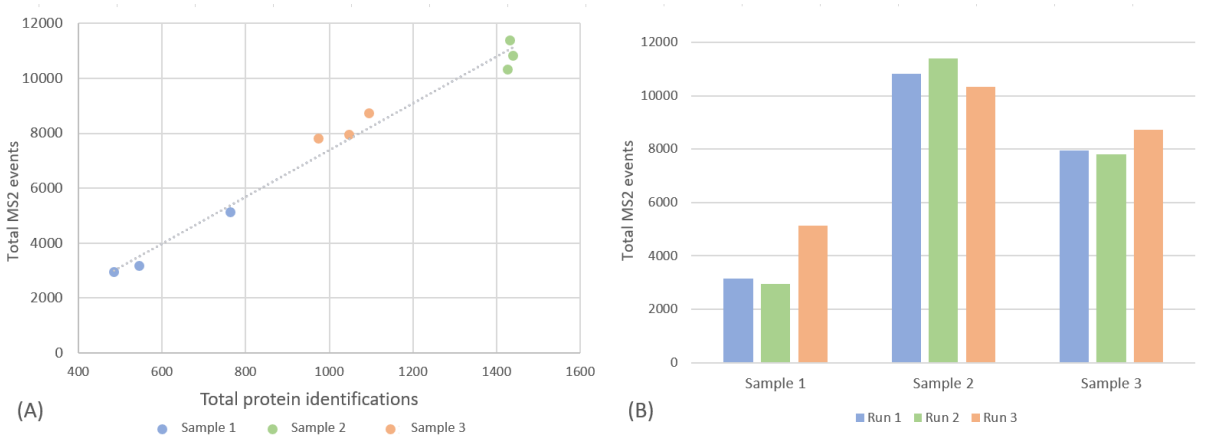

Figure 6 | **(A) Scatterplot showing the correlation between the total amount of protein identifications and the total amount of MS^2 events.** Sample 1 runs are shown in blue, sample 2 runs in green, and sample 3 runs in orange. The R^2 value for the linear trendline is 0,9809. **(B) Bar plot showing the amount of MS^2 events per sample.** Run 1 is shown in blue, run 2 is shown in green, and run 3 is shown in orange.

Looking at *Figure 6A* above, the amount of protein identifications correlates with the amount of fragments introduced to the second mass spectrometer (MS^2 events), which is expected. However, high discrepancies can be seen between the three samples (*Figure 6B*), sample 2 has a higher average amount of MS^2 events – and therefore more protein identifications – than samples 1 and 3. The high amount of variation between samples could possibly be due to the haemoglobin contamination. To confirm this hypothesis, a second scatterplot was made to determine the influence of haemoglobin-related peptides on the amount of total protein identifications (*Figure 7A*). From this figure, a slight correlation can be seen between the amount of detected haemoglobin-related peptide identifications, and the total protein identifications per sample. Moreover, sample 2 had considerably more total protein identifications in all three runs, compared to samples 1 and 3 (*Figure 7B*). Interestingly, the amount of haemoglobin subunit peptides also seems to be the lowest in sample 2, while being higher in samples 1 and 3.

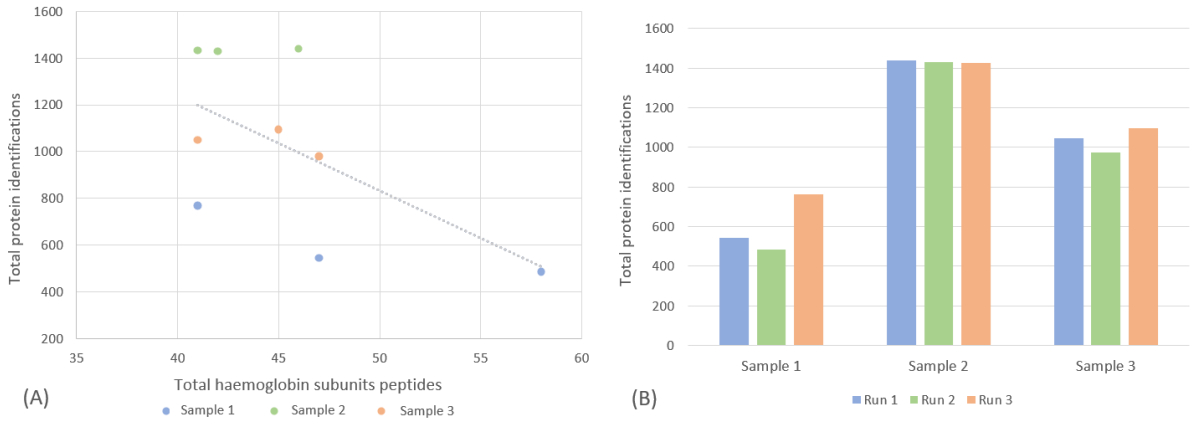

Figure 7 | **(A) Scatterplot showing the correlation between the amount of total haemoglobin-related peptides and the total amount of protein identifications.** Haemoglobin-related peptides taken into account are subunits alpha, beta, gamma-1, delta, and epsilon. Sample 1 runs are shown in blue, sample 2 runs in green, and sample 3 runs in orange. The R^2 value for the linear trendline is 0,3546. **(B) Bar plot showing the total amount of protein identifications per sample.** Run 1 is shown in blue, run 2 is shown in green, and run 3 is shown in orange.

Since the amount of identifications was drastically different for all three samples (*Figure 7B)*, possibly due to the haemoglobin contamination, further LC-MS analysis on actual patient and control samples was not possible and the focus of the thesis shifted towards two new projects. The clearance of already collected samples and the possible reasons for the haemoglobin contamination are discussed in *discussion section 4.1.*

3.2. Enzyme-linked immunosorbent assays for tryptophan and its metabolites

Each of the four different ELISAs was performed three times on pooled test blood samples from healthy volunteers to test the validity of the kits for future use on patient MDD and BD-D PBMC samples. The results of these ELISAs are summarized in *Figure 8* and *Table 4*.

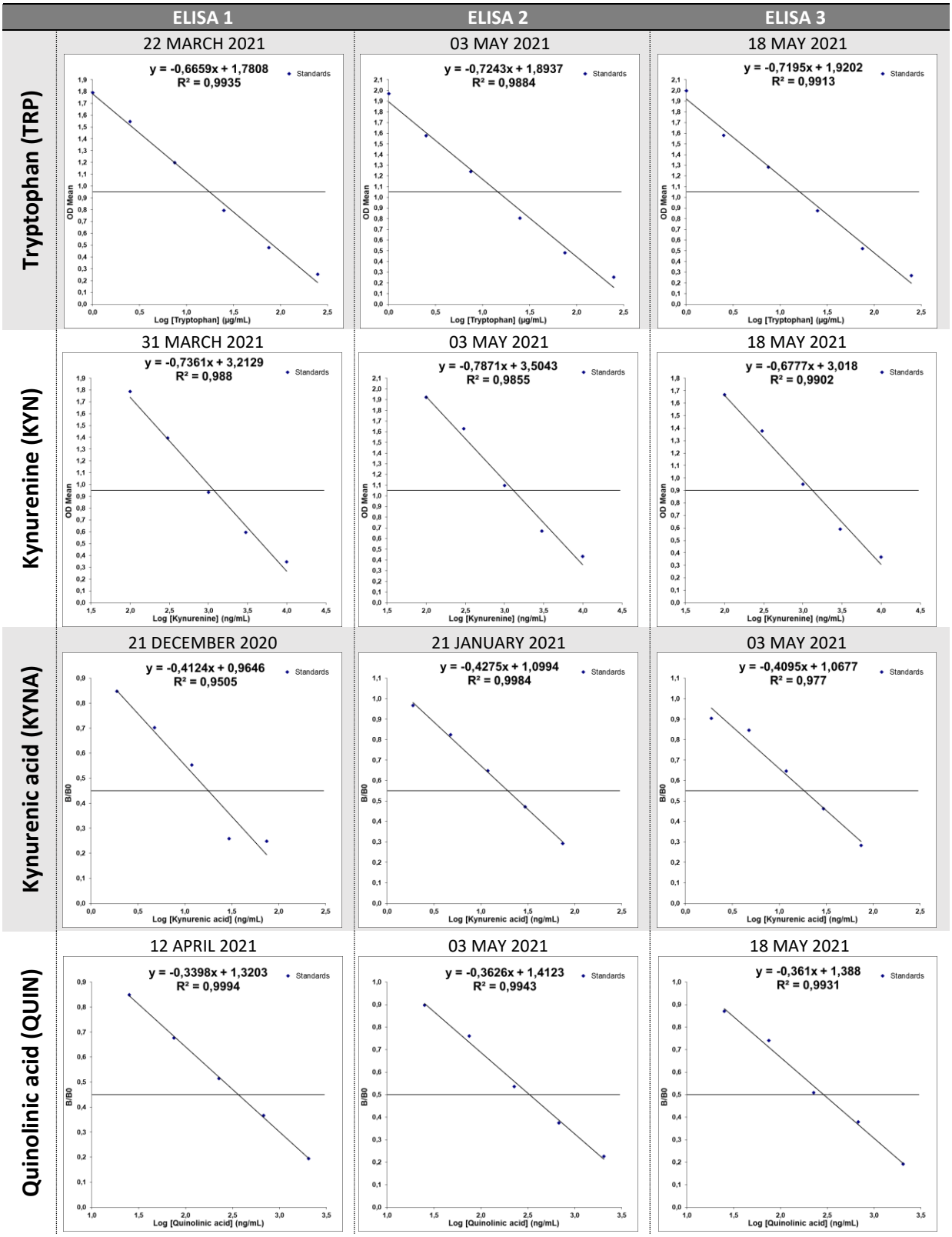

Figure 8 | **Overview of the ELISA standard curve results with their respective R²s.** The date on which each ELISA is carried out is noted above each standard curve.

In order to use the aforementioned ELISA kits for detection of TRYCAT in the peripheral bloodstream of MDD and BD-D patients, the ELISA kits had to be technically validated to ensure the performance, precision, validity and repeatability of the assays. As a first step, the standard curves were obtained for each triplicate of all four ELISAs by plotting the absorbance readings (tryptophan and kynurenine) or the B/B_0 values (kynurenic acid and quinolinic acid) of the standards on the y-axis, against the corresponding logarithmic standard concentrations on the x-axis. Linear regression was used for curve fitting. The coefficients of determination (R^2) were subsequently calculated for each standard curve to determine the capacity of the curve to reliably predict the unknown sample concentrations. For tryptophan, the average R^2 was 0,9911, for kynurenine 0,9879, for kynurenic acid 0,9753, and for quinolinic acid 0,9956. Since all these values are close to 1, the predictive capacity of these standard curves is high and thus reliable for further calculations of the sample concentrations.

At least one ELISA of each catabolite was performed on samples of plasma, gradient-residue plasma (GR-plasma), and serum (ELISA 1 for tryptophan, kynurenine and quinolinic acid; ELISA 2 for kynurenic acid) to validate their performance on bodily fluids derived from the peripheral bloodstream. The other ELISAs were performed on PBMC, since the main objective of the project is to find potential diagnostic biomarkers in PBMC in MDD and BD-D patients. Since TRYCAT concentrations in PBMC are expected to be lower than in serum or plasma, PBMC were isolated from 5mL and 10mL blood to assess the difference in TRYCAT concentrations in different concentrations of PBMC. Each sample was brought onto each plate in duplicate, whereafter the average OD was calculated. Using the standard curves shown in *Figure 8*, the concentrations in µg/mL (tryptophan) or ng/mL (kynurenine, kynurenic acid and quinolinic acid) were calculated for each sample. Additionally, tryptophan concentrations were converted to µM by multiplying the µg/mL concentrations by 4,89. Kynurenine, kynurenic acid and quinolinic acid concentrations were converted to nM by multiplying the ng/mL concentrations by 4,80, 5,286, and 5,98, respectively. All ODs and concentrations are shown in *Table 4*.

Table 4 | **Summary of the ELISA OD results and calculated concentrations.**

	TRYPTOPHAN (TRP)					
	Sample	**OD duplicate 1**	**OD duplicate 2**	**Average OD**	**[TRP] (µg/mL)**	**[TRP] (µM)**
ELISA 1	**Control 1**	1,159	1,062	1,111	10,15**	50
	Control 2	0,808	0,730	0,769	33,07**	162
	Serum	0,989	0,970	0,980	15,97	78
	Serum	0,943	1,002	0,973	16,36	80
	Plasma	1,075	1,035	1,055	12,30	60
	Plasma	1,168	1,053	1,111	10,15	50
	Plasma	1,019	1,025	1,022	13,79	67
	GR-plasma	1,098	1,052	1,075	11,48	56
	GR-plasma	1,071	1,040	1,056	12,28	30
	GR-plasma	1,058	1,004	1,031	13,37	65
ELISA 2	**Control 1**	1,199	1,232	1,216	8,63**	42
	Control 2	0,812	0,747	0,779	34,54**	169
	PBMC 5mL	1,799	1,876	1,837	1,20	6
	PBMC 10mL	1,782	1,743	1,763	1,52	7
ELISA 3	**Control 1**	1,118	1,148	1,133	12,42**	61
	Control 2	0,670	0,702	0,686	51,92**	254
	PBMC 5mL	1,969	1,880	1,925	0,99	5
	PBMC 10mL	1,492	1,635	1,564	3,13	15
	PBMC 5mL*	1,640	1,698	1,669	2,23	11
	PBMC 10mL*	1,596	1,539	1,568	3,09	15

Measuring range: 1,2 – 250µg/mL
* Two freeze/thaw cycles were performed instead of one
** Expected concentration Control 1: 10µg/mL, expected concentration Control 2: 30µg/mL

KYNURENINE (KYN)						
	Sample	OD duplicate 1	OD duplicate 2	Average OD	[KYN] (ng/mL)	[KYN] (nM)
ELISA 1	Control 1	1,322	1,312	1,317	376,36**	1807
	Control 2	0,712	0,707	0,710	2517,08**	12082
	Serum	1,382	1,496	1,439	256,96	1233
	Serum	1,392	1,403	1,398	292,58	1404
	Plasma	1,292	1,355	1,324	368,78	1770
	Plasma	1,336	1,528	1,432	262,65	1261
	GR-plasma	1,270	1,514	1,392	297,65	1429
	GR-plasma	1,437	1,489	1,463	238,37	1144
	PBMC 1,67mL	2,072	2,099	2,086	34,01	163
	PBMC 1,67mL	2,147	2,087	2,117	30,82	148
ELISA 2	Control 1	1,394	1,448	1,421	443,93**	2131
	Control 2	0,776	0,834	0,805	2689,15**	12908
	PBMC 5mL	2,427	2,278	2,350	29,27	140
	PBMC 10mL	2,218	2,087	2,152	52,19	251
ELISA 3	Control 1	1,252	1,371	1,312	329,67**	1582
	Control 2	0,761	0,685	0,723	2434,75**	11687
	PBMC 5mL	2,064	2,026	2,045	27,27	131
	PBMC 10mL	1,938	1,921	1,930	40,38	194
	PBMC 5mL*	2,013	2,088	2,051	26,77	128
	PBMC 10mL*	1,914	1,972	1,943	38,57	185

Measuring range: 63,3 – 10 000ng/mL
* Two freeze/thaw cycles were performed instead of one
** Expected concentration Control 1: 400ng/mL, expected concentration Control 2: 2000ng/mL

KYNURENIC ACID (KYNA)						
	Sample	OD duplicate 1	OD duplicate 2	Average OD	[KYNA] (ng/mL)	[KYNA] (nM)
ELISA 1	Control 1	0,559	0,841	0,700	5,05	27**
	Control 2	0,466	0,602	0,534	12,33	65**
	Plasma	0,886	0,823	0,855	2,20	12
	Plasma	0,760	0,776	0,768	3,50	19
	GR-plasma 5mL	0,838	0,870	0,854	2,20	12
	GR-plasma 5mL	0,774	0,851	0,813	2,75	15
	GR-plasma 10mL	0,841	0,951	0,896	1,76	9
	GR-plasma 10mL	0,820	0,838	0,829	2,52	13
	PBMC 5mL*	2,178	2,140	2,159	0,00	0
	PBMC 10mL*	2,161	2,199	2,180	0,00	0
ELISA 2	Control 1	1,854	1,432	1,643	3,82	20**
	Control 2	1,197	1,149	1,173	14,17	75**
	Serum	1,225	1,259	1,242	11,69	62
	Serum	1,246	1,273	1,260	11,14	59
	Plasma	1,453	1,350	1,402	7,50	40
	Plasma	1,409	1,565	1,487	5,91	31
	GR-plasma	1,387	1,473	1,430	6,92	37
	GR-plasma	1,384	1,426	1,405	7,42	39
	PBMC 10mL*	3,380	2,957	3,169	0,05	0
	PBMC 20mL*	3,467	3,133	3,300	0,04	0
ELISA 3	Control 1	1,555	1,577	1,566	3,89	21**
	Control 2	1,234	1,303	1,268	9,41	50**
	PBMC 5mL	2,195	2,484	2,340	0,39	2
	PBMC 10mL	2,524	2,552	2,538	0,22	1

Measuring range: 1,40 – 73,97ng/mL
* These PBMC were lysed chemically using a lysis buffer, not using a freeze/thaw cycle
** Expected concentration Control 1: 30nM, expected concentration Control 2: 75nM

QUINOLINIC ACID (QUIN)						
	Sample	OD duplicate 1	OD duplicate 2	Average OD	[QUIN] (ng/mL)	[QUIN] (nM)
ELISA 1	Control 1	2,045	2,270	2,158	48,68	291**
	Control 2	1,096	1,135	1,116	561,06	3355**
	Serum	2,659	2,603	2,631	16,03	96
	Serum	2,553	2,607	2,580	18,07	108
	Plasma	2,408	2,200	2,304	34,52	206
	Plasma	2,255	2,222	2,239	40,26	241
	GR-plasma	2,200	2,250	2,225	41,55	248
	GR-plasma	2,184	2,358	2,271	37,35	223
	PBMC 5mL	1,935	1,738	1,837	103,38	618
	PBMC 5mL	1,646	1,696	1,671	152,42	911
ELISA 2	Control 1	2,742	2,563	2,652	33,32	199**
	Control 2	1,262	1,274	1,268	576,75	3449**
	PBMC 5mL	2,914	3,066	2,990	16,62	99
	PBMC 10mL	2,949	2,928	2,939	18,47	110
ELISA 3	Control 1	2,188	2,183	2,186	57,76	345**
	Control 2	1,080	1,051	1,066	674,85	4036**
	PBMC 5mL	2,983	3,074	3,029	9,08	54
	PBMC 10mL	2,786	2,950	2,868	12,91	77
	PBMC 5mL*	3,047	3,039	3,043	8,79	53
	PBMC 10mL*	2,874	2,747	2,811	14,65	88

Measuring range: 25 – 2 000ng/mL
* Two freeze/thaw cycles were performed instead of one
** Expected concentration Control 1: 300nM, expected concentration Control 2: 3000nM

A table of all ODs and calculated concentrations for all four ELISAs. Values that fall below the measuring range are indicated in red and are thus not reliable.

Since all ELISAs carried out on PBMC – except for ELISA 2 and 3 of tryptophan and ELISA 1 of quinolinic acid – showed results under the measuring range (shown in red in *Table 4*), these results were not taken into account for further statistical analysis. Since the main goal of the project was to determine TRYCAT concentrations in PBMC, the decision was made to look further into the plasma, gradient-residue plasma (GR-plasma), and serum results. First, the average TRYCAT concentrations in plasma, GR-plasma, and serum were determined, whereafter the coefficients of variation (CVs) were calculated for each ELISA. These results are shown in *Table 5*. The CVs are a measure for the relative standard deviation and express the repeatability and precision of the ELISA. Generally, intra-assay replicate CVs are expected to be less than 10% (FDA Administration, 2020), while the average of all our CVs equals to 10,5%, which indicates an acceptable – albeit slightly high – variance.

Table 5 | **Calculations of plasma, gradient-residue-plasma and serum average concentrations and CVs.**

	PLASMA			GR-PLASMA			SERUM		
	[µg/mL]	AV	CV (%)	[µg/mL]	AV	CV (%)	[µg/mL]	AV	CV (%)
TRP	12,3 10,15 13,79	12,08	15	11,48 12,28 13,37	12,38	8	15,97 16,36	16,17	2
	[ng/mL]	AV	CV (%)	[ng/mL]	AV	CV (%)	[ng/mL]	AV	CV (%)
KYN	368,78 262,65	315,72	24	297,65 238,37	268,01	16	256,96 292,58	274,77	9
KYNA	7,5 5,91	6,71	17	6,92 7,42	7,17	5	11,69 11,14	11,42	3
QUIN	34,52 40,26	37,39	11	41,55 37,35	39,45	8	16,03* 18,07*	17,05*	8

* These values fall under the measuring range and are thus not reliable, but are used since no other serum values for quinolinic acid were available.

Additionally, the correlation between the presence of TRYCAT in GR-plasma and plasma on the one hand, and plasma and serum on the other hand, were evaluated for possible waste-reduction purposes in future assays. First, standard deviations (SDs) were calculated for the aforementioned average metabolite concentrations to determine the dispersion of the values around the mean. Additionally, F-tests and unpaired student's t-tests were used to determine whether significant differences were present within this data. Graphs were made to represent the differences between plasma, GR-plasma, and serum, for each metabolite ELISA. The calculated SDs are shown in *Table 6*, while F-test and student's t-test results are summarized in *Table 7*. The graphs with corresponding error bars representing the SDs can be found in *Figure 9*.

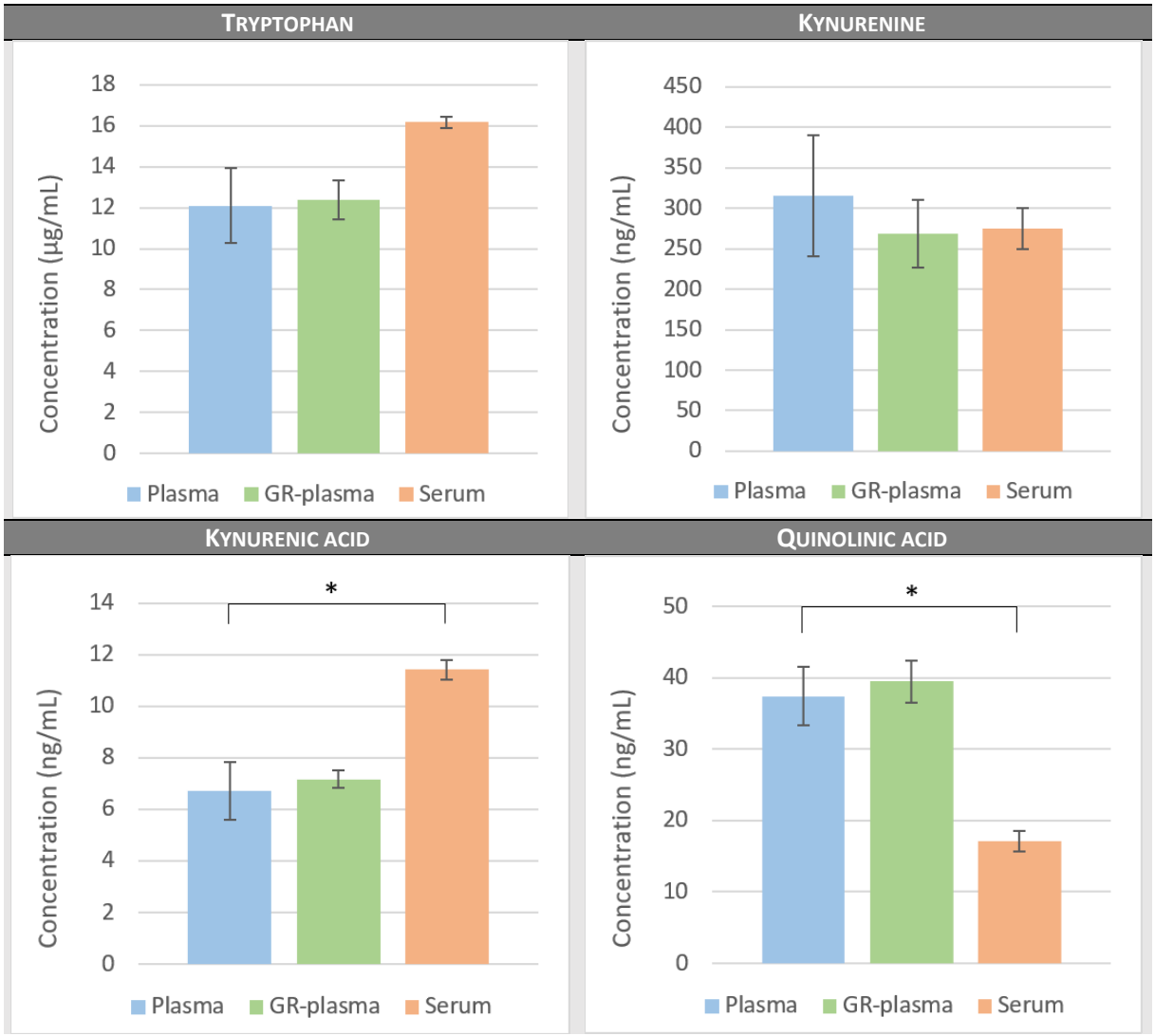

Figure 9 | **Graphs of all mean TRYCAT concentrations per sample source.** Plasma is shown in blue, gradient-residue plasma (GR-plasma) in green, and serum in orange. Error bars represent the calculated standard deviations (Table *6*). Significant differences are indicated with an asterisk. Tryptophan and kynurenine concentrations showed to be non-significantly different between all sample sources, although tryptophan concentrations indicated a trend for higher concentrations in serum than in plasma, however insignificant (p = 0,0587). For kynurenic acid, serum concentrations showed to be significantly higher (p = 0,0304) than those in plasma and GR-plasma. For quinolinic acid, the opposite could be observed, where the serum concentrations were significantly lower (p = 0,0217) compared to plasma. Furthermore, p-values indicating the difference between plasma and GR-plasma concentrations were all higher than 0,05 (p = 0,8154, p = 0,5147, p = 0,6330, and p = 6210 for all TRYCAT, respectively), indicating no significant differences between the use of plasma or GR-plasma for these ELISAs (all p-values can be found in Table *7*).

Table 6 | **Calculations of standard deviations (SD) for each TRYCAT metabolite in all sample sources.**

STANDARD DEVIATIONS			
	Plasma	**GR-plasma**	**Serum**
Tryptophan	1,83	0,95	0,28
Kynurenine	75,05	41,92	25,19
Kynurenic acid	1,12	0,35	0,39
Quinolinic acid	4,06	2,97	1,44

Table 7 | **F-test and unpaired student's t-test results for plasma vs. GR-plasma and plasma vs. serum.**

	PLASMA VS. GR-PLASMA		PLASMA VS. SERUM	
	F-test	**T-test**	**F-test**	**T-test**
Tryptophan	0,4236	0,8154	0,2119	0,0587
Kynurenine	0,6486	0,5147	0,4123	0,5406
Kynurenic acid	0,3879	0,6330	0,4240	0,0304*
Quinolinic acid	0,8043	0,6210	0,0864	0,0217*

If the result of the F-test is < 0,05, unequal variances are assumed when carrying out the student's t-test
If the result of the F-test is > 0,05, equal variances are assumed when carrying out the student's t-test
* Values are considered significant when p < 0,05

As can be deducted from *Figure 9* and *Table 7*, tryptophan and kynurenine concentrations in all three sample sources turned out to be insignificantly different from each other. However, serum tryptophan concentrations showed a consistent increase in comparison to plasma, with a p-value of 0,0587, which is barely over the cut-off for significance. For kynurenic acid, serum concentrations showed to be significantly higher than those in plasma (p-value of 0,0304), whereas in quinolinic acid, the opposite could be observed, with a p-value of 0,0217. Plasma and GR-plasma concentrations were not significantly different in any of the ELISAs. To visualize this further, a scatterplot was made by plotting the average plasma values against the average GR-plasma values. The coefficient of determination was also calculated, as can be seen in *Figure 10*. The average concentrations of all four TRYCAT in plasma have a high correlation with the concentrations in GR-plasma. The linear trendline has a coefficient of determination of 0,9994, converting to a Pearson's coefficient of correlation of 0,9997, which indicates an excellent correlation between the two sample source concentrations for all TRYCAT. In practice, this translates to the interchangeable use of plasma and GR-plasma when performing these ELISAs in the future, allowing for the use of GR-plasma instead of plasma and thus reducing the amount of whole blood required.

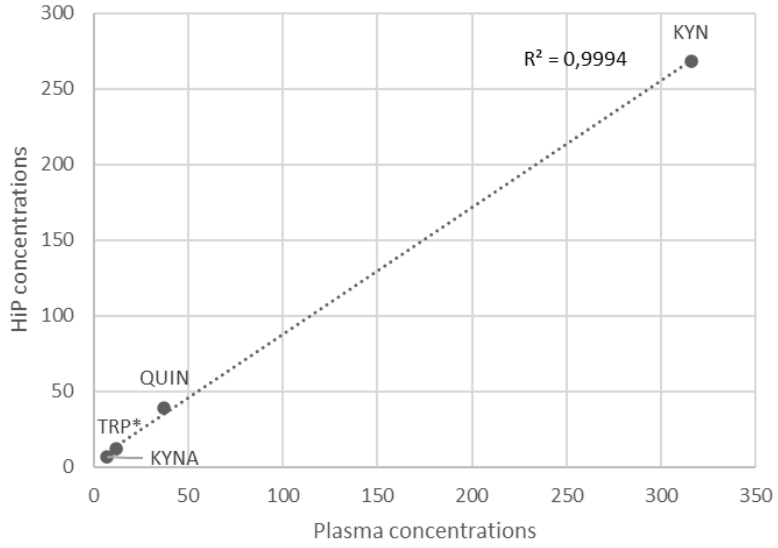

Figure 10 | **Scatterplot of average plasma concentrations vs. GR-plasma concentrations.** Average plasma concentrations are shown on the x-axis, average GR-plasma concentrations are plotted along the y-axis. A linear trendline was added for visualization of the correlation.
* Tryptophan concentration is depicted in µg/mL, the others are shown in ng/mL. Since only the correlation between GR-plasma and plasma concentrations is of importance, the difference in unit do not influence the results.

3.3. Proteomic analysis of extracellular vesicles isolated from plasma

3.3.1. *Nanoparticle Tracking Analysis*

The analysis on the ZetaView was performed on all samples in both scatter and fluorescence mode. During the first run, a 2% BSA – 0,1% Tween-20 buffer was used for storage of the samples, however this buffer caused very high background noise in scatter mode, causing an oversaturation of the sample cell. In fluorescence mode, no particles could be seen, only a high amount of background noise. For this reason, a different buffer was used during a new nEV isolation, namely Tris pH 7,5 buffer. This buffer showed no background and the results were within the measuring range of the ZetaView. The latter's results of samples which have had a pre-clearance step can be found in *Table 8* and *Figure 11.*

Table 8 | **Summary of the ZetaView results of the second run.**

SCATTER MODE				
Sample	**Median particle size (nm)**	**Average particle count per frame**	**Concentration (particles/mL)**	**Positions measured (of 11)**
A (+/+)	120,8	55	$1,1 \times 10^8$	8
B (-/+)	118,5	251	$4,9 \times 10^8$	7
C (+/-)	142,5	21*	$4,1 \times 10^7$	2
D (-/-)	130,2	89	$1,7 \times 10^8$	10
FLUORESCENCE MODE				
Sample	**Median particle size (nm)**	**Average particle count per frame**	**Concentration (particles/mL)**	**Positions measured (of 11)**
A (+/+)	197,5	19*	$1,5 \times 10^7$	6
B (-/+)	186,5	54	$4,2 \times 10^7$	10
C (+/-)	*No results*			
D (-/-)	170,0	26*	$3,0 \times 10^7$	1

Sample A: EV fraction + L1CAM-biotin complex, sample B: non-purified plasma + L1CAM-biotin complex, sample C: EV fraction + biotin only, sample D: non-purified plasma + biotin only. * Results are considered accurate when the average particle count per frame is over ±30, when lower than 30, these results are not reliable.

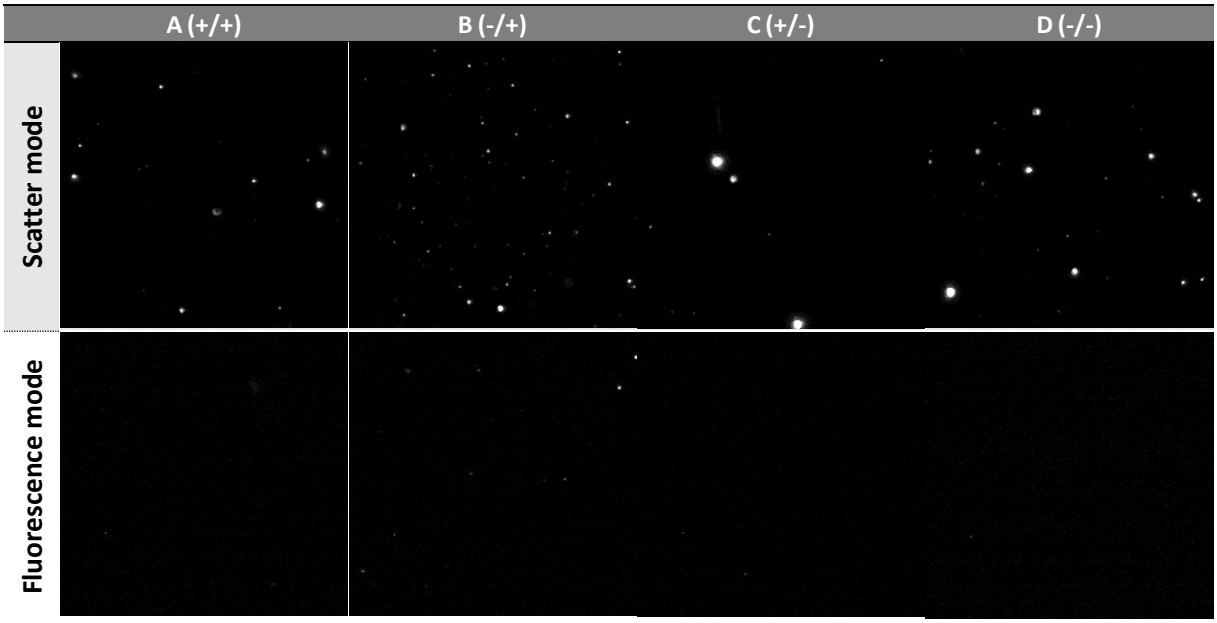

Figure 11 | **Screenshots of the ZetaView nanoparticle tracking analysis of the second run.** Sample A: EV fraction + L1CAM-biotin complex, sample B: non-purified plasma + L1CAM-biotin complex, sample C: EV fraction + biotin only, sample D: non-purified plasma + biotin only.

First, an analysis of all samples in scatter mode was performed to get a general overview of the amount and size of all particles that are present in each sample (*Table 8*). In all four samples, a median particle

size around 120nm to 140nm was measured. Also the concentrations for all samples were rather high, with a considerably lower amount in sample C, but this result is below the detection range and should thus not be deemed reliable. When looking at the results from the analysis in fluorescence mode – which only shows particles with a lipid membrane like EVs, but also lipoprotein contaminants – a higher median particle size can be observed. Additionally, the particle concentrations in each sample are still relatively high. For sample C, however, no results were acquired due to being under the detection limit. When looking at the screenshots the ZetaView has made during NTA (*Figure 11*), clear particles and no background signal can be seen in the images made in scatter mode. In the fluorescence mode images, only very few particles can be seen when closely zoomed in. Since nothing was detected in sample C, and samples A and D were under the detection limit of 30 particles per frame, these results are not considered reliable.

3.3.2. *Silver staining*

The silver staining protocol was performed twice. During the preparation of the SDS-PAGE gel for the first silver staining, samples without a pre-clearance step were loaded onto the gel. For sample A, the second elution was used since the first elution was lost during sonication, for samples B, C and D, the first elution was used. Additionally, three different concentrations of BSA were loaded onto the gel as controls. Since the results of the first silver staining showed a lot of background, a second SDS-PAGE gel was prepared, consisting of both elutions of all pre-cleared samples. Moreover, a sample of EVs isolated from cerebrospinal fluid (CSF) was loaded as a control sample, the beads on which samples A, B and C were isolated (the sample D beads did not fit on the gel), and the pre-clearance beads both for the EV-fraction (samples A and C) and the non-purified plasma (samples B and D). The results of these silver staining gels can be seen in *Figure 12*.

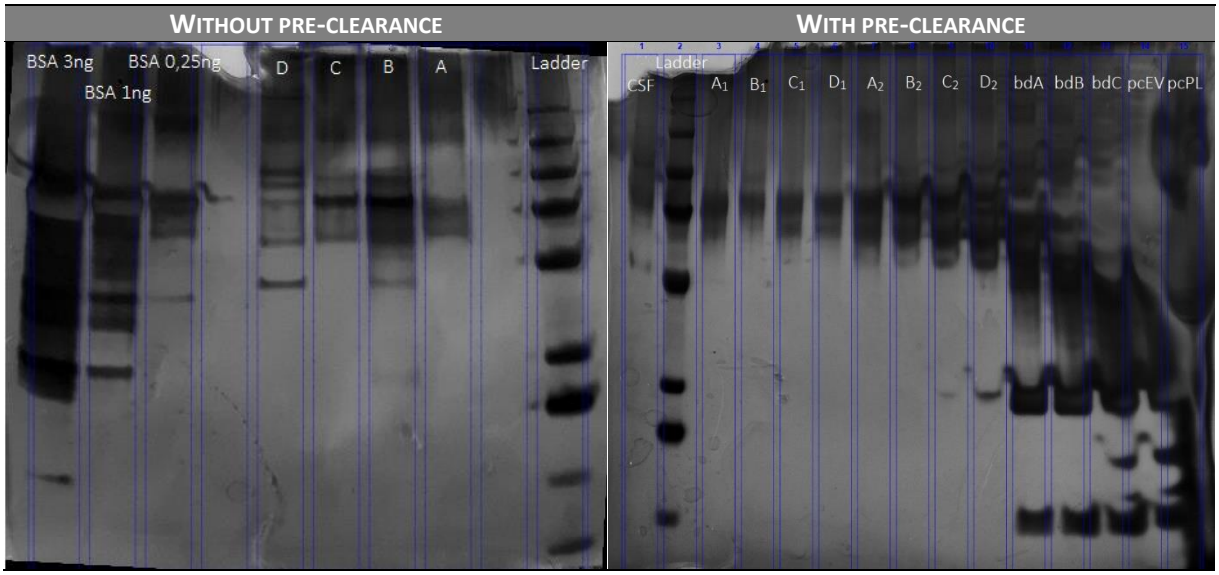

Figure 12 | **Photos of the SDS-PAGE gels after silver staining.** Sample A: EV fraction + L1CAM-biotin complex, sample B: non-purified plasma + L1CAM-biotin complex, sample C: EV fraction + biotin only, sample D: non-purified plasma + biotin only, BSA: Bovine Serum Albumin, CSF: cerebrospinal fluid, bdA: beads of sample A, bdB: beads of sample B, bdC: beads of sample C, pcEV: pre-clearance beads from EV fraction (samples A and C), pcPL: pre-clearance beads from non-purified plasma (samples B and D).

On the first silver staining which was performed on samples without additional pre-clearance step, it immediately became clear that a high amount of non-specific binding occurred in negative control samples C and D. Since the high amount of non-specific binding to biotin is detrimental to the accurate interpretation of the results, an additional pre-clearance step was added to the protocol of the newly isolated samples. On the silver staining of these pre-cleared samples, the lanes containing the beads that were used for the pre-clearance (pcEV and pcPL) still contain a lot of material, causing an

oversaturation on the right side of the gel and unclear lanes, indicating a very high amount of non-specific binding to biotin on these beads. When looking at the beads on which the samples were incubated after the pre-clearance step (bdA, bdB and bdC), two bands can be seen around the 25kDa and 50kDa marks, which are the anti-L1CAM light chain and heavy chain, respectively. For samples A-D, no clear bands can be seen, except for a black smear at the top of the gel. This could be an indication for ineffective breakage of the EVs during sonication.

3.3.3. *Western blot*

Four Western blots were carried out, each using a different antibody. For this purpose, two identical SDS-PAGE gels were prepared, on which pre-cleared samples were loaded of which the first and second elution were constituted. Additionally, a positive control cell line consisting of EVs extracted from human lung epithelium was loaded onto the gel, together with two EV CSF samples[6]. Both gels were cut in half around the 50kDa ladder mark. This way, anti-CD81 (28kDa) and anti-APOA1 (22-26kDa) could be incubated on the lower halves, and anti-albumin (67kDa) and anti-HSP70 (70kDa) on the upper halves of both gels. Photos of all four gels can be seen in *Figure 13*.

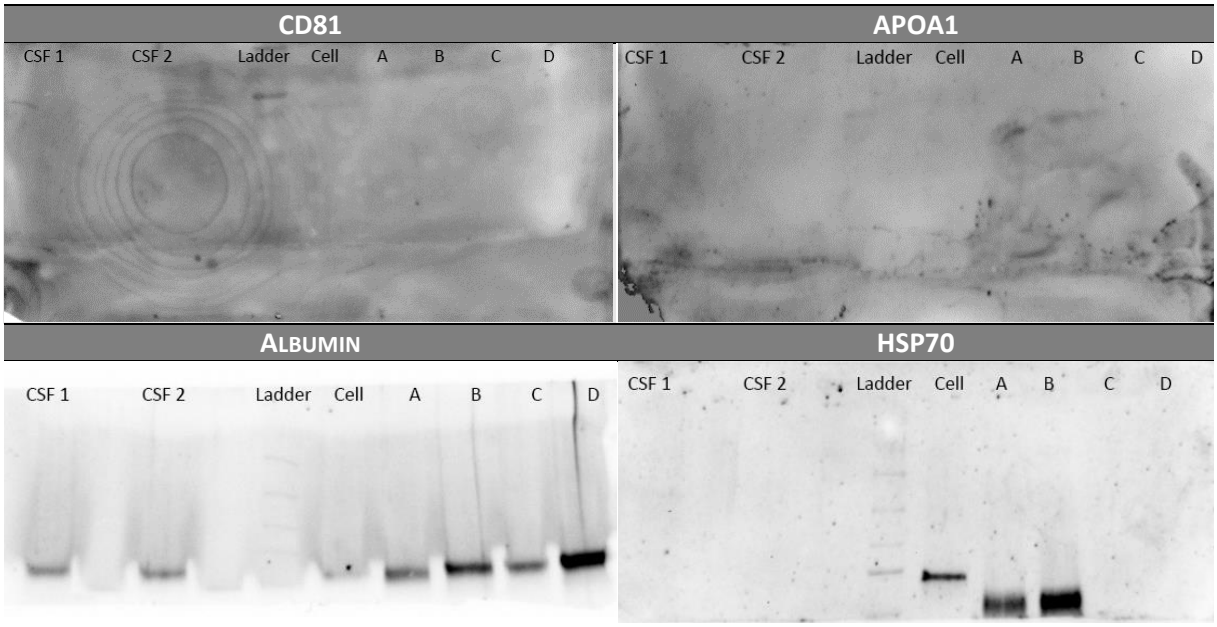

Figure 13 | **Photos of blots made with ChemiDoc XRS+ Imaging System.** Sample A: EV fraction + L1CAM-biotin complex, sample B: non-purified plasma + L1CAM-biotin complex, sample C: EV fraction + biotin only, sample D: non-purified plasma + biotin only, CSF 1: fraction 1 of cerebrospinal fluid control sample, CSF 2: fraction 2 of cerebrospinal fluid control sample, cell: EVs extracted from a human lung epithelial cell line NCI-H1975 used as a positive control sample.

Looking at the Western blot incubated with anti-CD81, which is EV-specific, no bands can be seen in any of the samples, except for the upper part of the ladder. However, at the left side of the blot, circular lines can be seen, which could indicate the emergence of a large air bubble during transfer, influencing the results. On the blot incubated with anti-APOA1 – a lipoprotein contaminant – not a single band can be seen, possibly indicating something went wrong during transfer or antibody incubation. On the blot incubated with anti-albumin (bulk protein, contaminant), however, bands can be seen in each lane, even in the negative control sample. When looking at the blot incubated with HSP70, which is also EV-specific, a clear band can be seen in the positive control cell sample, and two non-specific bands in samples A and B.

[6] The EV CSF samples are part of another ongoing project, but this is beyond the scope of this thesis.

3.3.4. *Mass spectrometry*

Analysis with the TimsTOF Pro LC-MS system was performed twice, once on samples without an additional pre-clearance step, and once on pre-cleared samples. During both runs, the resulting data was analysed for the presence of neuronal- and EV-specific proteins after MaxQuant LFQ match-between-runs, and compared to a list of the most abundant CSF proteins. Moreover, the amount of identifications after LFQ match-between-runs was acquired. These results are summarized in *Table 9*.

Table 9 | **Summary of the LC-MS TimsTOF Pro LC-MS results after MaxQuant LFQ match-between-runs.**

	WITHOUT PRE-CLEARANCE				WITH PRE-CLEARANCE			
	A (+/+)	**B (-/+)**	**C (+/-)**	**D (-/-)**	**A (+/+)**	**B (-/+)**	**C (+/-)**	**D (-/-)**
Serum albumin	X	X	X	X	X	X	X	X
Lactotransferrin	X	X	X	X	X	X	X	X
Alpha-1-antitrypsin	X	X	X	X	X	X		X
Serotransferrin	X	X	X	X				X
Apolipoprotein A1	X	X	X	X		X		X
Transthyretin*		X						X
Complement C3*	X	X	X	X	X	X		
Alpha-2- macroglobulin	X	X	X	X	X	X		
Haptoglobin		X	X	X	X			
Total identifications	447	467	523	619	203	173	127	163

A list of nine of the most abundant proteins in cerebrospinal fluid, their presence in each sample is indicated with an X. A red X indicates that the LFQ intensity in this sample was considerably higher than in the other samples of that run. * Transthyretin and complement C3 are the only two proteins on the list that are not among the 20 most abundant plasma proteins.

First, the results of both runs were analysed for the presence of EV-specific proteins. In the first run on samples without pre-clearance, four EV-specific proteins were detected, namely CD63 in samples C and D, HLA-B in samples B and D, and PDCD6IP and HSPA1B in all samples. In the second run on pre-cleared samples, no EV-specific proteins were detected after LFQ match-between-runs. Furthermore, when comparing the results of the first run to a list of most abundant CSF proteins (*Table 9*), it is clear that most proteins are present in all samples, besides a few exceptions. In the second pre-clearance run, however, considerably less CSF bulk proteins were detected. Ultimately, also a gene set enrichment analysis with DAVID (Database for Annotation, Visualization and Integrated Discovery) against the Homo sapiens proteome background was performed, to look at enriched functional-related gene groups of the pre-clearance sample run. For sample A, 168 out of 203 proteins or 84,4% (p-value = $4{,}5 \times 10^{-104}$) were associated with the Gene Ontology (GO)-term “extracellular exosome”. For sample B, 140 out of 173 proteins or 82,4% (p-value = $4{,}5 \times 10^{-85}$), for sample C, 104 out of 127 proteins or 83,2% (p-value = $4{,}9 \times 10^{-63}$), and for sample D, 124 out of 163 proteins or 78,0% (p-value = $2{,}0 \times 10^{-69}$) were enriched for this GO-term.

4. Discussion

4.1. Discriminatory diagnostic biomarkers for MDD vs. BD-D using LC-MS

When looking at the acquired results in *Figure 5*, it immediately became clear that our PBMC samples contained high amounts of haemoglobin subunit alpha and beta. This contamination was further illustrated in *Figure 7A*, where the amount of haemoglobin-related peptides slightly correlated with a decrease in protein identifications, which was also reflected in the low amount of triggered MS^2 events in *Figure 6A and 6B*. Because the high discrepancies in total numbers of identified proteins between the samples were detrimental to further analysis (see *Figure 7B*), the haemoglobin contamination became an important aspect of the continuation of the project. Haemoglobin contamination is caused by haemolysis of the red blood cells (RBC) in the blood sample and can be macroscopically observed as it stains the sample red. When new samples were collected after acquiring the LC-MS results, additional attention was therefore paid to the colour of the PBMC pellets. Different colours were detected in most of the samples, ranging from pure white, to dark red, with gradations of pink in-between. With this in mind, two objectives were established: (1) how to prevent this contamination in future PBMC sample collections, and (2) how to purify our already acquired PBMC samples from the haemoglobin contamination.

Regarding the first objective, it is important to look at the possible reasons of this contamination. A first possible cause for haemolysis stems from the blood withdrawal method, like the thinness of the needle, under-filling of the EDTA-tubes, and the time between disinfection of the skin and the puncture (Heireman et al., 2017). Also shaking of the sample and exposure to extreme temperatures could be causes for haemolysis (Lippi et al., 2008). Since all of the blood collections at SINAPS were performed by study nurses, while making use of sufficiently wide butterfly needles, the cause for haemolysis is most probably due to other factors. These factors can range from a delay between collection of the sample and gradient centrifugation could be another cause for haemolysis, to temperature and duration of storage (Lippi et al., 2008). Since the samples previously collected at SINAPS were all carried out using a standard PBMC gradient centrifugation protocol, we decided to change to SepMate tubes. These tubes have a barrier in the middle, causing a physical separation between the RBC and the PBMC. However, when using these SepMate tubes, a high amount of the resulting pellets still appeared red, instead of the expected white pellets. For this reason, a RBC lysis buffer (BioLegend, REF 420302, San Diego, California, USA) was acquired, as to try to lyse the RBC, and get the debris and haemoglobin in the supernatant after centrifugation. However, this buffer also caused lysis of our PBMC, instead of only the RBC, leading to the complete absence of a pellet. Additionally, we compared our own PBMC isolation protocol with that of the Laboratory of Experimental Haematology of Prof. Dr. Nathalie Cools. The most significant protocol differences were their use of 50mL SepMate tubes instead of the 15mL variant we use, EDTA-PBS instead of regular PBS, and that we did not dilute our blood before pipetting it on the density gradient. After carrying out our PBMC isolation according to their protocol, pellets were till visually red, although a potential impact on the results has yet to be objectified since the comparative LC-MS analysis of these samples is still ongoing at the moment of writing.

Since the cause for the haemolysis and resulting haemoglobin contamination of our PBMC samples is as of yet thus still unknown, the second objective came into place: purifying our already collected PBMC. A literature search was performed to look at commercially available products which could possibly clean up our samples. In literature, the commercial HemoVoid LC-MS on-bead (Biotech Support Group LLC, REF HVB-MS05, Monmouth Junction, New Jersey, USA) or HemogloBind (Biotech Support Group LLC, REF HO145-15, Monmouth Junction, New Jersey, USA) kits were mostly used for whole blood or RBC lysate samples, however only one article could be found where this was used on PBMC samples (Rubio-Navarro et al., 2015). Very recently, however, the HemogloBind kit has been used in research concerning COVID-19, where the kit was used to deplete haemoglobin from PBMC whole cell lysate samples (Kaneko et al., 2021). Nonetheless, since the HemoVoid kit had already been tried out by two Master's students at the Centre for Proteomics and was deemed insufficient for complete depletion due to filter saturation (*cf*. Master thesis by *Skorobogatov Jekaterina* and *Van*

Minnebruggen Julie), we looked at protein depletion columns. However, the most frequently used protein depletion column in literature (Multiple Affinity Removal Column Human 14, Agilent, REF 5188, Santa Clara, California, USA), which chromatographically removes fourteen high-abundant proteins from plasma samples, does not specifically eliminate haemoglobin (Tu et al., 2010). Furthermore, also other high-abundant proteins were present in our samples, namely gamma-actin, talin-1, filamin-A, myosin-9, and albumin, of which only the latter can be depleted with the aforementioned depletion column. Only gamma-actin and talin-1 had over 100 counts in sample 1 – which is the sample with the least amount of identifications – where a higher amount of gamma-actin peptides correlated with a decrease in identifications. Since actine is present in the cytoskeleton of both erythrocytes and PBMC, it being a possible contaminant can not be ruled out. If all high-abundant proteins need to be depleted from the samples, multiple kits and columns would be required, meaning a very high cost with relatively small gain. Since we, as of yet, have thus not found a cost-effective way of purifying our PBMC samples, we were recommended by the Centre for Proteomics to optimize our method of PBMC sample collection as to avoid haemoglobin contamination in the future, and use the already acquired samples for other purposes, not involving LC-MS analysis.

Unfortunately, our research question regarding this objective could thus not be answered and the MDD and BD-D patient PBMC samples were not utilized. In the future, these samples could possibly be used in targeted ELISA assays, since these are not affected by haemoglobin contamination. Because SINAPS already had multiple projects running regarding the kynurenine pathway, these samples could be used in the future for tryptophan catabolite and enzyme ELISAs, after thorough testing and technical validation has been completed (*see sections 2.2, 3.2, and 4.2).*

4.2. Enzyme-linked immunosorbent assays for tryptophan and its metabolites

ELISAs for tryptophan, kynurenine, kynurenic acid, and quinolinic acid were carried out on plasma, serum, and PBMC samples of healthy controls. Each ELISA was performed a total of three times to assess the repeatability of the results of each TRYCAT assay. Looking at the standard curves and their R^2-values for all performed ELISAs in *Figure 8*, we saw an overall average coefficient of determination of 0,9875. This means that 98,75% of the standard concentrations fit the linear regression model, indicating a high predictive capacity of these curves were reliable for further calculations of the unknown sample concentrations. After calculation of all the concentrations, which are shown in *Table 4*, we first looked at the TRYCAT concentrations in PBMC. Looking at the tryptophan results, PBMC concentrations were always at the lower limit of the measuring range, and consistently below the tryptophan levels in serum, plasma and GR-plasma, which was expected. Only one PBMC result fell below the detection limit, although the result was close to reaching the lower limit of the range. The tryptophan assay should be repeated with higher PBMC concentrations as to get more reliable results within the middle of the measuring range. When looking at the kynurenine results, however, all PBMC results fell below the measuring range. Nevertheless, the results for PBMC from 10mL blood were consistently higher than those from 5mL blood. Since kynurenine was still detected in PBMC – albeit below the measuring range – higher blood volumes (e.g., PBMC from 20mL blood) might result in concentrations within the measuring range and more reliable conclusions on the presence of kynurenine in PBMC of healthy controls. Next, the results of the kynurenic acid were evaluated, which showed extremely low concentrations in PBMC. Kynurenic acid concentrations were equal to zero in multiple PBMC concentrations, which might be an indication the kynurenine aminotransferase (KAT) enzyme is absent in PBMC . However, an interesting remark should be made regarding these results. The first two ELISAs used PBMC lysed using a lysis buffer, whereas the third ELISA used a freeze/thaw cycle. The results of the first two ELISAs were also considerably lower than those of the third, possibly indicating an influence of the lysis buffer on the kynurenic acid concentrations. This assay should be repeated using freeze/thaw cycles to rule out or confirm the influence of the lysis buffer on these results. Additionally, higher PBMC concentrations should be used to get results closer to or within the measuring range. Looking at the quinolinic acid results, an interesting observation was made. Concentrations in PBMC during the first ELISA were noticeably higher than those in serum, plasma and

GR-plasma. When the ELISA was repeated, however, concentrations fell below the measuring range. The reason for these conflicting results possibly lies in the amount of PBS the PBMC were diluted in. During the first ELISA, PBMC were used only for this assay, while in the other two ELISAs, PBMC from the same amount of blood were used for four different ELISAs, and thus diluted in a higher amount of PBS, ultimately leading to lower concentrations.

Since unfortunately, most of the TRYCAT concentrations in PBMC were under the detection limit, we were not able to do any statistical analysis on these results. Instead, we decided to look further into the acquired results for serum, plasma, and GR-plasma. For this purpose, we calculated CVs per ELISA per sample source, which are shown in *Table 5*. Since intra-assay replicate CVs are expected to be below 10% for accurate and repeatable results, we calculated the average CV for all the ELISAs. We found an intra-assay CV of 10,5%, which is slightly above the expected value, but still acceptable for the low sample size. An interesting observation was made, however, since the plasma results had consistently higher variances than the serum results, which is in line with previous findings (Deza-Cruz et al., 2019). Additionally, correlations between plasma and GR-plasma concentrations, and plasma and serum concentrations were evaluated. From these results, we found that tryptophan and kynurenine concentrations in all three sample sources were insignificantly different from each other. For kynurenic acid, however, serum concentrations were significantly higher than plasma concentrations, whereas in quinolinic acid, the opposite was observed. Since the results for GR-plasma and normal plasma were insignificantly different in all of the ELISAs, GR-plasma could be used instead of plasma in future assays. When looking at the visualisation in *Figure 10*, a coefficient of determination of 0,9994 was calculated, indicating an excellent correlation between both concentrations. With an eye to waste-reduction, this could be beneficial in future assays. With the same amount of blood, more PBMC can be isolated, since GR-plasma resulting from gradient centrifugation can be used instead of plasma.

An important footnote should be made regarding all the aforementioned results, however. Since the sample size was very small, these experiments should be repeated with bigger sample sizes to ensure the validity of these results. Even though repeatability of the assay seemed sufficient with an average intra-assay CV of 10,5%, these results are only based on two or three replicates per ELISA, per sample source. Additionally, since we got consistently low concentrations in PBMC, higher amounts of PBMC might be required to get results in the measuring range. Another possibility for the low concentrations in PBMC, might be improper breakage of the cells. A lysis buffer, as well as one or two freeze/thaw cycles were used, however we noticed that the latter method caused great difficulty in resuspending the pellets in PBS. Another possibility could be to use a RIPA-buffer, or sonicate the cells to ensure complete cell lysis. Nevertheless, the ELISA kits were successfully validated to ensure their performance and precision for future assays. If the PBMC collection and lysis protocols are further optimized and higher PBMC concentrations are used, these ELISAs can ultimately be used on MDD and BD-D patient samples to find differential expression of any of these catabolites between healthy controls and patients, or among MDD and BD-D patients.

4.3. Proteomic analysis of extracellular vesicles isolated from plasma

Different analyses of the nEV samples were performed with ZetaView, silver staining, Western blot, and LC-MS analysis. Nanoparticle tracking analysis with ZetaView was performed twice, since during the first run no usable results could be seen besides an oversaturation of the sample cell in scatter mode, and a high amount of background noise in fluorescence mode. Since the cause of this high background was unclear, the PBS – 2% BSA – 0,1% Tween-20 buffer was injected into the sample cell separately, which immediately showed a high amount of particles in scatter mode, and a high background noise in fluorescence mode after incubation of the buffer with CMG. Additionally, the optimal conditions for CMG measurements are carried out in a pH between 6 and 9. However, with the aforementioned buffer, only a pH of 5 could be reached, which is not optimal for fluorescent detection of CMG. For both reasons, during the second nEV isolation, a different buffer was used for sample storage, namely Tris pH 7,5 buffer. The use of this buffer was able to elevate the pH of the

elutions to pH 6, which is at the bottom of the optimal CMG range. When injecting these samples into the sample cell of the ZetaView, normal results could be acquired. The results in *Table 8* show a mean particle size in scatter mode between 120nm and 140nm. This is within the expected particle size for EVs, since the majority of EVs are smaller than 150nm, but larger than 30nm (Doyle and Wang, 2019). Concentrations for all samples were in the range of 10^7-10^8 particles/mL, but since scatter mode measures all particles present in the samples, this does not give an indication of the actual nEV concentration, which will ultimately be lower. Additionally, the particle concentration of sample C was noticeably lower than of the other samples, with also only 2 of 11 positions measured, meaning the other 9 positions were most probably under the detection limit of the ZetaView. The results of the analysis in fluorescence mode showed a higher mean particle size than in scatter mode, ranging between 170nm and 200nm. Since small non-lipid membrane particles and contaminants are not detected with fluorescence mode, the mean particle size is increased, better representing the size of the EVs present in the sample, even though slightly smaller particle sizes were expected. Particle concentrations of the samples are still high, albeit lower than in scatter mode, which is to be expected. These results give a good indication of the amount of EVs and other lipid membrane particles present in the sample. In sample C, however, no results could be acquired by the ZetaView due to being under the detection limit. Moreover, samples A and D both had an average count per frame of under 30, which means these results are not considered accurate and thus also not reliable. The results in *Figure 11* show clear particles without background noise in scatter mode, though this is not representative for the EVs present in the sample since scatter mode visualizes all particles. The results in fluorescence mode, however, showed barely any visible particles. Injected concentrations could have possibly be too low (even though a lower dilution is not possible due to the minimum ZetaView injection volume of 800-1000µL), or EVs could have been broken down, causing their lipid membranes to not be intact. If the latter is true, this could be due to the effect of pH during elution. Since the buffer which is used to elute is 0,2M glycine pH 2, the low pH could possibly have an effect on the stability of the exosomes. One study was found where a loss of EV concentration was observed during NTA when the EVs had been stored in a pH of 4, instead of a pH of 7 (Cheng et al., 2019). They suggested that an acidic environment could be destructive to the stability of EVs, however the opposite has also been observed (Ban et al., 2015). Since the ZetaView analysis was primarily done to give a general idea of the isolation and immunoprecipitation protocols, and if particles could be detected. However, this did not give us a sufficiently clear result of possible enrichment when comparing samples A with C, and B with D.

Similarly, the silver staining protocol was also performed twice, once on samples without additional pre-clearance step, and once on pre-cleared samples. During the first silver staining, as can be seen in *Figure 12*, a lot of background was visible on the gel, especially in the negative control lanes of samples C and D. This led us to believe a high amount of non-specific binding to the biotin took place during incubation, and an additional pre-clearance step of all samples was thus required. However, when comparing samples A and B, the lane for sample B had considerably more material than the lane for sample A. This is to be expected, since sample A had previously been enriched by using the SEC, whereas sample B had only been immunoprecipitated with anti-L1CAM. The anti-L1CAM antibody has thus presumably also bound to other material besides nEVs in sample B. When the silver staining protocol was repeated on a new gel with pre-cleared samples as described in *section 2.3.1.5*, the pre-clearance bead lanes (pcEV and pcPL) showed a very high amount of non-specific binding to biotin. This was expected, since the negative control samples C and D also had a high amount of non-specific binding to biotin. However, this caused an oversaturation of the gel, leading to a smear over the lanes of all the beads. In the future, these pre-clearance beads should thus not be loaded on the same gel as our samples since the oversaturation can be detrimental to a correct interpretation of the results. The lanes which contain the beads on which the samples were incubated after pre-clearance, show two clear bands around 25kDa and 50kDa, which are the anti-L1CAM light chain and heavy chain, respectively. This is an indication that the elution was successful, since the antibody remained on the beads and has not eluted together with the EVs. For samples A-D, the expected result would be to see a bands pattern along the length of the gel, with more material in A and B, compared to C and D,

respectively. Unfortunately this was not the case, since only a black smear can be seen at the top of the gel, possibly indicating ineffective breakage of the EVs during sonication. The first next stage in this silver staining analysis, is finding out the reason that no small proteins could be seen in the sample lanes. This could possibly be due to the silver staining protocol, however unlikely since the heavy and light chain of the anti-L1CAM antibody could be seen very clearly in the beads-lanes. Another possibility is the improper breakage of the EVs, for which we could try a methyl tert-butyl ether (MTBE) extraction protocol to perform a lipid extraction. This procedure has also been used for previous sample preparations of EV CSF samples, but has not been tested on plasma samples as of yet, and is thus the first next step. However, when comparing our protocol with the original protocols on which ours is based, there were some differences regarding the EV breakage procedure (Fiandaca et al., 2015; Mustapic et al., 2017). The most significant difference, is that the authors used Mammalian Protein Extraction Reagent (M-PER [Thermo Scientific, REF 78501, Rockford, Illinois, USA]), containing three times the suggested phosphatase and protease inhibitor concentrations to lyse their EVs. Furthermore, two freeze-thaw cycles were performed to ensure complete EV breakage. Since we did not use M-PER or inhibitor cocktails in the end, and neither did we perform freeze-thaw cycles, these adjustments could be made to our protocol to ensure better EV lysis and subsequent better silver staining results.

Western blots were only performed on pre-cleared sample gels with anti-CD81, anti-APOA1, anti-albumin, and anti-HSP70 antibodies. Western blots were carried out primarily to look whether EVs were present in our samples, and not only possible contaminants. Looking at the EV-specific CD81 blot in *Figure 13*, no results could be seen, except for the upper part of the ladder. On the left side of the blot, circles can be seen, which could be an indication for improper blotting because of the presence of an air bubble between one of the cassette layers. However, since our samples and the positive control sample were loaded on the right side of the blot where no bubbles were present, these results should not be influenced by this. Since no CD81 was detected in our positive control sample, this could be an indication for ineffective working of the antibody. The negative results of samples A-D should thus not be deemed reliable, since the positive control turned out to be negative. Looking at the other EV-specific blot, HSP70, one clear and specific band can be seen in the positive control sample lane. This is what was expected, since this positive control sample has a high amount of isolated EVs. However, in the sample lanes, no specific bands can be seen, only two non-specific smears at the bottom of lanes A and B. The reason no bands can be seen in the sample lanes is most probably due to insufficiently high concentrations. Since the two bands in lanes A and B are non-specific, they most likely result from non-specific binding from albumin, and not from HSP70. A possible cause for this could be the ineffective working from the blocking buffer if the blot was not properly incubated at this location of the blot. Looking at the APOA1 lipoprotein contaminant blot, not a single band was visible, not even the ladder. This could be an indication something went wrong during transfer or antibody incubation. The last blot, which looked at albumin contamination, showed interesting results, however. In each lane, clear results could be seen. For samples B and D, these bands were clearly darker than for samples A and C, which is what should be expected for sample B only. Since sample D is a negative control (not enriched with SEC and incubated with biotin-only beads), it was expected no material should be present in this lane. However, since a very dark band can be seen, this means a high amount of non-specific binding with biotin has occurred during incubation. In samples A and C, and samples B and D, approximately the same amount of albumin can be seen, respectively. This led us to believe albumin is the biggest cause for the non-specific binding on biotin, since the lanes that were enriched with SEC contain considerably less albumin. The SEC enrichment is thus certainly necessary to deplete the samples of the most contaminating proteins, since the non-purified plasma samples contain substantially more albumin. The reason our negative control seemingly contains the most amount of albumin binding, is still unclear. Potentially only one pre-clearance step is not enough to remove all non-specific bindings because the pre-clearance biotin beads were saturated, and an additional pre-clearance step may thus be required.

The last proteomic experiment, the LC-MS TimsTOF analysis, was performed once on samples without pre-clearance, and once on pre-cleared samples. This analysis was performed to look whether

or not EV-specific proteins were present in our samples. During the first run, four EV-specific proteins were detected (Théry et al., 2018), CD63 in samples C and D, HLA-B in samples B and D, and PDCD6IP and HSPA1B in all samples. CD63 is a non-tissue specific tetraspanin that is classically used as an EV marker present in the plasma membrane (Kowal et al., 2016). Since this tetraspanin was only found in negative control samples C and D, this could be an indication that EV isolation with L1CAM in samples A and B has been ineffective. HLA-B is a non-tissue specific MHC class I protein that is also frequently used as a marker for EVs in general (Synowsky et al., 2017). This protein was however only found in samples B and D – which are the samples that have not been enriched with SEC – also confirms the above findings of ineffective EV isolation. PDCD6IP or ALIX is an accessory protein in the ESCRT machinery with lipid protein-binding ability present in the cytosol of EVs, which also plays a role in EV biogenesis (Baietti et al., 2012). Since this protein was found in all samples, this cannot be used as an EV-specific marker in this case. Likewise, HSPA1B, which is a member of the HSP70 family, has been associated with EVs (Mathew et al., 1995). However, just like PDCD6IP, it has been detected in all samples and leads us to think EV isolation was not successful. In the second run on pre-cleared sample, not a single EV-associated marker was found in any of the samples. Additionally, the results from both runs were assessed for the presence of neuronal markers (L1CAM, synapsin 1, SNAP-25, NCAM, NS-enolase, NfL, MAP-2, and NeuN), astrocyte markers (GLAST, GLT2, GFAP, and GluSyn), microglial markers (TMEM119, P2Y12, IBA-1, and CD11b), and oligodendrocyte markers (PLP and CNP), but none of those were detected in either run. When comparing the results of both runs to a list of nine of the most abundant proteins in CSF (*Table 9*), it becomes clear that during the first run almost all CSF bulk proteins were detected. This comparison was repeated with the results of the pre-cleared samples and a lower amount of material (*see section 2.3.2.1*), where considerably less proteins present in CSF were detected. Additionally, when comparing this list to the most abundant bulk proteins in plasma, only transthyretin and complement C3 are specific to the most abundant CSF proteins, being present in samples D, and samples A and B, respectively. From the gene set enrichment analysis with DAVID, we found enrichments of 84,4% and 82,4% for the GO-term “extracellular exosome” for samples A and B, respectively. When comparing these enrichment percentages to negative control samples C (83,2%) and D (78,0%), they are not significantly different (p-value = 0,421) from each other. This implies EVs were not significantly enriched in the anti-L1CAM samples, compared to the biotin-only samples. It is thus as of yet unclear if any neuronal material was isolated from our plasma samples, since no neuronal markers were detected.

Since none of the analyses was able to give us a clear confirmation of successful EV isolation from plasma, the isolation and immunoprecipitation protocols need to be optimized before our hypothesis can be answered. Since L1CAM was not detected during LC-MS analysis, this may be a sign of ineffective immunoprecipitation with anti-L1CAM. Even though L1CAM is the most frequently used target for EV immunoprecipitation from plasma in literature (Fiandaca et al., 2015; Goetzl et al., 2015; Goetzl et al., 2016; Kapogiannis et al., 2015; Mustapic et al., 2017), some contradictory findings have recently emerged (Norman et al., 2020). L1CAM has been shown to have an alternative splicing isoform and hence exists as a soluble as well as a transmembrane form, and is also widely expressed outside of the brain (Angiolini et al., 2019). *Norman et al.* therefore suggests that, if L1CAM is alternatively spliced, anti-L1CAM may capture soluble L1CAM that is not associated with EVs. Moreover, the authors have performed SEC on plasma and CSF and found that EV-specific tetraspanins were detected in fractions 7-9, while L1CAM was detected in free protein fractions 11-14, with a similar distribution to albumin. They concluded that L1CAM thus behaves as a free protein – and not EV-associated – in plasma and CSF, where the CSF isoform is predominantly produced by cleavage, and the plasma isoform by alternative splicing excluding exon 25. Additionally, anti-L1CAM was found to bind non-specifically to alpha-synuclein, possibly explaining the alpha-synuclein enrichment in prior research (Niu et al., 2020; Zhao et al., 2019). Ultimately, it may thus be necessary to compare L1CAM to other neuronal antibodies such as anti-NCAM. When the isolation and immunoprecipitation protocols are fully optimized for the isolation from nEVs from plasma, this same protocol could be used at SINAPS for use in biomarker discovery for psychiatric disorders.

5. Conclusion

Psychiatric mood disorders are among the most debilitating mental illnesses, being associated with high mortality rates, life-long suffering, poor clinical outcomes, but also cognitive and functional impairment. Because of their multifactorial and complex etiopathogenesis, the biology of major depressive disorder and bipolar disorder still remains poorly understood. Since diagnosis solely relies on the subjective evaluation of clinical signs, misdiagnosis rates and consequential inappropriate psycho-pharmacotherapeutic treatment are high and often detrimental to the adequate treatment of psychiatric patients. It is thus of crucial importance to develop a more accurate and objective way of diagnosing patients as to treat each mood disorder more efficiently with proper pharmacotherapies. For this reason, the discovery of biological discriminatory differential biomarkers is key to markedly ameliorate diagnosis and treatment of psychiatric affective disorders like major depressive disorder and bipolar disorder.

This thesis focused on three research projects, primarily aiming to provide a broader future perspective concerning biomarker discovery. The first project was aimed at the discovery of differentially expressed proteins in peripheral blood mononuclear cells between healthy controls and patients. The second project was centred around the technical validation of tryptophan catabolite enzyme-linked immunosorbent assays, for future use on patient and healthy control samples for the discovery of differentially expressed proteins from the kynurenine pathway in the peripheral bloodstream. The last project was targeted on the successful isolation of neuronal extracellular vesicles from plasma, so in the future a new project could be started up looking for differential biomarkers derived from the brain, that may be present in these extracellular vesicles.

The first project was soon put on hold when severe haemoglobin contamination was discovered in the previously collected peripheral blood mononuclear cell samples. For future peripheral blood mononuclear cell collection, the protocol should be optimized as to prevent the presence and subsequent lysis of red blood cells in our samples. The second project showed successful validation of the acquired kits, which gave us promising results for future analysis after the protocol has been optimized. Higher initial cell numbers appear to be required, as well as an improved way of lysing the cells. For the third project, we unfortunately did not get any clear confirmation that we succeeded at isolating extracellular vesicles. Concentrations could have possibly been too low for most experiments, or optimizations to the used protocols might be necessary for effective isolation.

Further extensive research will be required to improve the state-of-the-art knowledge on psychiatric mood disorders. New projects will need to be focused predominantly on the differential diagnosis between multiple affective disorders by developing a biological biomarker panel. These could potentially be found in plasma, serum, or whole blood, though in the future the horizons of biomarker discovery could be broadened to discover proteins of interest in peripheral blood mononuclear cells or neuronal extracellular vesicles.

6. Acknowledgements

This Master's thesis and internship were performed at the Scientific Initiative for Neuropsychiatric and Psychopharmacological Studies (SINAPS), which is a collaboration between the Collaborative Antwerp Psychiatric Research Institute (CAPRI) of the University of Antwerp and the University Psychiatric Centre (UPC) Duffel. This dissertation would not have been possible without Prof. Dr. Violette Coppens and Prof. Dr. Manuel Morrens who gave me the opportunity to further discover my natural interest and fascination for psychiatric disorders. Promotor Prof. Dr. Violette Coppens is moreover sincerely thanked for her guidance through my internship and all the feedback on my written work. I would also like to thank my coach Jobbe Goossens for his advice and much appreciated support, both academically and mentally, during the whole duration of the internship. Also many thanks to Prof. Dr. Inge Mertens and Prof. Dr. Nathalie Cools for wanting to be my co-readers, their feedback and questions during the oral defences are greatly appreciated. Lab Manager Sofie Coolman is also sincerely thanked for being a fantastic mentor in the laboratory, but above all, for making me laugh and even offering a shoulder to cry on when needed. Yael Hirschberg is also wholeheartedly thanked for being my coach during the part of my internship at the Centre for Proteomics, for reading my work and for motivating me when I needed it. My co-interns Anouk, Ben, Pauline, and Valérie are also sincerely thanked for being great colleagues, but most of all, for being even better friends. To conclude, I would like to thank all members of SINAPS and the Centre for Proteomics for their hospitality during my internship, but also my friends and family for their encouraging words and sometimes much needed emotional support.

7. References

ALLEN, A. P., NAUGHTON, M., DOWLING, J., WALSH, A., O'SHEA, R., SHORTEN, G., SCOTT, L., MCLOUGHLIN, D. M., CRYAN, J. F., CLARKE, G. & DINAN, T. G. 2018. Kynurenine pathway metabolism and the neurobiology of treatment-resistant depression: Comparison of multiple ketamine infusions and electroconvulsive therapy. *Journal of Psychiatric Research,* 100**,** 24-32.

ANAND, A., LI, Y., WANG, Y., WU, J., GAO, S., BUKHARI, L., MATHEWS, V. P., KALNIN, A. & LOWE, M. J. 2005. Activity and connectivity of brain mood regulating circuit in depression: a functional magnetic resonance study. *Biol Psychiatry,* 57**,** 1079-88.

ANGIOLINI, F., BELLONI, E., GIORDANO, M., CAMPIONI, M., FORNERIS, F., PARONETTO, M. P., LUPIA, M., BRANDAS, C., PRADELLA, D. & DI MATTEO, A. J. E. 2019. A novel L1CAM isoform with angiogenic activity generated by NOVA2-mediated alternative splicing. 8**,** e44305.

ARNONE, D., SARAYKAR, S., SALEM, H., TEIXEIRA, A. L., DANTZER, R. & SELVARAJ, S. 2018. Role of Kynurenine pathway and its metabolites in mood disorders: A systematic review and meta-analysis of clinical studies. *Neurosci Biobehav Rev,* 92**,** 477-485.

BAIETTI, M. F., ZHANG, Z., MORTIER, E., MELCHIOR, A., DEGEEST, G., GEERAERTS, A., IVARSSON, Y., DEPOORTERE, F., COOMANS, C., VERMEIREN, E., ZIMMERMANN, P. & DAVID, G. 2012. Syndecan-syntenin-ALIX regulates the biogenesis of exosomes. *Nat Cell Biol,* 14**,** 677-85.

BAN, J.-J., LEE, M., IM, W. & KIM, M. 2015. Low pH increases the yield of exosome isolation. *Biochemical and Biophysical Research Communications,* 461**,** 76-79.

BELGE, J. B., VAN DIERMEN, L., SABBE, B., PARIZEL, P., MORRENS, M., COPPENS, V., CONSTANT, E., DE TIMARY, P., SIENAERT, P., SCHRIJVERS, D. & VAN EIJNDHOVEN, P. 2020. Inflammation, Hippocampal Volume, and Therapeutic Outcome following Electroconvulsive Therapy in Depressive Patients: A Pilot Study. *Neuropsychobiology,* 79**,** 222-232.

BERK, M., DODD, S., KAUER-SANT'ANNA, M., MALHI, G. S., BOURIN, M., KAPCZINSKI, F. & NORMAN, T. 2007. Dopamine dysregulation syndrome: implications for a dopamine hypothesis of bipolar disorder. *Acta Psychiatr Scand Suppl***,** 41-9.

BERTON, O. & NESTLER, E. J. 2006. New approaches to antidepressant drug discovery: beyond monoamines. *Nat Rev Neurosci,* 7**,** 137-51.

BIRNER, A., PLATZER, M., BENGESSER, S. A., DALKNER, N., FELLENDORF, F. T., QUEISSNER, R., PILZ, R., RAUCH, P., MAGET, A., HAMM, C., HERZOG-EBERHARD, S., MANGGE, H., FUCHS, D., MOLL, N., ZELZER, S., SCHÜTZE, G., SCHWARZ, M., REININGHAUS, B., KAPFHAMMER, H.-P. & REININGHAUS, E. Z. 2017. Increased breakdown of kynurenine towards its neurotoxic branch in bipolar disorder. *PloS one,* 12**,** e0172699-e0172699.

BLUMBERG, H. P., LEUNG, H. C., SKUDLARSKI, P., LACADIE, C. M., FREDERICKS, C. A., HARRIS, B. C., CHARNEY, D. S., GORE, J. C., KRYSTAL, J. H. & PETERSON, B. S. 2003. A functional magnetic resonance imaging study of bipolar disorder: state- and trait-related dysfunction in ventral prefrontal cortices. *Arch Gen Psychiatry,* 60**,** 601-9.

BOWDEN, C. L. 2005. A different depression: clinical distinctions between bipolar and unipolar depression. *J Affect Disord,* 84**,** 117-25.

CARVALHO, A. F., SHARMA, M. S., BRUNONI, A. R., VIETA, E. & FAVA, G. A. 2016. The Safety, Tolerability and Risks Associated with the Use of Newer Generation Antidepressant Drugs: A Critical Review of the Literature. *Psychother Psychosom,* 85**,** 270-88.

CASPI, A., SUGDEN, K., MOFFITT, T. E., TAYLOR, A., CRAIG, I. W., HARRINGTON, H., MCCLAY, J., MILL, J., MARTIN, J., BRAITHWAITE, A. & POULTON, R. 2003. Influence of life stress on depression: moderation by a polymorphism in the 5-HTT gene. *Science,* 301**,** 386-9.

CHEN, J., HUANG, C., SONG, Y., SHI, H., WU, D., YANG, Y., RAO, C., LIAO, L., WU, Y., TANG, J., CHENG, K., ZHOU, J. & XIE, P. 2015. Comparative proteomic analysis of plasma from bipolar depression and depressive disorder: identification of proteins associated with immune regulatory. *Protein Cell,* 6**,** 908-11.

CHEN, J. J., ZHAO, L. B., LIU, Y. Y., FAN, S. H. & XIE, P. 2017. Comparative efficacy and acceptability of electroconvulsive therapy versus repetitive transcranial magnetic stimulation for major depression: A systematic review and multiple-treatments meta-analysis. *Behav Brain Res,* 320**,** 30-36.

CHENG, Y., ZENG, Q., HAN, Q. & XIA, W. 2019. Effect of pH, temperature and freezing-thawing on quantity changes and cellular uptake of exosomes. *Protein & Cell,* 10**,** 295-299.

CHIRIŢĂ, A. L., GHEORMAN, V., BONDARI, D. & ROGOVEANU, I. 2015. Current understanding of the neurobiology of major depressive disorder. *Rom J Morphol Embryol,* 56**,** 651-8.

COPPENS, V., DE WACHTER, O., GOOSSENS, J., HENDRIX, J., MAUDSLEY, S., AZMI, A., VAN GASTEL, J., VAN SAET, A., LAUWERS, T. & MORRENS, M. 2020. Profiling of the Peripheral Blood Mononuclear Cell Proteome in Schizophrenia and Mood Disorders for the Discovery of Discriminatory Biomarkers: A Proof-of-Concept Study. *Neuropsychobiology,* 79**,** 324-334.

CRADDOCK, N. & SKLAR, P. 2013. Genetics of bipolar disorder. *The Lancet,* 381**,** 1654-1662.

DAGER, S. R., FRIEDMAN, S. D., PAROW, A., DEMOPULOS, C., STOLL, A. L., LYOO, I. K., DUNNER, D. L. & RENSHAW, P. F. 2004. Brain metabolic alterations in medication-free patients with bipolar disorder. *Arch Gen Psychiatry,* 61**,** 450-8.

DE JONG, R. A., NIJMAN, H. W., BOEZEN, H. M., VOLMER, M., TEN HOOR, K. A., KRIJNEN, J., VAN DER ZEE, A. G. J., HOLLEMA, H. & KEMA, I. P. 2011. Serum Tryptophan and Kynurenine Concentrations as Parameters for Indoleamine 2,3-Dioxygenase Activity in Patients With Endometrial, Ovarian, and Vulvar Cancer. 21**,** 1320-1327.

DE PICKER, L., FRANSEN, E., COPPENS, V., TIMMERS, M., DE BOER, P., OBERACHER, H., FUCHS, D., VERKERK, R., SABBE, B. & MORRENS, M. 2019. Immune and Neuroendocrine Trait and State Markers in Psychotic Illness: Decreased Kynurenines Marking Psychotic Exacerbations. *Front Immunol,* 10**,** 2971.

DE SÁ, A. S., CAMPOS, C., ROCHA, N. B., YUAN, T. F., PAES, F., ARIAS-CARRIÓN, O., CARTA, M. G., NARDI, A. E., CHENIAUX, E. & MACHADO, S. 2016. Neurobiology of Bipolar Disorder: Abnormalities on Cognitive and Cortical Functioning and Biomarker Levels. *CNS Neurol Disord Drug Targets,* 15**,** 713-22.

DEAN, J. & KESHAVAN, M. 2017. The neurobiology of depression: An integrated view. *Asian J Psychiatr,* 27**,** 101-111.

DEZA-CRUZ, I., MILL, A., RUSHTON, S. & KELLY, P. 2019. Comparison of the Use of Serum and Plasma as Matrix Specimens in a Widely Used Noncommercial Dengue IgG ELISA. *The American journal of tropical medicine and hygiene,* 101**,** 456-458.

DOOLIN, K., ALLERS, K. A., PLEINER, S., LIESENER, A., FARRELL, C., TOZZI, L., O'HANLON, E., RODDY, D., FRODL, T., HARKIN, A. & O'KEANE, V. 2018. Altered tryptophan catabolite concentrations in major depressive disorder and associated changes in hippocampal subfield volumes. *Psychoneuroendocrinology,* 95**,** 8-17.

DOYLE, L. M. & WANG, M. Z. 2019. Overview of Extracellular Vesicles, Their Origin, Composition, Purpose, and Methods for Exosome Isolation and Analysis. *Cells,* 8**,** 727.

DREVETS, W. C. 1998. Functional neuroimaging studies of depression: the anatomy of melancholia. *Annu Rev Med,* 49**,** 341-61.

DREVETS, W. C. 2001. Neuroimaging and neuropathological studies of depression: implications for the cognitive-emotional features of mood disorders. *Curr Opin Neurobiol,* 11**,** 240-9.

FDA ADMINISTRATION 2020. Bioanalytical Method Validation Guidance for Industry. *https://www.fda.gov/regulatory-information/search-fda-guidance-documents/bioanalytical-method-validation-guidance-industry*.

FELGER, J. C. & LOTRICH, F. E. 2013. Inflammatory cytokines in depression: Neurobiological mechanisms and therapeutic implications. *Neuroscience,* 246**,** 199-229.

FIANDACA, M. S., KAPOGIANNIS, D., MAPSTONE, M., BOXER, A., EITAN, E., SCHWARTZ, J. B., ABNER, E. L., PETERSEN, R. C., FEDEROFF, H. J., MILLER, B. L. & GOETZL, E. J. 2015. Identification of preclinical Alzheimer's disease by a profile of pathogenic proteins in neurally derived blood exosomes: A case-control study. *Alzheimers Dement,* 11**,** 600-7.e1.

FORTE, A., BALDESSARINI, R. J., TONDO, L., VÁZQUEZ, G. H., POMPILI, M. & GIRARDI, P. 2015. Long-term morbidity in bipolar-I, bipolar-II, and unipolar major depressive disorders. *J Affect Disord,* 178**,** 71-8.

FOUNTOULAKIS, K. N., VIETA, E., SANCHEZ-MORENO, J., KAPRINIS, S. G., GOIKOLEA, J. M. & KAPRINIS, G. S. 2005. Treatment guidelines for bipolar disorder: a critical review. *J Affect Disord,* 86**,** 1-10.

FRIES, G. R., LIMA, C. N. C., VALVASSORI, S. S., ZUNTA-SOARES, G., SOARES, J. C. & QUEVEDO, J. 2019. Preliminary investigation of peripheral extracellular vesicles' microRNAs in bipolar disorder. *Journal of Affective Disorders,* 255**,** 10-14.

FUNK, M., DREW, N., FREEMAN, M., FAYDI, E. & WORLD HEALTH, O. 2010. Mental health and development : targeting people with mental health conditions as a vulnerable group / Michelle Funk ... [et al]. Geneva: World Health Organization.

GAUTAM, S., JAIN, A., GAUTAM, M., VAHIA, V. N. & GROVER, S. 2017. Clinical Practice Guidelines for the management of Depression. *Indian J Psychiatry,* 59**,** S34-s50.

GHAEMI, S. N., BOIMAN, E. E. & GOODWIN, F. K. 2000. Diagnosing bipolar disorder and the effect of antidepressants: a naturalistic study. *J Clin Psychiatry,* 61**,** 804-8; quiz 809.

GOETZL, E. J., BOXER, A., SCHWARTZ, J. B., ABNER, E. L., PETERSEN, R. C., MILLER, B. L. & KAPOGIANNIS, D. 2015. Altered lysosomal proteins in neural-derived plasma exosomes in preclinical Alzheimer disease. *Neurology,* 85**,** 40-47.

GOETZL, E. J., KAPOGIANNIS, D., SCHWARTZ, J. B., LOBACH, I. V., GOETZL, L., ABNER, E. L., JICHA, G. A., KARYDAS, A. M., BOXER, A. & MILLER, B. L. 2016. Decreased synaptic proteins in neuronal exosomes of frontotemporal dementia and Alzheimer's disease. *FASEB journal : official publication of the Federation of American Societies for Experimental Biology,* 30**,** 4141-4148.

GOOSSENS, J., MORRENS, M. & COPPENS, V. 2021. The Potential Use of Peripheral Blood Mononuclear Cells as Biomarkers for Treatment Response and Outcome Prediction in Psychiatry: A Systematic Review. *Mol Diagn Ther,* 25**,** 283-299.

GORWOOD, P. 2008. Neurobiological mechanisms of anhedonia. *Dialogues in clinical neuroscience,* 10**,** 291-299.

GRIEVINK, H. W., LUISMAN, T., KLUFT, C., MOERLAND, M. & MALONE, K. E. 2016. Comparison of Three Isolation Techniques for Human Peripheral Blood Mononuclear Cells: Cell Recovery and Viability, Population Composition, and Cell Functionality. *Biopreserv Biobank,* 14**,** 410-415.

HAMPEL, H., KÖTTER, H. U. & MÖLLER, H. J. 1997. Blood-cerebrospinal fluid barrier dysfunction for high molecular weight proteins in Alzheimer disease and major depression: indication for disease subsets. *Alzheimer Dis Assoc Disord,* 11**,** 78-87.

HAN, Q., CAI, T., TAGLE, D. A. & LI, J. 2010. Structure, expression, and function of kynurenine aminotransferases in human and rodent brains. *Cell Mol Life Sci,* 67**,** 353-68.

HEBBRECHT, K., SKOROBOGATOV, K., GILTAY, E. J., COPPENS, V., DE PICKER, L. & MORRENS, M. 2021. Tryptophan Catabolites in Bipolar Disorder: A Meta-Analysis. *Front Immunol,* 12**,** 667179.

HEIREMAN, L., VAN GEEL, P., MUSGER, L., HEYLEN, E., UYTTENBROECK, W. & MAHIEU, B. 2017. Causes, consequences and management of sample hemolysis in the clinical laboratory. *Clinical Biochemistry,* 50**,** 1317-1322.

HIRSCHFELD, R. & WEISSMAN, M. RISK FACTORS FOR MAJOR DEPRESSION AND BIPOLAR DISORDER. 2002.

HIRSCHFELD, R. M. 2014. Differential diagnosis of bipolar disorder and major depressive disorder. *J Affect Disord,* 169 Suppl 1**,** S12-6.

HOOFNAGLE, A. N. & WENER, M. H. 2009. The fundamental flaws of immunoassays and potential solutions using tandem mass spectrometry. *Journal of Immunological Methods,* 347**,** 3-11.

HYE, A., LYNHAM, S., THAMBISETTY, M., CAUSEVIC, M., CAMPBELL, J., BYERS, H. L., HOOPER, C., RIJSDIJK, F., TABRIZI, S. J., BANNER, S., SHAW, C. E., FOY, C., POPPE, M., ARCHER, N., HAMILTON, G., POWELL, J., BROWN, R. G., SHAM, P., WARD, M. & LOVESTONE, S. 2006. Proteome-based plasma biomarkers for Alzheimer's disease. *Brain,* 129**,** 3042-50.

ILGıN, C. & TOPUZOĞLU, A. 2018. Extracellular Vesicles in Psychiatry Research in the Context of RDoC Criteria. *Psychiatry investigation,* 15**,** 1011-1018.

JAMES, S. L., ABATE, D., ABATE, K. H., ABAY, S. M., ABBAFATI, C., ABBASI, N., ABBASTABAR, H., ABD-ALLAH, F., ABDELA, J., ABDELALIM, A., ABDOLLAHPOUR, I., ABDULKADER, R. S., ABEBE, Z., ABERA, S. F., ABIL, O. Z., ABRAHA, H. N., ABU-RADDAD, L. J., ABU-RMEILEH, N. M. E., ACCROMBESSI, M. M. K., ACHARYA, D., ACHARYA, P., ACKERMAN, I. N., ADAMU, A. A., ADEBAYO, O. M., ADEKANMBI, V., ADETOKUNBOH, O. O., ADIB, M. G., ADSUAR, J. C., AFANVI, K. A., AFARIDEH, M., AFSHIN, A., AGARWAL, G., AGESA, K. M., AGGARWAL, R., AGHAYAN, S. A., AGRAWAL, S., AHMADI, A., AHMADI, M., AHMADIEH, H., AHMED, M. B., AICHOUR, A. N., AICHOUR, I., AICHOUR, M. T. E., AKINYEMIJU, T., AKSEER, N., AL-ALY, Z., AL-EYADHY, A., AL-MEKHLAFI, H. M., AL-RADDADI, R. M., ALAHDAB, F., ALAM, K., ALAM, T., ALASHI, A., ALAVIAN, S. M., ALENE, K. A., ALIJANZADEH, M., ALIZADEH-NAVAEI, R., ALJUNID, S. M., ALKERWI, A. A., ALLA, F., ALLEBECK, P., ALOUANI, M. M. L., ALTIRKAWI, K., ALVIS-GUZMAN, N., AMARE, A. T., AMINDE, L. N., AMMAR, W., AMOAKO, Y. A., ANBER, N. H., ANDREI, C. L., ANDROUDI, S., ANIMUT, M. D., ANJOMSHOA, M., ANSHA, M. G., ANTONIO, C. A. T., ANWARI, P., ARABLOO, J., ARAUZ, A., AREMU, O., ARIANI, F., ARMOON, B., ÄRNLÖV, J., ARORA, A., ARTAMAN, A., ARYAL, K. K., ASAYESH, H., ASGHAR, R. J., ATARO, Z., ATRE, S. R., AUSLOOS, M., AVILA-BURGOS, L., AVOKPAHO, E. F. G. A., AWASTHI, A., AYALA QUINTANILLA, B. P., AYER, R., AZZOPARDI, P. S., BABAZADEH, A., BADALI, H., BADAWI, A., BALI, A. G., et al. 2018. Global, regional, and national incidence, prevalence, and years lived with disability for 354 diseases and injuries for 195 countries and territories, 1990–2017: a systematic analysis for the Global Burden of Disease Study 2017. *The Lancet,* 392**,** 1789-1858.

KANEKO, T., ESMAIL, S., VOSS, C., MARTIN, C., SLESSAREV, M., HOVEY, O., LIU, X., YE, M., KIM, S., FRASER, D. & LI, S. 2021. *System-wide hematopoietic and immune signaling aberrations in COVID-19 revealed by deep proteome and phosphoproteome analysis*.

KANO, S.-I., DOHI, E. & ROSE, I. V. L. 2019. Extracellular Vesicles for Research on Psychiatric Disorders. *Schizophrenia bulletin,* 45**,** 7-16.

KAPOGIANNIS, D., BOXER, A., SCHWARTZ, J. B., ABNER, E. L., BIRAGYN, A., MASHARANI, U., FRASSETTO, L., PETERSEN, R. C., MILLER, B. L. & GOETZL, E. J. 2015. Dysfunctionally phosphorylated type 1 insulin receptor substrate in neural-derived blood exosomes of preclinical Alzheimer's disease. *FASEB journal : official publication of the Federation of American Societies for Experimental Biology,* 29**,** 589-596.

KIM, A. W., ADAM, E. K., BECHAYDA, S. A. & KUZAWA, C. W. 2020. Early life stress and HPA axis function independently predict adult depressive symptoms in metropolitan Cebu, Philippines. *Am J Phys Anthropol,* 173**,** 448-462.

KIM, N. S. & AHN, W. K. 2002. Clinical psychologists' theory-based representations of mental disorders predict their diagnostic reasoning and memory. *J Exp Psychol Gen,* 131**,** 451-76.

KOENIG, A. M. & THASE, M. E. 2009. First-line pharmacotherapies for depression - what is the best choice? *Pol Arch Med Wewn,* 119**,** 478-86.

KONČAREVIĆ, S., LÖßNER, C., KUHN, K., PRINZ, T., PIKE, I. & ZUCHT, H. D. 2014. In-depth profiling of the peripheral blood mononuclear cells proteome for clinical blood proteomics. *Int J Proteomics,* 2014**,** 129259.

KOWAL, J., ARRAS, G., COLOMBO, M., JOUVE, M., MORATH, J. P., PRIMDAL-BENGTSON, B., DINGLI, F., LOEW, D., TKACH, M. & THÉRY, C. 2016. Proteomic comparison defines novel markers to characterize heterogeneous populations of extracellular vesicle subtypes. *Proceedings of the National Academy of Sciences of the United States of America,* 113**,** E968-E977.

KRISHNAN, V. & NESTLER, E. J. 2008. The molecular neurobiology of depression. *Nature,* 455**,** 894-902.

LEE, Y., EL ANDALOUSSI, S. & WOOD, M. J. 2012. Exosomes and microvesicles: extracellular vesicles for genetic information transfer and gene therapy. *Hum Mol Genet,* 21**,** R125-34.

LIPPI, G., BLANCKAERT, N., BONINI, P., GREEN, S., KITCHEN, S., PALICKA, V., VASSAULT, A. J. & PLEBANI, M. 2008. Haemolysis: an overview of the leading cause of unsuitable specimens in clinical laboratories %J Clinical Chemistry and Laboratory Medicine. 46**,** 764-772.

LIU, H., DING, L., ZHANG, H., MELLOR, D., WU, H., ZHAO, D., WU, C., LIN, Z., YUAN, J. & PENG, D. 2018. The Metabolic Factor Kynurenic Acid of Kynurenine Pathway Predicts Major Depressive Disorder. 9.

MAES, M., MIHAYLOVA, I., RUYTER, M. D., KUBERA, M. & BOSMANS, E. 2007. The immune effects of TRYCATs (tryptophan catabolites along the IDO pathway): relevance for depression - and other conditions characterized by tryptophan depletion induced by inflammation. *Neuro Endocrinol Lett,* 28**,** 826-31.

MANSUR, R. B., DELGADO-PERAZA, F., SUBRAMANIAPILLAI, M., LEE, Y., IACOBUCCI, M., RODRIGUES, N., ROSENBLAT, J. D., BRIETZKE, E., COSGROVE, V. E., KRAMER, N. E., SUPPES, T., RAISON, C. L., CHAWLA, S., NOGUERAS-ORTIZ, C., MCINTYRE, R. S. & KAPOGIANNIS, D. 2020. Extracellular Vesicle Biomarkers Reveal

Inhibition of Neuroinflammation by Infliximab in Association with Antidepressant Response in Adults with Bipolar Depression. *Cells,* 9**,** 895.
MARTINS-DE-SOUZA, D., HARRIS, L. W., GUEST, P. C., TURCK, C. W. & BAHN, S. 2010. The role of proteomics in depression research. *Eur Arch Psychiatry Clin Neurosci,* 260**,** 499-506.
MATHEW, A., BELL, A. & JOHNSTONE, R. M. 1995. Hsp-70 is closely associated with the transferrin receptor in exosomes from maturing reticulocytes. *Biochemical Journal,* 308**,** 823-830.
MCINTYRE, R. S., ZIMMERMAN, M., GOLDBERG, J. F. & FIRST, M. B. 2019. Differential Diagnosis of Major Depressive Disorder Versus Bipolar Disorder: Current Status and Best Clinical Practices. *J Clin Psychiatry,* 80.
MILL, J. & PETRONIS, A. 2007. Molecular studies of major depressive disorder: the epigenetic perspective. *Mol Psychiatry,* 12**,** 799-814.
MIURA, H., OZAKI, N., SAWADA, M., ISOBE, K., OHTA, T. & NAGATSU, T. 2008. A link between stress and depression: shifts in the balance between the kynurenine and serotonin pathways of tryptophan metabolism and the etiology and pathophysiology of depression. *Stress,* 11**,** 198-209.
MORRENS, M., DE PICKER, L., KAMPEN, J. K. & COPPENS, V. 2020. Blood-based kynurenine pathway alterations in schizophrenia spectrum disorders: A meta-analysis. *Schizophr Res,* 223**,** 43-52.
MUNEER, A. 2016. The Neurobiology of Bipolar Disorder: An Integrated Approach. *Chonnam Med J,* 52**,** 18-37.
MUSETTI, L., DEL GRANDE, C., MARAZZITI, D. & DELL'OSSO, L. 2013. Treatment of bipolar depression. *CNS Spectr,* 18**,** 177-87.
MUSTAPIC, M., EITAN, E., WERNER, J. K., JR., BERKOWITZ, S. T., LAZAROPOULOS, M. P., TRAN, J., GOETZL, E. J. & KAPOGIANNIS, D. 2017. Plasma Extracellular Vesicles Enriched for Neuronal Origin: A Potential Window into Brain Pathologic Processes. *Front Neurosci,* 11**,** 278.
NASCA, C., DOBBIN, J., BIGIO, B., WATSON, K., ANGELIS, P., KAUTZ, M., ALBRIGHT, A., MATHÉ, A., KOCSIS, J., LEE, F., MURROUGH, J., MCEWEN, B. & RASGON, N. 2020. Insulin receptor substrate in brain-enriched exosomes in subjects with major depression: on the path of creation of biosignatures of central insulin resistance. *Molecular Psychiatry***,** 1-10.
NASRALLAH, H. A. 2015. Consequences of misdiagnosis: inaccurate treatment and poor patient outcomes in bipolar disorder. *J Clin Psychiatry,* 76**,** e1328.
NIU, M., LI, Y., LI, G., ZHOU, L., LUO, N., YAO, M., KANG, W. & LIU, J. J. E. J. O. N. 2020. A longitudinal study on α-synuclein in plasma neuronal exosomes as a biomarker for Parkinson's disease development and progression. 27**,** 967-974.
NORMAN, M., TER-OVANESYAN, D., TRIEU, W., LAZAROVITS, R., KOWAL, E. J. K., LEE, J. H., CHEN-PLOTKIN, A. S., REGEV, A., CHURCH, G. M. & WALT, D. R. 2020. L1CAM is not Associated with Extracellular Vesicles in Human Cerebrospinal Fluid or Plasma. 2020.08.12.247833.
PATEL, S. 2014. Role of proteomics in biomarker discovery: prognosis and diagnosis of neuropsychiatric disorders. *Adv Protein Chem Struct Biol,* 94**,** 39-75.
PENNER-GOEKE, S. & BINDER, E. B. 2019. Epigenetics and depression*Dialogues Clin Neurosci,* 21**,** 397-405.
PERUGI, G., MICHELI, C., AKISKAL, H. S., MADARO, D., SOCCI, C., QUILICI, C. & MUSETTI, L. 2000. Polarity of the first episode, clinical characteristics, and course of manic depressive illness: a systematic retrospective investigation of 320 bipolar I patients. *Compr Psychiatry,* 41**,** 13-8.
PREECE, R. L., HAN, S. Y. S. & BAHN, S. 2018. Proteomic approaches to identify blood-based biomarkers for depression and bipolar disorders. *Expert Rev Proteomics,* 15**,** 325-340.
PRUESSNER, M., HELLHAMMER, D. H., PRUESSNER, J. C. & LUPIEN, S. J. 2003. Self-reported depressive symptoms and stress levels in healthy young men: associations with the cortisol response to awakening. *Psychosom Med,* 65**,** 92-9.
QUAN, C., WANG, S., DUAN, K., MA, J., YU, H., YANG, M., HU, N., LONG, G., ZENG, G. & HUANG, Z. 2020. The role of kynurenine pathway and kynurenic aminotransferase alleles in postpartum depression following cesarean section in Chinese women. *Brain and behavior,* 10**,** e01566-e01566.
RACHID, F. 2017. Repetitive Transcranial Magnetic Stimulation and Treatment-emergent Mania and Hypomania: A Review of the Literature. *J Psychiatr Pract,* 23**,** 150-159.
REN, J., ZHAO, G., SUN, X., LIU, H., JIANG, P., CHEN, J., WU, Z., PENG, D., FANG, Y. & ZHANG, C. 2017. Identification of plasma biomarkers for distinguishing bipolar depression from major depressive disorder by iTRAQ-coupled LC-MS/MS and bioinformatics analysis. *Psychoneuroendocrinology,* 86**,** 17-24.
RHEE, S. J., HAN, D., LEE, Y., KIM, H., LEE, J., LEE, K., SHIN, H., KIM, H., LEE, T. Y., KIM, M., KIM, S. H., AHN, Y. M., KWON, J. S. & HA, K. 2020. Comparison of serum protein profiles between major depressive disorder and bipolar disorder. *BMC Psychiatry,* 20**,** 145.

ROLLINS, B., MARTIN, M. V., MORGAN, L. & VAWTER, M. P. 2010. Analysis of whole genome biomarker expression in blood and brain. *Am J Med Genet B Neuropsychiatr Genet,* 153b**,** 919-36.

RUBIO-NAVARRO, A., AMARO VILLALOBOS, J. M., LINDHOLT, J. S., BUENDÍA, I., EGIDO, J., BLANCO-COLIO, L. M., SAMANIEGO, R., MEILHAC, O., MICHEL, J. B., MARTÍN-VENTURA, J. L. & MORENO, J. A. 2015. Hemoglobin induces monocyte recruitment and CD163-macrophage polarization in abdominal aortic aneurysm. *International Journal of Cardiology,* 201**,** 66-78.

SAATCIOGLU, O. & GUDUK, M. 2009. Electroconvulsive therapy-induced mania: a case report. *J Med Case Rep,* 3**,** 94.

SAEEDI, S., ISRAEL, S., NAGY, C. & TURECKI, G. 2019. The emerging role of exosomes in mental disorders. *Translational Psychiatry,* 9**,** 122.

SAMANTA, S., RAJASINGH, S., DROSOS, N., ZHOU, Z., DAWN, B. & RAJASINGH, J. 2018. Exosomes: new molecular targets of diseases. *Acta Pharmacol Sin,* 39**,** 501-513.

SCHWIELER, L., SAMUELSSON, M., FRYE, M. A., BHAT, M., SCHUPPE-KOISTINEN, I., JUNGHOLM, O., JOHANSSON, A. G., LANDÉN, M., SELLGREN, C. M. & ERHARDT, S. 2016. Electroconvulsive therapy suppresses the neurotoxic branch of the kynurenine pathway in treatment-resistant depressed patients. *Journal of Neuroinflammation,* 13.

SEN, S., DUMAN, R. & SANACORA, G. 2008. Serum brain-derived neurotrophic factor, depression, and antidepressant medications: meta-analyses and implications. *Biological psychiatry,* 64**,** 527-532.

SHAH, N., GROVER, S. & RAO, G. P. 2017. Clinical Practice Guidelines for Management of Bipolar Disorder. *Indian J Psychiatry,* 59**,** S51-s66.

SHIM, I. H., WOO, Y. S., KIM, M.-D. & BAHK, W.-M. 2017. Antidepressants and Mood Stabilizers: Novel Research Avenues and Clinical Insights for Bipolar Depression. *International journal of molecular sciences,* 18**,** 2406.

SIM, K., LAU, W. K., SIM, J., SUM, M. Y. & BALDESSARINI, R. J. 2015. Prevention of Relapse and Recurrence in Adults with Major Depressive Disorder: Systematic Review and Meta-Analyses of Controlled Trials. *Int J Neuropsychopharmacol,* 19.

SINGH, T. & RAJPUT, M. 2006. Misdiagnosis of bipolar disorder. *Psychiatry (Edgmont),* 3**,** 57-63.

SOARES, E., REIS, J., RODRIGUES, M., RIBEIRO, C. F. & PEREIRA, F. C. 2021. Circulating Extracellular Vesicles: The Missing Link between Physical Exercise and Depression Management? *International journal of molecular sciences,* 22**,** 542.

SULLIVAN, P. F., NEALE, M. C. & KENDLER, K. S. 2000. Genetic epidemiology of major depression: review and meta-analysis. *Am J Psychiatry,* 157**,** 1552-62.

SUZUKI, Y., SUDA, T., FURUHASHI, K., SUZUKI, M., FUJIE, M., HAHIMOTO, D., NAKAMURA, Y., INUI, N., NAKAMURA, H. & CHIDA, K. 2010. Increased serum kynurenine/tryptophan ratio correlates with disease progression in lung cancer. *Lung Cancer,* 67**,** 361-365.

SYNOWSKY, S. A., SHIRRAN, S. L., COOKE, F. G. M., ANTONIOU, A. N., BOTTING, C. H. & POWIS, S. J. 2017. The major histocompatibility complex class I immunopeptidome of extracellular vesicles. *The Journal of biological chemistry,* 292**,** 17084-17092.

TAURINES, R., DUDLEY, E., GRASSL, J., WARNKE, A., GERLACH, M., COOGAN, A. N. & THOME, J. 2011. Proteomic research in psychiatry. *J Psychopharmacol,* 25**,** 151-96.

THÉRY, C., WITWER, K. W., AIKAWA, E., ALCARAZ, M. J., ANDERSON, J. D., ANDRIANTSITOHAINA, R., ANTONIOU, A., ARAB, T., ARCHER, F., ATKIN-SMITH, G. K., AYRE, D. C., BACH, J.-M., BACHURSKI, D., BAHARVAND, H., BALAJ, L., BALDACCHINO, S., BAUER, N. N., BAXTER, A. A., BEBAWY, M., BECKHAM, C., BEDINA ZAVEC, A., BENMOUSSA, A., BERARDI, A. C., BERGESE, P., BIELSKA, E., BLENKIRON, C., BOBIS-WOZOWICZ, S., BOILARD, E., BOIREAU, W., BONGIOVANNI, A., BORRÀS, F. E., BOSCH, S., BOULANGER, C. M., BREAKEFIELD, X., BREGLIO, A. M., BRENNAN, M. Á., BRIGSTOCK, D. R., BRISSON, A., BROEKMAN, M. L., BROMBERG, J. F., BRYL-GÓRECKA, P., BUCH, S., BUCK, A. H., BURGER, D., BUSATTO, S., BUSCHMANN, D., BUSSOLATI, B., BUZÁS, E. I., BYRD, J. B., CAMUSSI, G., CARTER, D. R., CARUSO, S., CHAMLEY, L. W., CHANG, Y.-T., CHEN, C., CHEN, S., CHENG, L., CHIN, A. R., CLAYTON, A., CLERICI, S. P., COCKS, A., COCUCCI, E., COFFEY, R. J., CORDEIRO-DA-SILVA, A., COUCH, Y., COUMANS, F. A., COYLE, B., CRESCITELLI, R., CRIADO, M. F., D'SOUZA-SCHOREY, C., DAS, S., DATTA CHAUDHURI, A., DE CANDIA, P., DE SANTANA, E. F., DE WEVER, O., DEL PORTILLO, H. A., DEMARET, T., DEVILLE, S., DEVITT, A., DHONDT, B., DI VIZIO, D., DIETERICH, L. C., DOLO, V., DOMINGUEZ RUBIO, A. P., DOMINICI, M., DOURADO, M. R., DRIEDONKS, T. A., DUARTE, F. V., DUNCAN, H. M., EICHENBERGER, R. M., EKSTRÖM, K., EL ANDALOUSSI, S., ELIE-CAILLE, C., ERDBRÜGGER, U., FALCÓN-PÉREZ, J. M., FATIMA, F., FISH, J. E., FLORES-BELLVER, M., FÖRSÖNITS, A., FRELET-BARRAND, A., et al. 2018. Minimal information for studies of extracellular

vesicles 2018 (MISEV2018): a position statement of the International Society for Extracellular Vesicles and update of the MISEV2014 guidelines. *Journal of extracellular vesicles,* 7**,** 1535750-1535750.

TU, C., RUDNICK, P. A., MARTINEZ, M. Y., CHEEK, K. L., STEIN, S. E., SLEBOS, R. J. & LIEBLER, D. C. 2010. Depletion of abundant plasma proteins and limitations of plasma proteomics. *J Proteome Res,* 9**,** 4982-91.

TYRING, S., GOTTLIEB, A., PAPP, K., GORDON, K., LEONARDI, C., WANG, A., LALLA, D., WOOLLEY, M., JAHREIS, A., ZITNIK, R., CELLA, D. & KRISHNAN, R. 2006. Etanercept and clinical outcomes, fatigue, and depression in psoriasis: double-blind placebo-controlled randomised phase III trial. *The Lancet,* 367**,** 29-35.

VAKILI, S., AHOOYI, T. M., YARANDI, S. S., DONADONI, M., RAPPAPORT, J. & SARIYER, I. K. 2020. Molecular and Cellular Impact of Inflammatory Extracellular Vesicles (EVs) Derived from M1 and M2 Macrophages on Neural Action Potentials. *Brain sciences,* 10**,** 424.

VAN DEN AMEELE, S., COPPENS, V., SCHUERMANS, J., DE BOER, P., TIMMERS, M., FRANSEN, E., SABBE, B. & MORRENS, M. 2017. Neurotrophic and inflammatory markers in bipolar disorder: A prospective study. *Psychoneuroendocrinology,* 84**,** 143-150.

VAN DEN AMEELE, S., VAN NUIJS, A. L., LAI, F. Y., SCHUERMANS, J., VERKERK, R., VAN DIERMEN, L., COPPENS, V., FRANSEN, E., DE BOER, P., TIMMERS, M., SABBE, B. & MORRENS, M. 2020. A mood state-specific interaction between kynurenine metabolism and inflammation is present in bipolar disorder. *Bipolar Disord,* 22**,** 59-69.

VARGHESE, F. P. & BROWN, E. S. 2001. The Hypothalamic-Pituitary-Adrenal Axis in Major Depressive Disorder: A Brief Primer for Primary Care Physicians. *Primary care companion to the Journal of clinical psychiatry,* 3**,** 151-155.

WALKER, E. R., MCGEE, R. E. & DRUSS, B. G. 2015. Mortality in mental disorders and global disease burden implications: a systematic review and meta-analysis. *JAMA Psychiatry,* 72**,** 334-41.

XU, H. B., ZHANG, R. F., LUO, D., ZHOU, Y., WANG, Y., FANG, L., LI, W. J., MU, J., ZHANG, L., ZHANG, Y. & XIE, P. 2012. Comparative proteomic analysis of plasma from major depressive patients: identification of proteins associated with lipid metabolism and immunoregulation. *Int J Neuropsychopharmacol,* 15**,** 1413-25.

YOUNG, J. J., SILBER, T., BRUNO, D., GALATZER-LEVY, I. R., POMARA, N. & MARMAR, C. R. 2016. Is there Progress? An Overview of Selecting Biomarker Candidates for Major Depressive Disorder. *Front Psychiatry,* 7**,** 72.

ZHAO, Z.-H., CHEN, Z.-T., ZHOU, R.-L., ZHANG, X., YE, Q.-Y. & WANG, Y.-Z. J. F. I. A. N. 2019. Increased DJ-1 and α-synuclein in plasma neural-derived exosomes as potential markers for Parkinson's disease. 10**,** 438.

8. Appendix

Table 10 | **List of differentially expressed proteins between MDD and BD-D, MDD and HC, and BD-D and HC. Ranked according to decreasing MDD/BD-D discriminatory potential, as identified by *Coppens et al.***

PROTEIN	MDD/BDD 2SD = 0.16	MDD/HC 2SD = 0.19	BDD/HC 2SD = 0.21
HLA class I histocompatibility antigen, A-24 alpha chain	0,64	0,11	-0,53
Keratin, type II cytoskeletal 1	0,63	-0,01	-0,64
HLA class I histocompatibility antigen, B-18 alpha chain	0,62	0,14	-0,48
HLA class II histocompatibility antigen, DRB1-16 beta chain	**-0,59**	**-0,21**	**0,38**
Keratin, type I cytoskeletal 9	0,58	-0,06	-0,63
HLA class I histocompatibility antigen, A-2 alpha chain	0,47	-0,02	-0,49
Histone H2A type 1	0,46	-0,62	-1,09
Interferon-induced GTP-binding protein Mx1	-0,45	-0,05	0,40
Keratin, type I cytoskeletal 10	0,43	0,04	-0,39
Plexin-A4	-0,39	-0,38	0,01
Retinoblastoma-like protein 1	-0,39	0,19	0,58
High mobility group nucleosome-binding domain-containing protein 4	0,37	0,13	-0,25
HD domain-containing protein 2	0,37	-0,04	-0,41
cGMP-inhibited 3',5'-cyclic phosphodiesterase B	-0,35	-0,42	-0,07
Galectin-10	0,33	0,41	0,08
Beta-hexosaminidase	0,32	-0,33	-0,65
Haemoglobin subunit gamma-1	0,30	0,64	0,33
HLA class I histocompatibility antigen, A-68 alpha chain	-0,30	-0,02	0,28
Non-histone chromosomal protein HMG-14	0,30	0,20	-0,09
HLA class I histocompatibility antigen, Cw-1 alpha chain	0,29	0,30	0,00
Bardet-Biedl syndrome 12 protein	-0,28	-0,33	-0,06
NCK-interacting protein with SH3 domain	-0,27	-0,21	0,06
CAP-Gly domain-containing linker protein 2	-0,26	-0,22	0,05
Keratin, type II cytoskeletal 2 epidermal	0,26	0,00	-0,25
40S ribosomal protein S28	0,25	0,29	0,04
Histone H2A type 2-C	0,25	0,04	-0,21
Neutrophil gelatinase-associated lipocalin	0,25	0,53	0,27
OCIA domain-containing protein 2	0,25	-0,22	-0,47
Mitogen-activated protein kinase 13	0,24	0,02	-0,22
Tubulin beta-3 chain	-0,24	-0,60	-0,36
Histone H1.4	0,24	0,29	0,04
Trem-like transcript 1 protein	-0,24	-0,71	-0,47
Haemoglobin subunit gamma-2	0,23	0,36	0,13
PHD finger protein 6	0,23	-0,10	-0,33
Protein IWS1 homolog	0,23	-0,15	-0,38
Tropomyosin beta chain	-0,23	0,00	0,22
Peptidyl-prolyl cis-trans isomerase G	0,22	-0,09	-0,32
39S ribosomal protein L28, mitochondrial	0,22	-0,01	-0,23
Carcinoembryonic antigen-related cell adhesion molecule 8	0,22	0,27	0,05

Alpha-ketoglutarate-dependent dioxygenase FTO	0,22	-0,04	-0,26
Bactericidal permeability-increasing protein	0,22	0,52	0,30
Endoplasmic reticulum aminopeptidase 2	-0,21	-0,45	-0,24
Lactotransferrin	0,21	0,60	0,39
RNA-binding protein 42	0,21	0,00	-0,21
N-sulphoglucosamine sulphohydrolase	0,21	-0,11	-0,31
Platelet glycoprotein Ib alpha chain	-0,21	-0,23	-0,03
Cytochrome b-c1 complex subunit 9	0,20	-0,26	-0,46
ADP-ribosylation factor-like protein 8B	0,20	0,35	0,15
Platelet glycoprotein VI	-0,20	-0,24	-0,04
Cathelicidin antimicrobial peptide	0,20	0,63	0,43
Protein disulphide-isomerase A5	-0,20	-0,24	-0,04
Macrophage migration inhibitory factor	0,20	-0,11	-0,31
HLA class II histocompatibility antigen, DRB1-11 beta chain	-0,19	-0,46	-0,26
Histone H2B type 3-B	0,19	-0,06	-0,25
Liver carboxylesterase 1	0,19	-0,12	-0,31
E3 ubiquitin-protein ligase RNF123	0,19	-0,06	-0,25
HLA class I histocompatibility antigen, B-7 alpha chain	0,19	-0,08	-0,27
Histone H1.2	0,18	0,20	0,02
GTPase IMAP family member 5	-0,18	-0,26	-0,08
Prenylcysteine oxidase-like	-0,18	0,13	0,31
WD repeat-containing protein 43	0,18	-0,24	-0,42
Mitochondrial-processing peptidase subunit alpha	0,17	-0,12	-0,29
Granzyme H	0,17	-0,35	-0,52
Tyrosine-protein phosphatase non-receptor type 7 (Fragment)	0,17	-0,08	-0,25
Protein preY, mitochondrial	0,17	-0,05	-0,21
Granulysin (Fragment)	0,17	-0,34	-0,51

Red: increased expression in disease compared to HC; Green: decreased expression in disease compared to HC; Black: non-significant differential expression compared to HC, **bold**: significantly contraregulated expression in MDD compared to BD-D.